Universitat Politècnica de Catalunya
Facultat de Matemàtiques i Estadística

Degree in Mathematics

Bachelor's Degree Thesis

Stability of intracellular calcium in cardiac myocytes

Montserrat Torres Garcia

Supervised by Blas Echebarria Dominguez and Inmaculada Rodriguez Cantalapiedra

May, 2019

Thanks to my supervisors for all the help, and specially for understanding my circumstances during this project.

Thanks to my partner, for all the help and endless support, I would have not made it without you.

A special mention to everyone who has cheered for me during this last two hard years.

Abstract

The relationship between alternations in cardiac contractions, known as alternans, and the dynamics of intracellular calcium has been proven in several studies. In this paper, we will study a simple model two-variable model that sets the conditions for alternans due to refractoriness in calcium release. To perform this study, a theoretical background on dynamical systems will be provided, specially focused on the geometrical point of view and the use of Poincaré maps. A second chapter of theoretical background will focus on bifurcation theory and the main types of local bifurcations will be reviewed. The goal of this is to have enough knowledge to perform a complete study of the model while understanding the biological part of it and, eventually, link period doubling bifurcations to cardiac alternans.

Keywords

Dynamical Systems, Bifurcation theory, Cardiac alternan, Cardiac dynamics, Calcium stability

Contents

1. Previa

Calcium alternans have been related to cardiac fibrillations, one of the main causes of heart attacks. The purpose of this thesis is double: on one hand to gain enough theoretical knowledge about dynamical systems to be able to make a good study of a simple model, and to analyze a model of calcium alternans, understanding the biological processes and concepts that are related to it.

In the first chapter, from a really low level, a dynamical systems theory course is written. The first sections are dealt briefly, and as the study goes on, the geometrical point of view becomes central. The goal of the first chapter is to learn about Poincaré maps, how are they related to periodic orbits and their behaviour.

In the second chapter we focus on the study of local bifurcations, first by understanding what happens qualitatively at the system when they occur, and later we deal with the most common types of bifurcations of equilibria and periodic orbits.

The third chapter is about the study of the minimal model of calcium alternans due to refractoriness of RyR2. Giving first the concepts needed to understand it, the model is built, and with MatLab software it is analysed to test, mainly, how Poincaré maps can be useful for period doubling bifurcations.

2. Dynamical Systems

2.1 First-order systems of ODEs

We consider a system of first-order ODEs of the form

$$\frac{dx}{dt} = \dot{x} = f(x) \tag{2.1.1}$$

where $x(t) \in \mathbb{R}^n$ is a vector function of an independent variable, usually time, and $f : U \to \mathbb{R}^n$ is a smooth function defined on some subset $U \subseteq \mathbb{R}^n$. We may regard (2.1.1) as describing the evolution in continuous time t of a dynamical system with finite-dimensional state $x(t)$ of dimension n. In our case, because the vector field f does not depend explicitly on time, the system is called autonomous and we have that solutions are invariant under translations in time: if $x(t)$ is a solution, then so is $x(t + t_0)$ for any constant $t_0 \in \mathbb{R}$. Other types of ODEs can be put in the form (2.1.1):

- Non-autonomous systems. They have the form

  $$\dot{x} = f(x, t) \tag{2.1.2}$$

  They describe systems governed by laws that vary in time. They can be rewritten as autonomous if we consider the new variable $y = (x, s) \in \mathbb{R}^{n+1}$, with $s = t$, then we get

  $$\frac{dy}{ds} = f(y)$$

  Note that even if the system has a solution like $f(x^*, t) = 0$, the rewritten system does not have that constant solution for y.

- Higher-order ODEs. Systems with higher order derivatives such as $\ddot{x}(t)$, $x'''(t)$, etc; can be rewritten as first order systems by the introduction of derivatives as new dependent variables. For example, with the system

  $$\frac{dx^2}{d^2t} = \ddot{x}(t) = f(x, \dot{x})$$

  This can be rewritten as a first-order system for $z = (x, y) \in \mathbb{R}^{2n}$ with $y(t) = \dot{x}(t)$ as

  $$\dot{y} = f(x, y)$$

2.2 Existence and Uniqueness of solutions

The vector field f generates a **flow** $\phi_t : U \subseteq \mathbb{R}^n \to \mathbb{R}^n$, where $\phi_t(x) = \phi(x, t)$ is a smooth function defined for all $x \in U$ and $t \in I = [a, b] \subseteq \mathbb{R}^n$ and $\phi_t(x)$ is a solution to (2.1.1) because

$$\frac{d}{dt}(\phi(x, t))\Big|_{t=\tau} = f(\phi(x, \tau))$$

The flow, for autonomous systems, satisfies the following properties:

1. $\phi_0 = id$
2. $\phi_{t+s}(x) = (\phi_t \circ \phi_s)(x) = \phi(\phi(x, s), t)$

An initial value problem (IVP) for (2.1.1) consists of solving the ODE given an initial condition for $x(t)$, $x_0 \in \mathbb{R}^n$ a constant vector:

$$\begin{aligned} \dot{x} &= f(x) \\ x(0) &= x_0 \end{aligned} \tag{2.2.1}$$

Since we work with autonomous systems, there is no loss of generality in imposing the initial condition at $t = 0$ rather than some other time t_0. In this case, we seek a solution $\phi(x_0, t)$ such that $\phi(x_0, 0) = x_0$. The flow $\phi(x_0, \cdot) : I \subseteq \mathbb{R} \to \mathbb{R}^n$ defines a **solution curve**, **trajectory** or **orbit** of (2.1.1) based at x_0. [1] We have that $\phi(x_0, t)$ maps the initial data x_0 to the solution at time t and it's important to remark that it is not defined for all $t \in \mathbb{R}$, $x_0 \in \mathbb{R}^n$ unless solutions exist globally. The second property of the flows means that solving the ODE for time $t + s$ is equivalent to solving it for time s then for time t. Moreover, the flow depends on both the initial and final time, not just their difference, and satisfies

3. $\phi_{t,s} \circ \phi_{s,r} = \phi_{t,r}$

To state the fundamental local existence and uniqueness theorem for IVPs, due to Picard and Lindlof, we will need to describe what a *manifold* is though it will not be the main topic on this study of dynamical systems. Roughly speaking, a manifold is a topological space that locally resembles Euclidean space near each point, that is, each point of an n-dimensional manifold has a neighbourhood that is homeomorphic to $\mathbb{R}^n$ [1]. In particular, we will deal with differentiable manifolds which are topological spaces with a globally defined differential structure. However, in discussing submanifolds of solutions such as the stable manifolds, we will usually be able to work with copies of real Euclidean spaces defined locally by graphs.

Theorem 2.2.1. Local existence and uniqueness *Let $U \subset \mathbb{R}^n$ be an open subset of real Euclidean space (or of a differentiable manifold M), let $f : U \to \mathbb{R}^n$ be a continuously differentiable (C^1) map and let $x_0 \in U$. Then there is some constant $c > 0$ and a unique solution $\phi(x_0, \cdot) : (-c, c) \to U$ satisfying the differential equation $\dot{x} = f(x)$ with initial condition $x(0) = x_0$. [2]*

Two main remarks should be done about this theorem:

- Solutions of IVPs need not exist for all times because it is only a local existence theorem, it only assures the existence of a solution for sufficiently small times next to the initial time. Even for arbitrarily smooth functions f the solution of a nonlinear IVP may fail to exist for all times, like if $f(x)$ grows faster than a linear function of x. In fact, we could easily make up vector fields $f : U \to \mathbb{R}^n$ such that the solution $x(t)$ leaves any subset $U \subset \mathbb{R}^n$ in finite time.
- Actually, f only needs to be Lipschitz, thus we can deal with piecewise linear functions. However, solutions need not be unique if f is not Lipschitz continuous. If $f(x)$ is only assumed to be a continuous function of x, then solutions for (2.2.1) always exist due to Peano Existence's Theorem, but may fail to be unique.

[1] For first-order systems we only need to impose data for $x(t)$. For higher order systems, we would need to impose initial data for the same number of derivatives as the order of the system.

2.2.1 Fixed points and stability

Fixed points, also called **equilibrium solutions**, **zeroes** or **steady state solutions** are an important class of solutions of an ODE. They are $x^* \in \mathbb{R}^n$ defined by

$$f(x^*) = 0 \tag{2.2.2}$$

Thus, the ODE has the constant solution $x(t) = x^*$.

An equilibrium is said to be **stable** (or Liapunov stable) if small perturbations of the solution decay, or at least remain bounded, for all time. That is, for every neighbourhood V of $x^* \in U$, there is a neighbourhood $V_1 \subset V$ such that every solution $x(x_0, t)$ with $x_0 \in V1$, is defined and lies in V for all $t > 0$. If, in addition, V_1 can be choosen to that $x(t) \to x^*$ as $t \to \infty$ then x^* is said to be **asymptotically stable**. Usually, asymptotically stable fixed points are called *sinks* and unstable fixed points (those which are not stable) are known as *sources*.
If we work with the flow of the ODE, we get that equilibria solutions satisfy

$$\phi_t(x^*) = \phi(x^*, t) = x^*$$

which explains why equilibria are sometimes referred as fixed points of the flow map. Moreover, we can state precise definitions of stability in terms of the flow: an equilibrium x^* is *stable* if for every $\epsilon > 0$ there exists $\delta > 0$ shuch that if $|x - x^*| < \delta$ then $|\phi_t(x) - x^*| < \epsilon$ for all $t \geq 0$. Also, an equilibrium is *asymptotically stable* if its stable and there exists $\eta < 0$ such that if $|x - x^*| < \eta$ then $\phi_t(x) \to x^*$ as $t \to \infty$.
Thus, stability means that the solutions which start sufficiently close to equilibrium remain arbitrarily close for all $t \geq 0$, while asymptotic stability means that in addition, nearby solutions approach the equilibrium as $t \to \infty$. Stability does not imply asymptotic stability since nearby solutions might oscillate about an equilibrium without decaying toward it. Also, it is not sufficient for asymptotic stability that all nearby solutions approach the equilibrium, because they could make large excursions before approaching the equilibrium, which would violate the definition of stability [3].
Note that these notions of stability are local, they only relate to the behaviour of solutions near the fixed point x^*. Even if such solutions remain bounded for all time, other solutions may not exist globally.

One way to figure out the stability of a fixed point is by using Lyapunov functions. The method relies on finding a positive definite function $V : U \to \mathbb{R}$, the **Lyapunov function**, which decreases along solution curves of the ODE.

Theorem 2.2.2. *[4] Let x^* be a fixed point for (2.1.1) and $V : W \to \mathbb{R}$ be a differentiable function defined on some neighbourhood $W \subseteq U$ of x^* such that:*

1. *$V(x^*) = 0$ and $V(x) > 0$ if $x \neq x^*$*
2. *$\dot{V}(x) \leq 0$ in $W \setminus \{x^*\}$*

Then x^* is stable. Moreover, if

3. *$\dot{V}(x) < 0$ in $W \setminus \{x^*\}$*

then x^* is asymptotically stable.

In the state of the theorem, we have used

$$\dot{V}(x) = \sum_{j=1}^{n} \frac{\partial V}{\partial x_j} \dot{x}_j = \sum_{j=1}^{n} \frac{\partial V}{\partial x_j} f_j(x)$$

If we can choose $W = U = \mathbb{R}^n$ in case (3), then x^* is said to be **globally asymptotically stable** and we can conclude that all solutions remain bounded and approach to x^* as $t \to \infty$. Thus, the stability of equilibria and boundedness of solutions can be tested without explicitly solving the ODE. However, there are no general methods for finding suitable Lyapunov functions.
For problems with multiple equilibria, there is an alternative to finding local Lyapunov functions and it is finding a compact hypersurface $S \subset \mathbb{R}^n$ such that the vector field is directed inward everywhere on S. If such surface exists, then any solution starting on or the inside of S can never leave the interior of S and thus, it must remain bounded for all time. Thus, the local existence theorem becomes global when we work on compact manifolds instead of open spaces like $\mathbb{R}^n$.

Going back to the existence of solutions, if we want solutions that exist globally in time, we need to add conditions to the theorem (2.2.1). In fact, the only way in which global existence can fail is if the solution escapes to infinity, i.e., it *blows-up*. The extension of solutions implies that we can extend a solution of the ODE as long as it remains bounded, and by the ODE we have that the derivative $\dot{x}(t)$ remains bounded if the solution $x(t)$ does so too.

Theorem 2.2.3. *[5] The differential equation $\dot{x} = f(x)$, $x \in M$, with M a compact manifold, and $f \in C^1$, has solution curves defined for all $t \in \mathbb{R}$.*

Thus, the flows on spheres and tori are globally defined because there is no way in which solutions can escape such manifolds. On the other hand, the local theorem can be extended to show that solutions depend on initial conditions:

Theorem 2.2.4. *[6] Let $U \subseteq \mathbb{R}^n$ can be open and suppose $f : U \to \mathbb{R}^n$ has a Lipschitz constant K. Let $y(t)$ and $z(t)$ be solutions to $\dot{x} = f(x)$ on the closed interval $[t_0, t_1]$. Then, for all $t \in [t_0, t_1]$*

$$|y(t) - z(t)| \leq |y(t_0) - z(t_0)| e^{K(t-t_0)}$$

However, these continuous dependence does not preclude the exponentially fast separation of solutions, like the one that happens near a saddle point. Note that the local exponential divergence (or contraction) of trajectories may be different in different directions and is measured by the *Lyapunov exponent* of the system.

2.3 Linear systems of ODEs

An IVP for a homogenous, autonomous, first-order linear system of ODEs has the form

$$\begin{aligned} \dot{x} &= f(x) = Ax \\ x(0) &= x_o \end{aligned} \tag{2.3.1}$$

where A is a $n \times n$ matrix with constant coefficients and $x_0 \in \mathbb{R}^n$. It has a unique global solution, given explicitly by

$$x(x_0, t) = e^{tA}x_0 \tag{2.3.2}$$

where $t \in (-\infty, \infty)$ and the matrix exponential is the convergent series defined as

$$e^{tA} = I + tA + \frac{1}{2}t^2A^2 + ... + \frac{1}{n!}t^nA^n + ...$$

The matrices e^{tA} verify

1. $e^{t_1A}e^{t_2A} = e^{(t_1+t_2)A}$
2. $\frac{d}{dt}e^{tA} = Ae^{tA}$
3. $det(e^{tA}) = e^{tr(A)t}$

A **general solution** to $\dot{x} = Ax$ can be obtained by linear superposition on n linearly independent solutions $\{x_1(t), ..., x_n(t)\}$

$$x(t) = \sum_{j=1}^{n} c_j x_j(t)$$

where the n unknown constants c_j are to be determined by the initial conditions.
If A has n linearly independent eigenvectors v_j, $j = 1 \div n$, then we may take as a basis for the space of solution the vector valued functions

$$x_j(t) = e^{\lambda_j t}v_j$$

where λ_j is the eigenvalue associated with v_j. For complex eigenvalues without multiplicity, $\lambda_j = \alpha_j \pm i\beta_j$ having eigenvectors $Re(v_j) \pm iIm(v_j)$ we may take

$$x_j = e^{\alpha_j t}(Re(v_j)cos(\beta_j t) - Im(v_j)sin(\beta_j t))$$
$$x_{j+1} = e^{\alpha_j t}(Re(v_j)cos(\beta_j t) + Im(v_j)sin(\beta_j t))$$

as the associated pair of real linearly independent solutions.
We denote the **fundamental solution matrix** having these n solutions for its columns as

$$X(t) = [x_1(t), ..., x_n(t)] \tag{2.3.3}$$

The columns $x_j(t)$ of $X(t)$ form a basis of the space of solutions of $\dot{x} = Ax$. Thus, we have that

$$e^{tA} = X(t)X(0)^{-1} \tag{2.3.4}$$

The system $\dot{x} = Ax$ may also be solved by first finding an invertible transformation T which diagonalizes A, or at least puts it into Jordan normal form. Then, the system becomes

$$\dot{y} = Jy$$

where $J = T^{-1}AT$ and $x = Ty$. Now, the exponential e^{tA} may be computed as

$$e^{tA} = Te^{tJ}T^{-1}$$

It is important to note that if v_j is an eigenvector belonging to a real eigenvalue λ_j of A, then v_j is also an eigenvector belonging to the eigenvalue e^{λ_j} of e^A. Moreover, if $span\{Re(v_j), Im(v_j)\}$ [2] is an eigenspace belonging to a complex conjugate pair of eigenvalues λ_j, $\overline{\lambda_j}$, then it is also an eigenspace belonging to e^{λ_j}, $e^{\overline{\lambda_j}}$.

The matrix e^{tA} can be understood as a mapping from $\mathbb{R}^n$ to $\mathbb{R}^n$: given any point x_0 in $\mathbb{R}^n$, $x(x_0, t) = e^{tA}x_0$ is the point at which the solution based at x_0 lies after time t. Thus, e^{tA} defines a flow on $\mathbb{R}^n$ generated by the vector field Ax, defined on $\mathbb{R}^n$,and it can be thought of as the set of all solutions to $\dot{x} = Ax$. In this set, those solutions which lie in the linear subspaces spanned by the eigenvectors play a special role. These subspaces are invariant under e^{tA} and in particular, if v_j is a real eigenvector of A, and hence of e^{tA}, then a solution based at a point $c_j v_j \in \mathbb{R}^n$ remains on $span\{v_j\}$ for all time. Similarly, the two-dimensional subspace spanned by $Re(v_j)$, $Im(v_j)$ when v_j is a complex eigenvector, is invariant under e^{tA} [7].

As a recap, the eigenspaces of A are invariant subspaces for the flow. The subspaces spanned by eigenvectors can be divided into three classes:

- The **stable subspace**, $E^s = span\{v_1, ..., v_{n_s}\}$. Where $v_1, ..., v_{n_s}$ are the n_s generalized eigenvectors whose eigenvalues have *negative real parts*.
- The **unstable subspace**, $E^u = span\{u_1, ..., u_{n_u}\}$. Where $u_1, ..., u_{n_u}$ are the n_u generalized eigenvectors whose eigenvalues have *positive real parts*.
- The **center subspace**, $E^c = span\{w_1, ..., w_{n_c}\}$. Where $w_1, ..., w_{n_c}$ are the n_c generalized eigenvectors whose eigenvalues have *null real parts*.

The names reflect the facts that solutions lying on E^s are characterized by exponential decay (either monotonic or oscillatory), those lying on E^u are characterized by exponential growth and those lying in E^c by neither. In the absence of multiple eigenvalues, these latter either oscillate at constant amplitude (if λ, $\overline{\lambda} = \pm i\beta$) or remain constant (if $\lambda = 0$). When there are multiple eigenvalues for which algebraic and geometric multiplicities differ, then one may have growth of solutions in E^c.

2.3.1 Stability of solutions

Considering the linear system $\dot{x} = Ax$, we will classify their solutions in: unstable, stable or asymptotically stable. These definitions are global when we talk about linear systems and become only local when the system has non-linear terms.

Theorem 2.3.1. *[8]* **Stability of linear systems with constant terms**. *The system $\dot{x} = Ax$ is:*

1. *Asymptotically stable $\Leftrightarrow$ All eigenvalues of A have strictly negative real part.*
2. *Stable $\Leftrightarrow$ All eigenvalues of A have negative or zero real part.*

[2] Given a vector space V over a field K, the span of a set S of vectors is defined to be the intersection W of all subspaces of V that contain S.

3. *Unstable* $\Leftrightarrow$ *There's an eigenvalue with positive real part or an eigenvalue with zero real part and its algebraic and geometric multiplicities differ.*

2.4 Non-linear systems of ODEs

We now consider a non-linear system

$$\dot{x} = f(x) \tag{2.4.1}$$

and the initial value problem associated

$$\begin{aligned} \dot{x} &= f(x) \\ x(0) &= x_0 \end{aligned} \tag{2.4.2}$$

Since we cannot give a general formula analogous to the one for the linear case we need to find a different approach to solve, or at least understand the behaviour, of non-linear ODEs. A good place to start the study is by finding the fixed points of f, also referred as **stationary solutions**.

2.4.1 Linear stability analysis

Suppose that we have a fixed point x^*, so that $f(x^*) = 0$, and we want to characterize the behaviour of solutions near x^*. We do this by linearizing (2.4.1) at x^*. Consider $x \in \mathbb{R}^n$ near $x^* \in \mathbb{R}^n$. Then,

$$x = x^* + \delta x \qquad \delta \ll 1 \tag{2.4.3}$$

With this new point, we can rewrite (2.4.1) as

$$\frac{dx^*}{dt} + \frac{d(\delta x)}{dt} = f(x^* + \delta x)$$

As we have that $f : \mathbb{R}^n \to \mathbb{R}^n$, we get for $i = 1 \div n$

$$\frac{d(\delta x_i)}{dt} = f_i(x_1^* + \delta x_1, ..., x_n^* + \delta x_n)$$

Now we can compute the Taylor expansion for each f_i, $i = 1 \div n$, and obtain

$$\frac{d(\delta x_i)}{dt} = f_i(x^*) + \sum_{j=1}^{n} \left.\frac{df_i}{dx_j}\right|_{x^*} \delta x_j$$

Note that the Jacobian matrix of f is exactly what we are writing on the second term of the right side, so we have

$$\frac{d(\delta x)}{dt} \simeq f(x^*) + Df(x^*)\delta x \tag{2.4.4}$$

where $Df(x^*)$ is a matrix with constant coefficients. Since we are only considering a linearization around the fixed point, higher derivatives are not taken into consideration when using the Taylor expansion and, therefore, we do not have an equality at (2.4.4) but a semiequality. However, for now we will take the

expression as an equality because it's easier to work with. Thus, if we take into account that $f(x^*) = 0$, we have that the linearization of the system around a fixed point x^* has the equation

$$\frac{d(\delta x)}{dt} = Df(x^*)\delta x \tag{2.4.5}$$

which is a linear system and its solutions are of the form $\delta x(t) = e^{tDf(x^*)}\delta x(0)$ having the following properties [9]:

- If we use as an initial condition a point $\delta x(0)$ which position compared to x^* is given by an eigenvector of $Df(x^*)$ associated to an eigenvalue of **strictly positive real part**, λ_+: $\delta x(0) = v_{\lambda_+}$; then $||\delta x(t)||$ increases along the direction given by v_+ and the system goes away from x_0. Those eigenvectors give the unstable or dilatant directions.

- If we use as an initial condition a point $\delta x(0)$ which position compared to x^* is given by an eigenvector of $Df(x^*)$ associated to an eigenvalue of **strictly negative real part**, λ_-: $\delta x(0) = v_{\lambda_-}$; then $||\delta x(t)||$ decreases along the direction given by v_- and the system goes to x_0. Those eigenvectors give the stable or contractant directions.

- The eigenvalues of null real part are problematic. In this case, the nonlinear terms may cause the growth or decay of perturbations from equilibrium and the behaviour of solutions of the nonlinear system near the equilibrium may differ qualitatively from that of the linearized system.

When an equilibrium x^* of (2.4.1) is such that $Df(x^*)$ has no eigenvalues with zero real part, x^* is called **hyperbolic**. For a hyperbolic equilibrium, all solutions of the linearized system grow or decay exponentially in time, as we have already seen. According to the Hartman-Grobman theorem, if x^* is hyperbolic, then the flows of the linearized and nonlinear system are topologically equivalent near the equilibrium. In particular, the stability of the nonlinear equilibrium is the same as the stability of the equilibrium of the linearized system.

Theorem 2.4.1. Hartman-Grobman *[10]. If $Df(x^*)$ has no zero or purely imaginary eigenvalues then there is a homeomorphism h defined on some neighbourhood U of x^* in $\mathbb{R}^n$ locally taking orbits of the nonlinear flow ϕ_t of (2.4.2), to those of the linear flow $e^{tDf(x^*)}$ of the linearization. The homeomorphism preserves the sense of orbits and can also be chosen to preserve parametrization by time.*

Before the next result, we will need to define two type of manifolds

- **Local Stable Manifold**

$$W^s_{loc}(x^*) = \{x \in U |\ \phi_t(x) \to x^* \text{ as } t \to \infty, \text{ and } \phi_t(x) \in U \text{ for all } t \geq 0\} \tag{2.4.6}$$

- **Local Unstable Manifold**

$$W^u_{loc}(x^*) = \{x \in U |\ \phi_t(x) \to x^* \text{ as } t \to -\infty, \text{ and } \phi_t(x) \in U \text{ for all } t \leq 0\} \tag{2.4.7}$$

where $U \subset \mathbb{R}^n$ is a neighbourhood of the fixed point x^*. The invariant manifolds W^s_{loc} and W^u_{loc} provide nonlinear analogues of the flat stable and unstable eigenspaces E^s, E^u of the linearization. In fact, as we can see in the next theorem, W^s_{loc}, W^u_{loc} are tangent to E^s and E^u at x^*.

Theorem 2.4.2. Stable Manifold Theorem for a Fixed Point *[11]. Suppose that $\dot{x} = f(x)$ has a hyperbolic fixed point x^*. Then there exist local stable and unstable manifolds W^s_{loc}, W^u_{loc}, of the same dimension n_s, n_u as those of the eigenspaces E^s, E^u of the linearized system at x^*, and tangent to E^s, E^u at x^*. W^s_{loc}, W^u_{loc} are as smooth as the function f.*

Note that we have not yet said anything about a center manifold, tangent to E^c at x^* and only have dealt with hyperbolic cases in which E^c does not exist. This is because nonhyperbolic cases will be dealt with later, on the second chapter.

The local invariant manifolds have global analogues W^s, W^u obtained by letting points in W^s_{loc} flow backwards in time and those in $W^u loc$ flow forwards:

$$\begin{aligned} W^s(x^*) &= \bigcup_{t\leq 0} \phi_t(W^s_{loc}(x^*)) \\ W^u(x^*) &= \bigcup_{t\geq 0} \phi_t(W^u_{loc}(x^*)) \end{aligned} \tag{2.4.8}$$

Existence and uniqueness of solutions of (2.4.2) ensure that two stable (or unstable) manifolds of distinct fixed points x_1^*, x_2^* cannot intersect nor can $W^s_{loc}(x^*)$ (or $W^u(x^*)$) intersect itself. However, intersections of stable and unstable manifolds of distinct fixed points or the same fixed point can occur and, in fact, are a source of much of the complex behaviour found in dynamical systems.

2.4.2 Phase space

Very few nonlinear systems of ODEs are explicitly solvable. Therefore, rather than looking for individual analytical solutions it's best to try to understand the qualitative behaviour of their solutions.
We may represent the solutions of $\dot{x} = f(x)$ by solution curves or trajectories $x(t)$ in the *phase space* $\mathbb{R}^n$. These trajectories are integral curves of the vector field f, meaning that they are tangent to f at every point. The existence-uniqueness theorem implies that if the vector field f is smooth, then a unique trajectory passes through each point of phase space and that trajectories cannot cross. We may visualize f as the steady velocity field of a fluid that occupies phase space and the trajectories as particles paths of the fluid. In the fluid analogy, ϕ_t may be interpreted as the map that takes a particle from its initial location at time 0 to its location at time t.

One way to organize the study of dynamical systems is by the dimension of their phase space. In one or two dimensions, the non-intersection of trajectories strongly restricts their possible behaviour: in one dimension, solutions can only increase or decrease monotonically to an equilibrium or to infinity; in two dimensions, oscillatory behaviour can occur. In three dimensions complex behaviour, including chaos, is possible.

2.4.3 1D Case

Consider the autonomous non-linear system

$$\frac{dx}{dt} = \dot{x} = f(x) \tag{2.4.9}$$

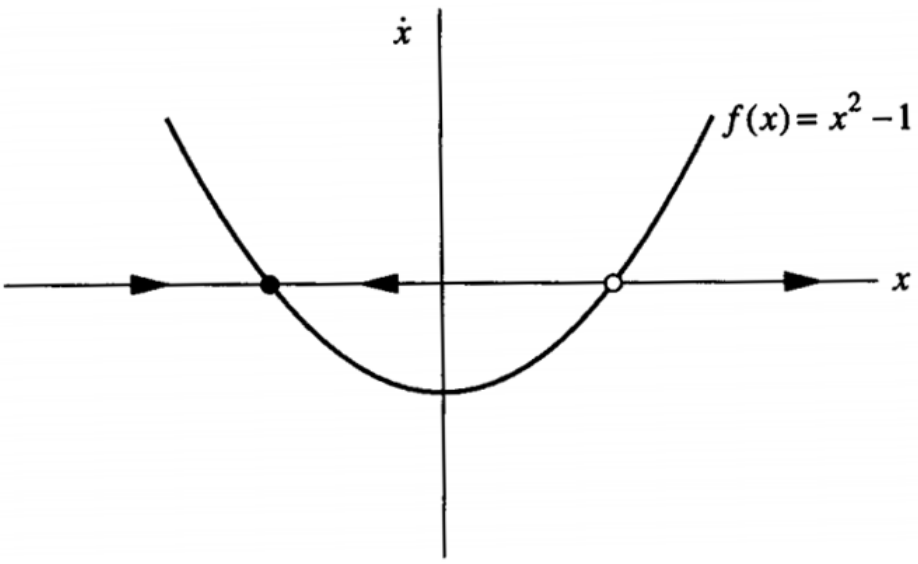

Figure 1: Phase portrait. Image from [3]

with $x \in \mathbb{R}$ and $f : \mathbb{R} \to \mathbb{R}$. We think of t as time, x as position and $\dot{x}$ as velocity. We can draw the graph of $f(x)$ and use it to sketch the vector field on the x-axis. Imagine that a fluid is flowing along the real line with a local velocity $f(x)$. The flow is to the right where $f(x) > 0$ and to the left where $f(x) < 0$. To find the solution to the ODE starting form an arbitrary initial condition x_0, we place an imaginary particle (*phase point*) at x_0 and watch how it is carried along by the flow. As time goes on, the phase point moves along the x-axis according to some function $x(t)$, called *trajectory* based at x_0, and it represents the solution of the ODE starting at the initial condition x_0. A picture that shows all the qualitatively different trajectories of the system is called **phase portrait**. The appearance of the phase portrait is controlled by the fixed points x^*, defined by $f(x^*) = 0$, that represent the equilibrium solutions. Also, we can see the stability of the fixed points by seeing whether the arrows point towards the fixed point (stable fixed point) or they point in the opposite direction (unstable fixed point).

Example 1 [3]. For the system $\dot{x} = x^2 - 1$ the phase portrait would be the one on Figure 1.

In this example all small disturbances to $x^* = -1$ will decay, but a large disturbance that sends x to the right of $x = 1$, will not decay but will be repelled to infinity. Thus, we have that $x^* = -1$ is locally stable.

Example 2 [3]. We consider the system $\dot{x} = k - \frac{x}{c}$. There's only one fixed point, $x^* = kc$, so if we sketch the phase portrait we get what shows on Figure 2:

The flow is always towards x^* so we say that x^* is asymptotically stable since it's approached from all initial conditions.
In this case we can also sketch $x(t)$ as can be seen on Figure 3. To do so, we start a phase point at the origin and imagine how it would move. The flow carries monotonically the phase point towards x^* and its speed, $\dot{x}$, decreases linearly as it approaches the fixed point, therefore $x(t)$ is increasing and concave down.

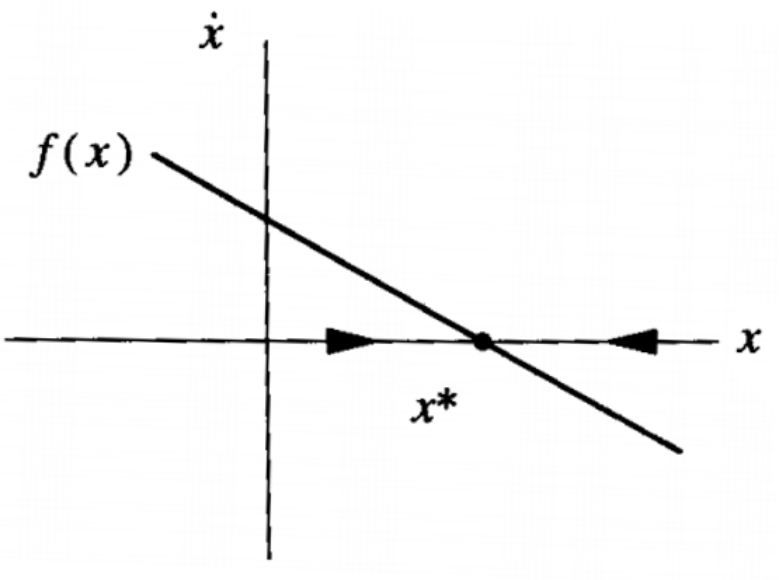

Figure 2: Phase portrait. Image from [3]

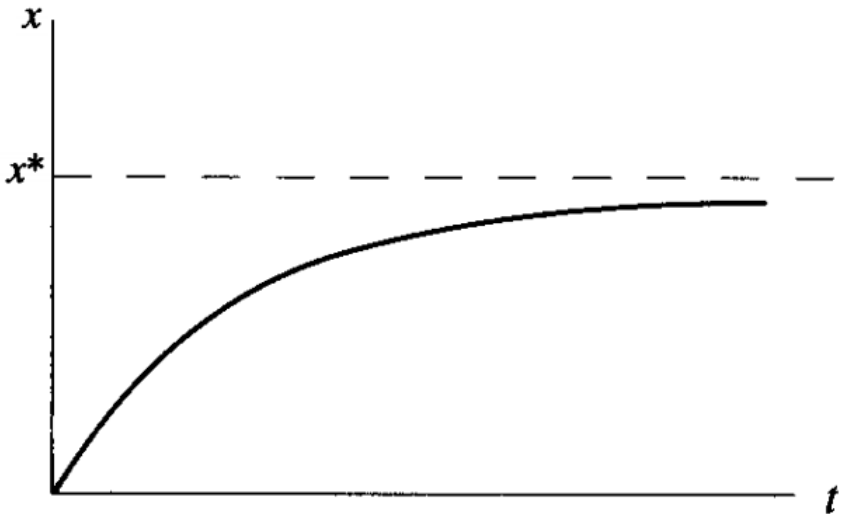

Figure 3: Solution portrait. Image from [3]

For the phase line, the linearization about a fixed point can be thought as $\dot{\delta} = f'(x^*)\delta + O(\delta^2)$, where $\delta(t) = x(t) - x^*$. When $f'(x^*) = 0$ the $O(\delta^2)$ terms are not negligible and non linear analysis is needed to determine stability. But when $f'(x^*) \neq 0$, the linearization is:

$$\dot{\delta} = \delta f'(x^*) \tag{2.4.10}$$

and this shows that the perturbation $\delta(t)$ grows exponentially if $f'(x^*) > 0$ and decays if $f'(x^*) < 0$. The magnitude of $f'(x^*)$ plays the role of an exponential growth or decay rate, and its inverse determines the time required for $x(t)$ to vary significantly in the neighborhood of x^*.

Fixed points dominate the dynamics of first order problems. Trajectories either approach a fixed point or diverge to infinity, and those are the only things that can happen for a vector field on the real line. The reason is that trajectories are forced to increase or decrease monotonically, or remain constant, never reversing direction. Thus, a fixed point is regarded as an equilibrium solution and the approach to it is always monotonic (overshoot and damped oscillations can never happen in a first order system). For the same reason, undamped oscillations are impossible. Hence, there are no periodic solutions to $\dot{x} = f(x)$ and this reflects the fact that this ODE corresponds to a flow on a line. [3]

2.4.4 2D Case

In the bidimensional case a dynamical system is of the form

$$\begin{aligned} \dot{x_1} &= f_1(x_1, x_2) \\ \dot{x_2} &= f_2(x_1, x_2) \end{aligned} \tag{2.4.11}$$

If we consider a small perturbation close to a fixed point $x^* = (x_1^*, x_2^*)$

$$x = x^* + \delta x = (x_1^* + \delta x_1, x_2^* + \delta x_2)$$

then we can linearize the system (2.4.11) around x^*

$$\begin{aligned} \dot{\delta} x_1 &= f_1(x_1^* + \delta x_1, x_2^* + \delta x_2) \\ \dot{\delta} x_2 &= f_2(x_1^* + \delta x_1, x_2^* + \delta x_2) \end{aligned}$$

that with Taylor's expansion becomes

$$\begin{aligned} \dot{\delta} x_1 &= f_1(x_1^*, x_2^*) + \left.\frac{\partial f_1}{\partial x_1}\right|_{x^*} \delta x_1 + \left.\frac{\partial f_1}{\partial x_2}\right|_{x^*} \delta x_2 \\ \dot{\delta} x_2 &= f_2(x_1^*, x_2^*) + \left.\frac{\partial f_2}{\partial x_1}\right|_{x^*} \delta x_1 + \left.\frac{\partial f_2}{\partial x_2}\right|_{x^*} \delta x_2 \end{aligned}$$

Using $D_{ij} = \left.\frac{\partial f_i}{\partial x_j}\right|_{x^*}$, we have

$$\begin{aligned} \dot{\delta x_1} &= D_{11}\delta x_1 + D_{12}\delta x_2 \\ \dot{\delta x_2} &= D_{21}\delta x_1 + D_{22}\delta x_2 \end{aligned}$$

[3] Note that if we are dealing with a circle rather than a line we could eventually return to the starting place.

which is exactly the same as

$$\frac{d}{dt}\begin{pmatrix}\delta x_1\\ \delta x_2\end{pmatrix} = \begin{pmatrix}D_{11} & D_{12}\\ D_{21} & D_{22}\end{pmatrix}\begin{pmatrix}\delta x_1\\ \delta x_2\end{pmatrix}$$

To determine the spectrum of D, we compute the characteristic polynomial $P(\lambda)$

$$\begin{aligned} Det(D-\lambda I) &= \begin{vmatrix}D_{11}-\lambda & D_{12}\\ D_{21} & D_{22}-\lambda\end{vmatrix}\\ &= (D_{11}-\lambda)(D_{22}-\lambda) - D_{12}D_{21}\\ &= \lambda^2 - (D_{11}+D_{22})\lambda + D_{11}D_{22} - D_{12}D_{21}\end{aligned}$$

which gives

$$P(\lambda) = \lambda^2 - Tr(D)\lambda + Det(D) \tag{2.4.12}$$

We can now consider all the possible cases for the roots of this polynomial [9].

2.4.4.1 Different real roots and non null

The characteristic polynomial can be factorized in the form:

$$P(\lambda) = (\lambda-\lambda_1)(\lambda-\lambda_2) \tag{2.4.13}$$

and the matrix is diagonalizable. Any initial condition $\delta x(0)$ can be decomposed in a basis formed by the eigenvectors v_1, v_2 associated to the eigenvalues λ_1, λ_2 respectively.

$$\delta x(0) = \alpha_1 v_1 + \alpha_2 v_2$$

where α_1, α_2 are two real constants. The linear behaviour with time of $\delta x(t)$ is then given by

$$\delta x(t) = \alpha_1 e^{\lambda_1} v_1 + \alpha_2 e^{\lambda_2} v_2$$

Depending on the signs of λ_1, λ_2 we can have the following behaviours:

1. Both roots have the same sign. Then the fixed point is called a **node** and its representation can be seen in Figure 4 and Figure 5. The node is *stable* when the two roots are negative and it is *unstable* when they are positive. The red lines are the directions given by the eigenvectors. The blue curves are examples of trajectories in the phase space.

2. The roots have opposite signs. Then the fixed point is call a **saddle node** and it is *always unstable*. The representation can be seen in Figure 6, where the red lines are the directions given by the eigenvectors. The blue curves are examples of trajectories in the phase space.

2.4.4.2 Complex conjugate roots

The characteristic polynomial cannot be factorized in $\mathbb{R}$. The complex conjugate eigenvalues can be written as

$$\begin{aligned}\lambda_1 &= \sigma + i\omega\\ \lambda_2 &= \sigma - i\omega\end{aligned}$$

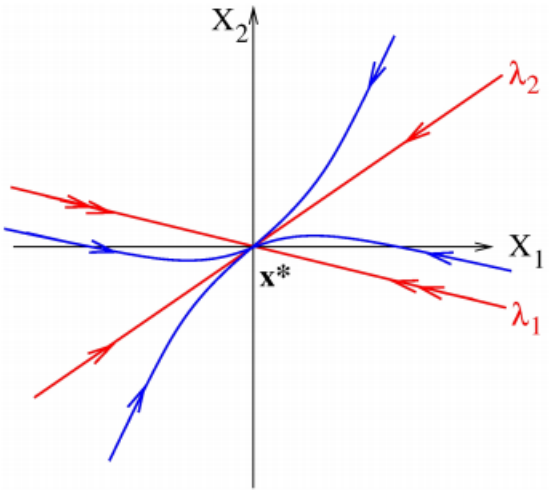

Figure 4: Stable node. Image from [9]

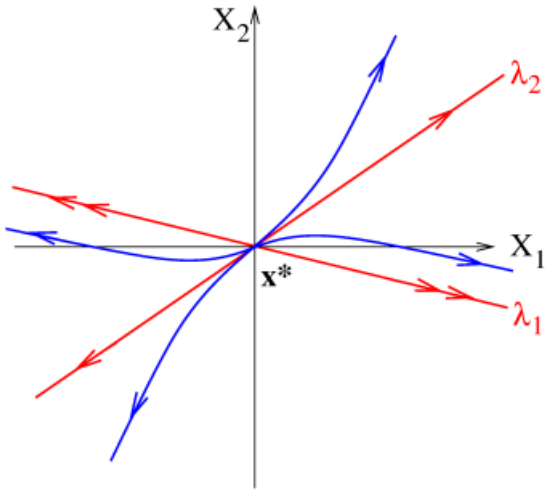

Figure 5: Unstable node. Image from [9]

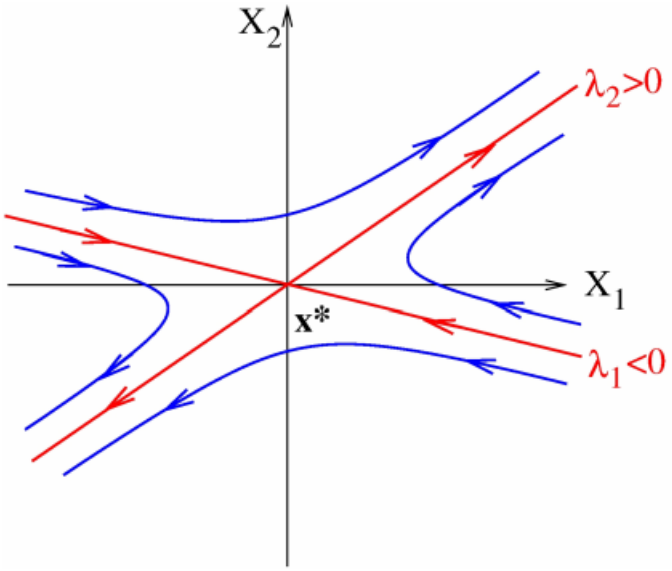

Figure 6: Saddle point. Image from [9]

with σ and ω reals. There is a change of coordinates that allows to write the system as

$$\dot{y_1} = \sigma y_1 + \omega y_2$$
$$\dot{y_2} = -\omega y_1 + \sigma y_2$$

The solutions of the system for an initial condition y^0 are

$$\begin{aligned} y_1(t) &= e^{\sigma t}(y_1^0 \cos \omega t + y_2^0 \sin \omega t) \\ y_2(t) &= e^{\sigma t}(-y_1^0 \sin \omega t + y_2^0 \cos \omega t) \end{aligned} \tag{2.4.14}$$

The $\cos(\omega)t$ and $\sin(\omega)t$ parts of the solution lead to oscillations with time. Such oscillations exist only when the imaginary part of the eigenvalues, ω, is different from 0. Concerning the stability of the fixed point, it is determined by the $e^{\sigma t}$ function, which is defined by the real part of the complex conjugate eigenvalues. Thus, the real part of the eigenvalues determine the stability of the fixed point. We have two cases:

1. $\sigma \neq 0$. Then the fixed point is called a **spiral**. It is *stable* for $\sigma < 0$ and *unstable* for $\sigma > 0$. The representation can be seen in Figure 7 where the blue curves are examples of trajectories in the phase space and the unstable spiral has the same figure but with reverse arrows.

2. $\sigma = 0$. The fixed point is called a **center**. The stability of the fixed point cannot be determined by a linear analysis: the nonlinearities will determine if the point is stable or unstable. These points can be named *neutrally stable*. A representation can be found in Figure 8.

2.4.4.3 Double non-null root

We have $\lambda_1 = \lambda_2$ and the characteristic polynomial is $P(\lambda) = (\lambda - \lambda_1)^2$. We have two possibilities:

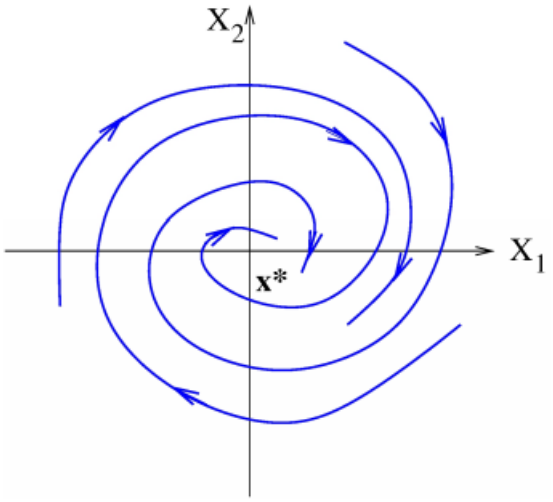

Figure 7: Stable spiral. Image from [9]

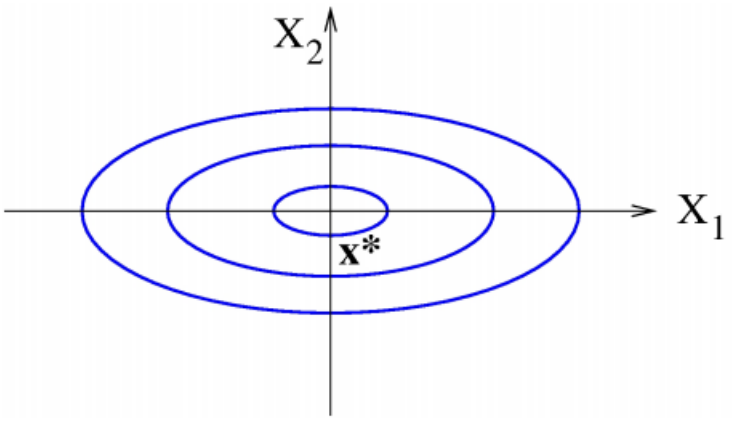

Figure 8: Center. Image from

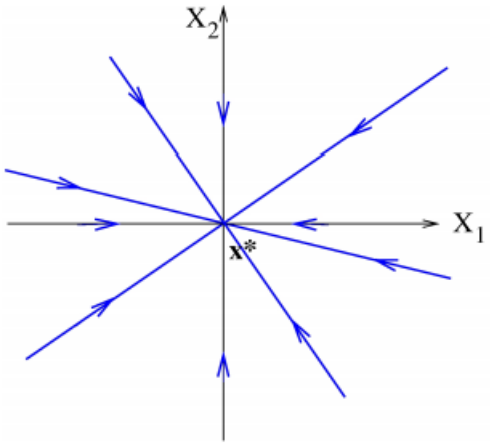

Figure 9: Stable star node. Image from [9]

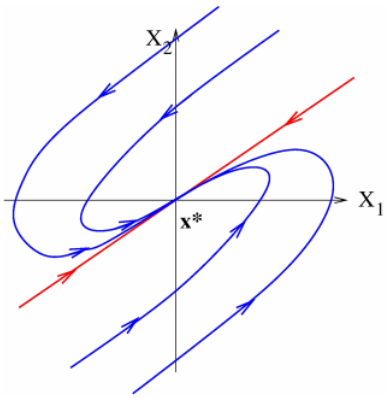

Figure 10: Stable degenerated node. Image from [9]

1. The matrix is diagonalizable. Then, the fixed point is a **star node**. It can be stable or unstable depending on wheter the sign of λ_1 is positive (then is unstable) or if it is negative (then is stable). In Figure 9 can be found a representation, where all lines going to the origin are trajectories; the representation for the unstable star node is the same with reversed arrows.

2. The matrix is no diagonalizable. Then, the matrix can be transformed to its Jordan form and the solutions are

$$\begin{aligned} y_1(t) &= (y_1^0 + y_2^0 t)e^{\lambda_1 t} \\ y_2(t) &= y_2^0 e^{\lambda_1 t} \end{aligned} \tag{2.4.15}$$

   The fixed point is then a **degenerated node**. Depending on the sign of λ_1, it is stable if it is negative or unstable otherwise. A stable degenerated node is represented in Figure 10, where the blue curves are examples of trajectories in the phase space. The representation of the unstable node is obtained by reversing the arrows.

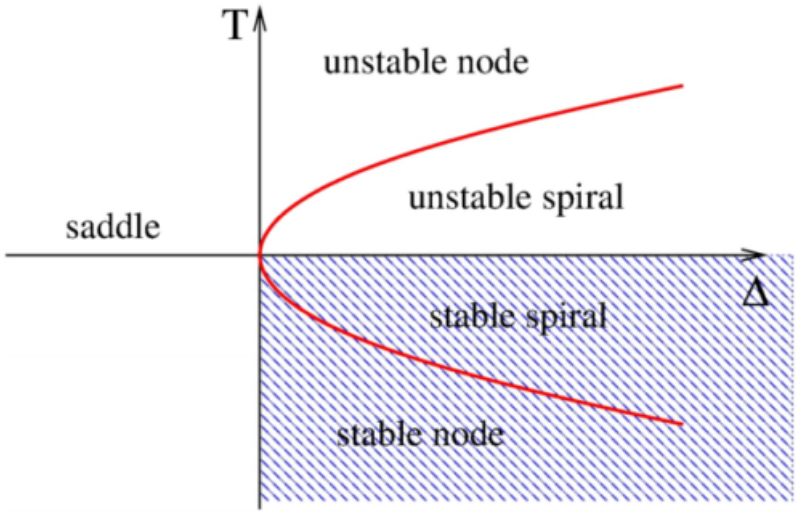

Figure 11: Summary for 2D. Image from [9]

2.4.4.4 Summary of the 2D case

In the two-dimensional case, the eigenvalues of the matrix can be deduced from the trace (T) and the determinant (Δ) of the matrix. As the characteristic polynomial of the Jacobian matrix is

$$P(\lambda) = \lambda^2 - T\lambda + \Delta \tag{2.4.16}$$

and its roots are given by

$$\begin{aligned} \lambda_\pm &= \frac{T}{2} \pm \sqrt{\frac{T^2}{4} - \Delta} \qquad when \frac{T^2}{4} > \Delta \\ \lambda_\pm &= \frac{T}{2} \pm i\sqrt{\Delta - \frac{T^2}{4}} \qquad when \frac{T^2}{4} < \Delta \end{aligned} \tag{2.4.17}$$

We can gather all the previous cases in the Figure 11, where the hatched part of the plane corresponds to the stable fixed points. In conclusion, in 2D, one fixed point is stable if T is negative and Δ is positive, where $T = Trace(Df(x^*))$ and $\Delta = Det(Df(x^*))$.

2.4.5 Higher dimensions Case

In the case of higher dimensions, the eigenvalues are still roots of the characteristic polynomial and it is necessary to determine the sign of the real part of all the eigenvalues, λ_i, to determine the stability of the fixed point. It has been said that if all eigenvalues verify $Re(\lambda_i) \neq 0$, the fixed point is called *hyperbolic*. The dynamics deduced from the linearization are an accurate representation of the true nonlinear dynamics if the fixed point is hyperbolic. These cases are *robust* because their dynamics is not modified by small perturbations of the model.
Hyperbolic fixed point or not, the general rule is [9]:

- If one (or more) eigenvalue has the **real part strictly positive**, the fixed point is **unstable**.

- If all eigenvalues have the **real part strictly negative**, then the fixed point is **stable**.
- If all the eigenvalues have the real part non-positive but at least one has null real part, the linearization of the system does not allow to deduce the dynamics around the fixed point, non-linear terms determine the stability of the system.

2.5 Linear and nonlinear maps

We have seen that the linear system $\dot{x} = Ax$ gives rise to the flow map $e^{tA} : \mathbb{R}^n \to \mathbb{R}^n$ when e^{tA} is an $n \times n$ matrix. Now, for fixed $t = \tau$ we consider $B = e^{\tau A}$, a constant matrix, and the difference equation

$$()x_{n+1} = Bx_n \tag{2.5.1}$$

(2.5.1) is the **discrete dynamical system** obtained from the flow of $\dot{x} = Ax$.
Similarly, the flow of a nonlinear system, $\phi_t(x)\big|_{t=\tau}$ gives rise to a nonlinear map $G(x)$ and the difference equation

$$x_{n+1} = G(x) \tag{2.5.2}$$

2.5.2 is the **discrete dynamical system** obtained from the flow of $\dot{x} = f(x)$. In this case, if $\phi_t(x)$ is smooth, then $G(x)$ is smooth map and has an smooth inverse, that is, it is a *diffeomorphism*.

A fixed point for discrete dynamical system is defined as

$$\begin{aligned} Bx^* &= x^* \qquad \textit{for linear maps} \\ G(x^*) &= x^* \qquad \textit{for nonlinear maps} \end{aligned} \tag{2.5.3}$$

in this case, $x_n = x^*$ for all n. An orbit of a map is a sequence of points $\{x_i\}_{i \geq -\infty}$ defined by the difference equations (2.5.1) and (2.5.2). In the case of linear maps, any initial point generates a unique orbit due to the fact that B has no zero eigenvalues. In both cases, if the maps are invertible, then its orbits exist forward and backward in time [12].
The stable, unstable and center spaces for linear maps are defined the same way as for linear vector fields:

- **Stable space** E^s is the span of the n_s generalized eigenvectors whose eigenvalues have modulus < 1. It is a contraction space.
- **Unstable space** E^u is the span of the n_u generalized eigenvectors whose eigenvalues have modules > 1. It is an expansion space.
- **Center space** E^c is the span of the n_c generalized eigenvectors whose eigenvalues have modulus $= 1$. It is a non transformation space.

If there are no multiple eigenvalues, then the contraction and the expansion are bounded by geometric series, that is, there exist constants $c > 0$, $\alpha < 1$ such that for $n \geq 0$

$$\begin{aligned} |x_n| &\leq c\alpha_n |x_0| \qquad \textit{if } x_0 \in E^s \\ |x_{-n}| &\leq c\alpha_n |x_0| \qquad \textit{if } x_0 \in E^s \end{aligned}$$

If multiple eigenvalues occur, then the contraction (or the expansion) need not to be exponential. However, an exponential bound can still be found if $|\lambda_i| < 1$ for all eigenvalues. In spite of problems caused by multiplicities, if B has no eigenvalues of unit modulus, the eigenvalues alone serve to determine the stability of the system. In this case, $x = 0$ is a **hyperbolic fixed point** and, in general, if x^* is a fixed point for G and $DG(x^*)$ has no eigenvalues of unit modulus, then x^* is called a hyperbolic fixed point. The linearization theorem of Hartman-Grobman and the invariant manifold results apply to maps just as for flows, and global stable and unstable manifolds are defined as for flows too, by taking unions of backward and forward iterates of the local manifolds.

It is important to remark that flows and maps differ crucially in that, while the orbit $\phi_t(p)$ of a flow is a curve in $\mathbb{R}^n$, the orbit $\{G^n(p)\}$ of a map is sequence of points. Thus, while the invariant manifolds of flows are composed of the unions of solution curves, those of maps are unions of discrete orbit points [12].

$G^n(p)$ means the nth iterate of p under G. Thus, if there is a cycle of k distinct points $p_j = G^j(p_0)$, for $j = 1 \div n$ and $G^k(p_0) = p_0$, we have a **periodic orbit** of period k. The stability of such an orbit is determined by the linearized map $DG^k(p_0)$ which by the chain rule is

$$DG^k(p_0) = DG(G^{k-1}(p_0))...DG(G(p_0))DG(p_0)$$

Stability of the linear map

The linear system (2.5.1) has the unique fixed point $x^* = 0$. The behaviour of the linear map is governed by the eigenvalues and eigenvectors of B. In general, the stability type of the fixed point $x = 0$ is determined by the magnitude of the eigenvalues of B. If $|\lambda_i| > 1$ for all eigenvalues we have a source; if $|\lambda_i| < 1$ for all eigenvalues we have a sink; and if $|\lambda_i| > 1$ for some eigenvalues and $|\lambda_i| < 1$ for the others, we have a saddle point. If $|\lambda_i| = 1$ for any eigenvalues then a norm is preserved in the directions v_i associated to those eigenvalues (unless they are multiple with nontrivial Jordan blocks). If an even number of eigenvalues have negative real parts, the map is orientation preserving while if an odd number have negative real parts it reverses orientation [12].

2.6 Asymptotic behaviour and structural stability

In this section, first we will define various limit sets which represent asymptotic behaviour of certain classes of solutions and then we will discuss the equivalence relations. Most of the definitions will be general, but our aim focus will concentrate on two-dimensional flows and maps.

2.6.1 Asymptotic behaviour

We define an **invariant set** S for a flow $\phi_t(x)$ or map G on $\mathbb{R}^n$ as a subset $S \subset \mathbb{R}^n$ such that

$$\phi_t(x) \in S \quad (\text{or } G(x) \in S) \qquad \text{for } x \in S \qquad \text{for all } t \in \mathbb{R} \tag{2.6.1}$$

Examples for stable and unstable manifolds would be a fixed point or a periodic orbit. However, the nonwandering set is the most important set to study the long-term behaviour. Fixed points and closed orbits represent the stationary or repeatable behaviour and a generalization of these sets is the nonwandering set. A point p is called **nonwandering for the flow** ϕ_t (respectively the map G) if for any neighbourhood U of p, there exists arbitrarily large t (respectively $n > 0$) such that $\phi_t(p) \cap U \neq \emptyset$ (respectively $G^n(U) \cap U \neq \emptyset$).

The **nonwandering set** Ω is set of all such points p. Thus, a nonwandering point lies on or near orbits which come back within a specified distance of themselves. Fixed points and periodic orbits are clearly nonwandering. However, not all invariant sets consist of nonwandering points [13].

Since the set of wandering points is open, Ω is closed and it must contain the closure of the set of fixed points and periodic orbits. Wandering points correspond to transient behaviour, while long-term or asymptotic behaviour corresponds to orbits of nonwandering points.
A point p is an ω-**limit point of** x if there are points $\phi_{t_1}(x)$, $\phi_{t_2}(x)$, ... on the orbit of x such that $\phi_{t_i}(x) \to p$ when $t_i \to \infty$. A point q is an α-**limit point** if such a sequence exists with $\phi_{t_i}(x) \to q$ when $t_i \to -\infty$. For maps G the t_i are integers. The α-limit and ω-limit sets, $\alpha(x)$ and $\omega(x)$, are the sets of α and ω limit points of x. A closed invariant set $A \subset \mathbb{R}^n$ is called **attracting set** if there is some neighbourhood U of A such that $\phi_t(x) \in U$ for $t \geq 0$ and $\phi_t(x) \to A$ as $t \to \infty$ for all $x \in U$. The set $\cup_{t \leq 0} \phi_t(U)$ is the **domain of attraction of** A (the stable manifold A). An attracting set ultimately captures all orbits starting in its domain of attraction. A **repelling set** is defined analogously, replacing t by $-t$. Domains of attraction of disjoint attracting sets are necessarily nonintersecting and separated by the stable manifolds of nonattracting sets.
In many problems we are able to find a "trapping region", a closed connected set $D \subset \mathbb{R}^n$ such that $\phi_t(D) \subset D$ for all $t > 0$. For this, it is sufficient to show that the vector field is directed everywhere inward the boundary of D. In this case, we can define the associated attracting set as $A = \bigcap_{t \geq 0} \phi_t(D)$. For maps, a closed set A is an attracting set if it has some neighbourhood U such that $G^n(U) \to A$ as $n \to \infty$. As in the case of flows, if D is a trapping region such that $G(U) \subset U$, then the associated attracting set is $A = \bigcap_{n \geq 0} G^n(D)$ [13].

We note that we have not specified that an attractor should be persistent with respect to small perturbations of the vector field or map, this will be dealt in the following subsection.

2.6.2 Structural stability

Given a map $F \in C^r(\mathbb{R}^n)$ we first need to specify what is meant by a perturbation G of F [14]. If $F \in C^r(\mathbb{R}^n)$ $r, k \in \mathbb{Z}^+$ $k \leq r$ and $\epsilon > 0$, then G is a C^k **perturbation of size** ϵ if there is a compact set $K \subset \mathbf{R}^n$ such that $F + G$ on the set $\mathbb{R}^n - K$ and for all $(i_1, ..., i_n)$ with $\sum_{m=1}^{n} i_k = i \leq k$ we have that

$$|\frac{\partial^i}{\partial x_1^{i_1} ... \partial x_n^{i_n}}(F - G)| < \epsilon$$

Note that F and G can be either maps or vector fields.

Given two maps F and G, we consider them C^k **equivalent**, with $k \leq r$, if there exists a C^k diffeomorphism h such that $h \circ F = G \circ h$. When $k = 0$ we call the equivalence **topological**. This definition implies that h takes and orbit $\{F^n(x)\}$ to an orbit $\{G^n(x)\}$, something that also applies when instead of working with maps we deal with vector fields. Two C^r vector fields f and g are said to be C^k equivalent if there exists a C^k diffeomorphism h which takes orbits $\phi_t^f(x)$ of f to orbits $\phi_t^g(x)$ of g preserving orientation but not necessarily parametrization by time. In general, the parametrization cannot be preserved because the periods of closed orbits in flows can differ, altough if it does preserve parametrization by time, then h is called a **conjugation**. The definition of equivalence implies that for any x and t_1 then there is a t_2 such that

$$h(\phi_{t1}^f(x)) = \phi_{t2}^g(h(x))$$

Now we can state the definition of structurally stable. A map $F \in C^r(\mathbb{R}^n)$ (or a vector field f) is

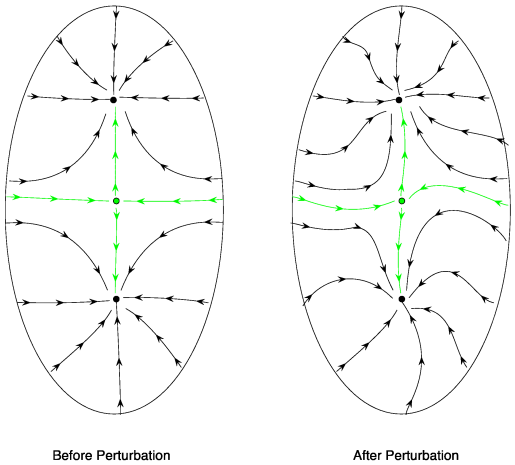

Figure 12: The phase portraits are homeomorphic. Image from [15]

structurally stable if there is an $\epsilon > 0$ such that all C^1 perturbations of F (or f) are topologically equivalent to F. It's important to remark that structural stability implies that the phase portrait of one system and its perturbation are homeomorphic as can be seen in Figure **??**. However, this equivalence does not distinguish among nodes, improper nodes and foci though it can distinguish between sinks, saddles and sources if the equivalence relation is type C^0.

Example 2.6.1. [14] Consider the two dimensional linear differential equation

$$\dot{x} = Ax \qquad x \in \mathbb{R}^2 \tag{2.6.2}$$

and the map

$$x \mapsto Bx \qquad x \in \mathbb{R}^2 \tag{2.6.3}$$

Suppose that A has no eigenvalues with zero real part and that B has no eigenvalues of unit modulus. We want to see that if these conditions hold, then both systems are structurally stable.

Consider a small perturbation of (2.6.2) such as follows:

$$\dot{x} = Ax + \epsilon f(x)$$

where $f(x)$ has support in the same compact set. Since A is invertible, we can use the Implicit Function Theorem and say that the equation

$$Ax + \epsilon f(x) = 0$$

has a unique solution $x^* = 0 + O(\epsilon)$ near $x = 0$ for sufficiently small ϵ. Moreover, since the matrix of the linearized system

$$\dot{\zeta} = [A + \epsilon Df(\dot{x})]\zeta$$

has eigenvalues which depend continuously on ϵ, no eigenvalues can cross the imaginary axis if it remains small respect to the magnitude of the real parts of the eigenvalues of A. Thus, the perturbed system has a unique fixed point with eigenspaces and invariant manifolds of the same dimensions as those of the initial system, and which are ϵ-close locally in position and slope to the unperturbed manifolds.

Similar observations apply to the discrete system and a corresponding small perturbation. However, in both cases the problem lays on finding a homeomorphism which takes orbits of the linear system to those of the perturbed, nonlinear, one. In the particular case of discrete systems, the goal is to prove that such homeomorphism makes the diagram in Figure 13 commute:

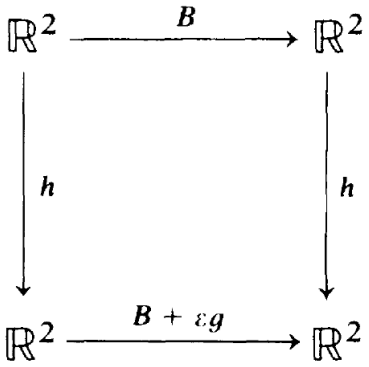

Figure 13: Diagram to be commutative by the existence of h. Image from [14]

An important note in order to particularise structurally stable systems is that a vector field (or a map) that has a non-hyperbolic fixed point cannot be structurally stable. That is because if the linearized matrix is noninvertible, a small perturbation can remove it; alternatively, if the matrix has only imaginary eigenvalues, then the small perturbation can turn the point into a hyperbolic sink, a saddle or a source. Same argument holds for periodic orbits, which leads us to state an important conclusion:

Theorem 2.6.2. *[14] In order to be structurally stable, a system needs to have all fixed points and closed orbits hyperbolic. However, this condition alone does not guarantee structural stability.*

To summarize, we say that a system is structurally stable if any sufficiently close system has the same qualitative behaviour. However, it can be extremely complex to determine since it is not a generic property, that is, we can find structurally unstable systems which remain unstable under small perturbations. It is also important to note that the definition is relative to the class of systems considered, and that we have used C^1 ϵ perturbations by C^r vector fields on $\mathbb{R}^n$.

2.7 Periodic Orbits

2.7.1 Periodic Orbits

A periodic orbit is a special type of solution which repeats itself in time. Formally, given a dynamical system

$$\dot{x} = f(x) \qquad x \in \mathbb{R}^n \tag{2.7.1}$$

a non-constant solution $x(t)$ is periodic if there exists a constant $T > 0$ such that $x(t) = x(T + t)\ \forall t \in \mathbb{R}$. The image of the periodicity interval $[0, T]$ under $x(t)$ in the state space $\mathbb{R}^{\ltimes}$ is called the **periodic orbit**.

In arbitrary dimensions, there are several techniques to prove analytically that a periodic orbit exists though the most important are only useful for a planar vector field.

For any dimension, we will just talk about gradient systems.

A **gradient system** is a dynamical system of the form: $\dot{x} = -\nabla V(x)$ for a given function $V(x) \in \mathbb{R}^n$. Only with this assumption, we can state

Theorem 2.7.1. *[16] Gradient systems cannot have periodic orbits.*

Proof. Suppose that $\gamma : t \to x(t)$ is a periodic orbit of the gradient system $\dot{x} = -\nabla V(x)$ with period T. Then

$$0 = V(x(T)) - V(x(0)) = \int_0^T \frac{dV}{dt} dt = \int_0^T \nabla V \cdot \dot{x} dt = -\int_0^T ||\dot{x}||^2 dt < 0$$

Second equality holds by Barrow's Rule, the third one by the chain rule and the last one because it is a gradient system. □

A similar idea is behind the next result:

Theorem 2.7.2. *[17] If a dynamical system $\dot{x} = V(x)$ has a Lyapuno-like function $V(x)$, ie, $V(x)$ is monotonically decreasing along trajectories, there cannot be any periodic orbit.*

The proof is analogous to the previous one.

The following results are specific for the plane, which will be the focus later on.

Two-Dimensional Flows

The fact that solution curves are one dimensional, make the range of solution types on the plane rather limited. Systems on two manifolds other than $\mathbb{R}^2$ one more complicated and are beyond the purpose of this text.

Hence, suppose we are given

$$\begin{aligned} \dot{x} &= f(x, y) \\ \dot{y} &= g(x, y) \end{aligned} \qquad (x, y) \in U \subset \mathbb{R}^2$$

with f and g sufficiently smooth. The first step to study the system is to seek fixed points, that is, find solutions to $f(x, y) = 0 = g(x, y)$.

Linearizing the system at (x^*, y^*) with $\alpha = (\alpha_1, \alpha_2)$ and $F = (f, g)$, we get

$$\begin{pmatrix} \dot{\alpha}_1 \\ \dot{\alpha}_2 \end{pmatrix} = \begin{pmatrix} \frac{\delta f}{\delta x}(x^*, y^*) & \frac{\delta f}{\delta y}(x^*, y^*) \\ \frac{\delta g}{\delta x}(x^*, y^*) & \frac{\delta g}{\delta y}(x^*, y^*) \end{pmatrix} \begin{pmatrix} \alpha_1 \\ \alpha_2 \end{pmatrix} \leftrightarrow \dot{\alpha} = DF(x^*, y^*)\alpha$$

If the eigenvalues of the matrix $DF(x^*, y^*)$ have non-zero real parts, then the solution $\alpha(t) = e^{tDF(x^*, y^*)}\alpha(0)$ not only yields local asymptotic behaviour, but, by Hartman's theorem and the stable manifold theorem also provides the local topological structure of the phase portrait.

After locating the fixed points and studying their stability we want to ascertain whether it has any periodic orbits. The following theorem is a good strategy to explore that.

Theorem 2.7.3. Dulac's criterion *[16]. Let R be a simply connected region in $\mathbb{R}^2$ and a dynamical system given by*

$$\begin{aligned} \dot{x} &= f(x, y) \\ \dot{y} &= g(x, y) \end{aligned}$$

with f and $g \in C^1$ in $\mathbb{R}$. Suppose that there exists $h(x, y) \in C^1(\mathbb{R})$ so that $\nabla \cdot h(fe_x + ge_y)$ has a finite sign in $\mathbb{R}$ (it does not change). Then the dynamical system cannot have any periodic orbits in R.

Proof. Let's suppose that the dynamical system has a periodic orbit γ contained in R and let be A the area enclosed by it. Since R is simply connected, A lies entirely in R. By Green's theorem:

$$\iint_A \nabla \cdot h(fe_x + ge_y)\, dx\, dy = \oint_\gamma h(fe_x + ge_y) \cdot n\, dl$$

where n is the outward normal to γ.

The left side of the expression is different from zero because of the sign-definiteness. However, the right side is zero because $(fe_x + ge_y)$ is tangent to γ. Therefore we have a contradiction and therefore it does not exist $\gamma \in \mathbb{R}$. □

Corollary 2.7.4. Bendixson's criterion. *If on a simply connected region $R \subseteq \mathbb{R}^2$ the expression $\frac{\partial f}{\partial x} + \frac{\partial g}{\partial y}$ is not identically zero and does not change sign, then the dynamical system has no closed orbits lying entirely in D.*

In addition, to fixed points and closed orbits, for planar flows all the non wondering possible sets fall into three classes:

- fixed points
- closed orbits
- the unions of fixed points and the trajectories connecting them

The latter are named **heteroclinic orbits** when they connect distinct points and the **homoclinic orbits** when they connect a point to itself. The closed paths formed of heteroclinic orbits are called **homoclinic cycles** and the fixed points contained in them must all be saddle points (if they are hyperbolic) because sinks and sources have wondering points in their neighborhoods [18].

Note that the homoclinic orbit is not a periodic orbit because it takes an infinite amount of time to reach the fixed point. Homoclinic orbits and heteroclinic cycles (several heteroclinic trajectories forming a loop) can act as attractors (or repellers) for other trajectories or as divisors between regions of separated dynamics. It is also possible that isolated closed orbits, not containing fixed points, act as attractors/repellers. Such orbits are called limits cycles.

Thus, in two-dimensional flows the global structures of solution curves are generally far richer than those of one-dimensional systems, in which periodic orbits cannot occur and the fixed points are ordered and necessary connected to their immediate neighbours and only to them.

2.7.2 Index Theory

Another useful approach to figure out whether a planar system has periodic orbits or not, is index theory. First we consider the general idea of the index: given a planar flow, we draw a simple closed curve C not passing through any equilibrium points and consider the orientation of the vector field at a points $p = (x, y) \in C$. Letting p traverse C counter clockwise, the vector $(f(x, y), g(x, y))$ rotates continuously and, when it returns to the original position, it must have rotated through an angle $2\pi k$ for some $k \in \mathbb{Z}$. The integer k is the **index of the closed curve** C and it can be shown that it is independent of the form of C in the sense that it is determined solely by the character of the fixed points inside C [18].

Intuitively, one can consider the index of a curve as the number of times the vector field rotates in counter clockwise fashion when traversing the curve once.

The index satisfies a number of elementary topological properties [16]

1. when C and C' are two closed curves that can be continuously deformed into each other (without moving the curve over one of the fixed points of the vector field) then $I_C = I_{C'}$.
2. If C does not enclose any fixed points, then $I_C = 0$.
3. The index is unchanged when the direction of the vector field is reversed.
4. If C is a trajectory of the system, then $I_C = 1$.

The **index of a fixed point** I_{x^*} is defined as the I_C of the curve that endorses only x^* and is independent of the choice of curve.

An important lemma related is the following:

Lemma 2.7.5. *[16] If a closed curve C encloses n fixed points $x_1^*, ..., x_n^*$ then*

$$I_C = I_{x*_1} + ... + I_{x*_n}$$

Lemma 2.7.6. *[18] The following are true:*

1. *The index of a sing, a source of a center is $+1$.*
2. *The index of a hyperbolic saddle point is -1.*
3. *The index of a closed orbit is $+1$*
4. *Inside any closed orbit C there must be at least one fixed point. If all the fixed points within C are hyperbolic, then there must be one odd number $(2n+1)$ of which n are saddles and $n+1$ either sinks or sources.*

These can be used to rule out the existence of closed orbits because we have seen that if the vector field has no fixed points there cannot be any periodic orbits. Furthermore, if the system has only one fixed point, it cannot be hyperbolic, it has to be a sink, a source or a center.

2.7.3 Stability

We have seen ways to figure out whether there are, or not, periodic solutions for a given dynamical system. Now we wonder about the stability of those solutions. First, it is important to note that the definition of stability used for fixed points no longer applies. This discrepancy between stabilities is not avoidable as we will see now.

Consider an autonomous system

$$\begin{aligned} \dot{x} &= f(x) \\ x(0) &= p \end{aligned} \tag{2.7.2}$$

that has a periodic solution $\varphi(t)$ with period T. The linearized system in the neighbourhood of the T-periodic solution is given by

$$\dot{x} = A(t)x \qquad , \qquad A(t+T) = A(t) \qquad t \in \mathbb{R} \tag{2.7.3}$$

with $A(t) = f_x(\varphi(t))$. If $\phi(t)$ is the fundamental matrix solution of this equation [4] reducing to Id when $t = 0$, then the Floquet multiplier matrix [5] is $M = \phi(T)$.

If all eigenvalues of M were less than one in modulus, we could easily infer asymptotic stability like the one that works for fixed points. However, the following statement is always true:

Proposition 2.7.7. *[19] For an autonomous system, M has always at least one eigenvalue equal to one.*

Proof. Differentiating the equation $\frac{d\psi}{dt} = f(\psi(t))$ with respect to t we get $\frac{d}{dt} = A(t)\frac{d\psi}{dt}$, ie, $\xi(t) = \frac{\delta\psi}{\delta t}$ is a solution to the linearized system (2.7.3). Therefore, it has a representation $\xi(t) = \phi(t) \cdot C$ for $C \in \mathbb{R}^n$ constant, and we can assume that $\phi(0) = I$ so $C = \xi(0)$.

Since this solution is T-periodic, evaluation at $t = T$ shows that $Mc = C$, that is, the Floquet matrix M has 1 as eigenvalue, with a corresponding eigenvector $C = \xi(0) = \dot{\psi}(0) = f(\psi(0))$ which is tangent to the orbit at the point $\psi(0)$. □

Let the T-periodic solution $\psi(t)$ determine the orbit γ, so

$$\gamma = \{x | x = \psi(t) \text{ for some } t\}$$

Given some choice of norm $||.||$, the distance between two points is $d(x, y) = ||x - y||$ and the distance from a point to a set S is:

$$d(x, S) = \inf_{y \in S} d(x, y)$$

Definition 2.7.8. The periodic solution ψ with orbit δ is orbitally **stable** if given $\xi > 0$ there exists a $\delta > 0$ such that $d(\phi(t, x), \gamma) < \xi \ \forall t > 0$ and $\forall x$ such that $d(x, y) < \delta$. It is orbitally asymptotically stable if it is orbitally stable and $d(\phi(t, x), \gamma) \to 0$ as $t \to \infty$.

There exist two main ways to determine the stability of a periodic orbit: Floquet Theory (some of whose concepts have already been used in this section) or Poincaré Maps (which involve the use of maps, seen former in this chapter).

2.8 Poincaré Maps

2.8.1 Floquet Theory

An analytical approach to determine the stability of a periodic orbit is based on the Floquet theorem. Previous to that, we need to consider some theory about linear systems with periodic coefficients. It is important to remark that not all solutions of a periodic system have to be periodic.

Stability of a periodic solution x^* manifests itself in the way neighboring trajectories behave. A trajectory that stands from the perturbed initial vector $y = x_0^* + \delta x_0^*$ will, after one period T, be displaced by

$$\delta x^*(T) = \phi(T; x_0^* + \delta x_0^*) - \phi(T; x_0^*)$$

To first order, this displacement is given by:

$$\delta x^*(T) = \frac{\partial \phi(T; x_0^*)}{\partial x_0} \cdot \delta x_0^*$$

[4] $\phi(t)$ is a matrix-valued function whose columns are linearly independents solutions of the system
[5] will be defined later on

It is clear that the matrix $\frac{\partial\phi(T;x_0^*)}{\partial x_0}$ determines whether initial perturbations from the periodic orbit decay or grow. This matrix is called the **monodromy matrix**. Some properties of the flow ϕ are useful to find another representation of the matrix. Since ϕ satisfies the autonomous equations the monodromy matrix is the same as $\Phi(T)$ where $\Phi(t)$ is the fundamental matrix solution for the linearized equation about the periodic orbit $x^*(t)$:

$$\dot{\Phi} = Df(x^*)\Phi \qquad \text{with } \Phi(0) = Id$$

So we have that the monodromy matrix of a periodic solution with a T period and initial value x_0^* is [20]:

$$\Phi(T) = \frac{\partial\phi(T;x_0^*)}{\partial x_0}$$

Now, we need to define the logarithm of a non-singular matrix. This definition is based on the series expansion about the origin of the complex function $ln(1+z)$.

Lemma 2.8.1. *[19] Lec C be a constant, non singular matrix (real or complex). There exists a matrix D, called the logarithm of C, such that $e^D = C$.*

Proof of this is seen with the Jordan form of C and since the details are not relevant for this text, it will be skipped.

As with ordinary logarithm in the complex plane, D is not uniquely defined. In general, even if C is real, D will be complex. However, it is possible to show that if C is real, then C^2 has a real logarithm matrix.

We are considering the system $\dot{x} = A(t)x$ with $A(t+T) = A(t)$ and we can state the following about it:

Theorem 2.8.2. Floquet's Theorem *[19]: Let A be continuous and T-periodic. Then if Φ is any fundamental matrix solution of the system, there exists a matrix P defined where A is, and periodic there with period T and a constant matrix Q such that*

$$\Phi(t) = P(t)e^{Qt}$$

Proof. Let $\Psi(t) = \Phi(T+t)$. Then $\Psi(t)$ is also a fundamental matrix solution to the system. It is clear (and easy to see) that there exists a non-singular, constant matrix M such that $\phi(T+t) = \phi(t)M$. The matrix M is called **Floquet multiplier matrix**. Since M is non-singular, we can find Q such that $e^{TQ} = M$ with T, the period. Now consider the matrix $P(t)$ defined $\forall t$ by the formula

$$P(t) = \Phi(t)e^{-Qt}$$

It only remains to see that $P(t)$ is periodic with period T:

$$P(T+t) = \phi(t+T)e^{-Q(t+T)} = \phi(t)Me^{-QT}e^{-Qt} = \phi(t)e^{-Qt} = P(t)$$

□

Some remarks need to be done about this theorem:

1. The theorem does not require that T is the least period of A.
2. If the fundamental matrix Φ is chosen so that it reduces to Id at $t = 0$, then $M = \Phi(T)$.
3. Suppose $A(t)$ is real. The Floquet multiplier matrix M can then also be chosen real, but the matrices P and Q of the theorem will need to be complex in general.

Stability of periodic orbits

Since $\Phi(0) = Id$ we have $\Phi(T) = e^{QT}$ and the behaviour of solutions in the neighbourhood of $x^*(t)$ is determined by the eigenvalues of the constant matrix e^{QT}. These eigenvalues $\rho_1, ..., \rho_n$ are called the Floquet (or characteristic) multipliers and each complex number λ_j such that $\rho_j = e^{\lambda_j T}$ is called the **characteristic exponent** of the closed orbit.

The multiplier associated with perturbations along $x^*(t)$ is always unity; let this be ρ_n. The moduli of the remaining $(n-1)$ determine the stability of $x^*(t)$. Although the matrix Q is not determined uniquely by the solutions of the linearized system, the eigenvalues of e^{QT} are uniquely determined. However, to compute this eigenvalues we still need a representation of e^{QT} and this can only be obtained by generating a set of n linearly independent solutions to form $\Phi(t)$. This is generally difficult analytically [20].

About the behaviour of solutions related to the remaining values of the module of the eigenvalues there are three options:

- if all the remaining eigenvalues have their module strictly less than one, then the orbit is stable.
- if at least one of the remaining eigenvalues has its module strictly greater than one, then the periodic orbit is unstable.
- if all the eigenvalues have modulus equal or minus to one and at least one is strictly equal to one, then linear stability analysis is not conclusive.

2.8.2 Poincaré maps

A more geometrical view to discuss the stability of closed orbits are Poincaré Map, which seek a geometric depiction of the trajectories in a lower dimensional space.

Let γ be a periodic orbit of a flow ϕ_t in $\mathbb{R}^n$ arising from a non-linear vector field $f(x)$. We take a local cross section $\Sigma \subset \mathbb{R}^n$ of dimension $(n-1)$. The hypersurface Σ need not to be planar but must be chosen so that the flow is everywhere transverse to it. This means $f(x) \cdot n(x) \neq 0 \ \forall x \in \Sigma$ where $n(x)$ is the unit normal to Σ at x. We denote the point where γ intersects Σ by p and let $U \subseteq \Sigma$ be some neighbourhood of p. [6]

Definition 2.8.3. The first return or Poincaré map $P : U \to \Sigma$ is defined for a point $q \in U$ by $P(q) = \phi_\tau$ with $\tau = \tau(q)$ is the time taken for the orbit $\phi_t(q)$ based at q to first return to Σ.

Note that usually τ depends on q and need not to be equal to $T = T(p)$ the period of γ. However, $\tau \to T$ as $q \to p$.

It is obvious that p is a fixed point for the map P and it reflects the stability of γ for the flow ϕ_t. In particular, if p is hyperbolic and $DP(p)$ the linearized map, it has n_s eigenvalues with modulus less than one and n_u with modulus greater than one; and $n_s + n_u = n - 1$. Moreover, $dim(W^s(p)) = n_s$ and $din(W^u(p)) = n_u$ for the map [21]. Since the orbits of P lying in W^s and W^u are formed by intersections of orbits of ϕ_t with Σ, the dimensions of $W^s(\gamma)$ and $W^u(\gamma)$ are each one greater than those for the map. This figure can easily be seen in the sketches of Figure 14.

[6] If there are multiple intersections of γ with Σ, then Σ can be shrinked until there is only one left.

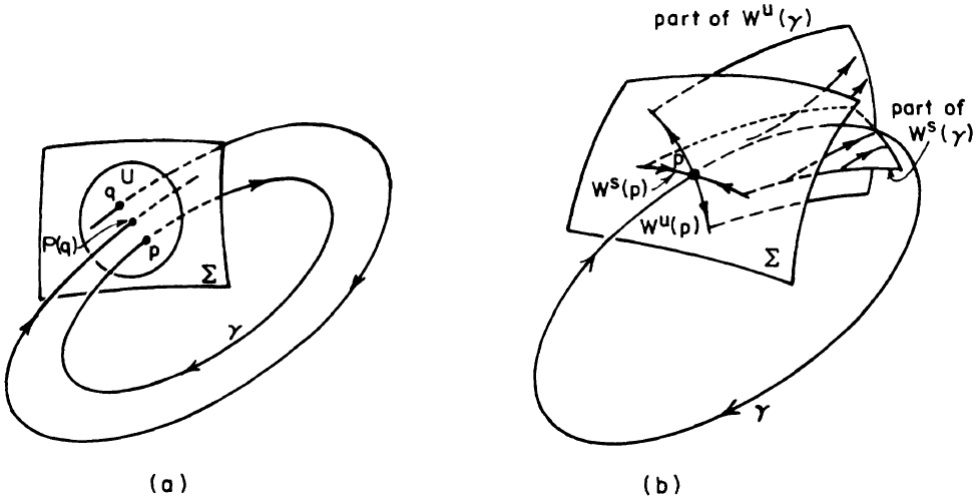

Figure 14: The Poincaré map. (a) The cross section and the map; (b) a closed orbit. Image from [21]

Poincaré maps and orbit stability

Let $x^*(t) = x^*(t+T)$ be a solution lying on the closed orbit γ based at $x(0) = p \in \Sigma$. Linearizing about γ we get:

$$\dot{\xi} = DF(x^*(t))\xi \tag{2.8.1}$$

with $DF(x^*(t))$ a $n \times nT$-periodic matrix. We have seen that if $X(t)$ is a fundamental solution matrix of that system then it can be written as:

$$X(t) = Z(t)e^{tR} \; ; \; Z(t) = Z(t+T)$$

with X,Z and R $n \times n$ matrices. Furthermore, if we choose $X(0) = Z(0) = Id$ then $X(T) = e^{TR}$ and the behaviour of solutions in the neighbourhood of γ is determined by the eigenvalues of e^{TR} (this is essentially Floquet theory). Choosing the basis appropriately so that the last column of e^{TR} is $(0, ..., 0, 1)^T$, the matrix $DP(p)$ of the linearized Poincaré map is simply the $(n-1) \times (n-1)$ matrix obtained by deleting the n-th row and column of e^{TR}. Thus, the first $n-1$ Floquet multipliers $\lambda_1, ..., \lambda_{n-1}$ are the eigenvalues of the Poincaré map.

Although R is not uniquely determined by the solutions of (2.8.1) the eigenvalues of e^{TR} are. However, to compute these eigenvalues it is still necessary a representation of e^{TR} and this can only be obtained by actually generating a set of n linearly independent solutions to form $X(t)$. Usually, this is a difficult task and requires perturbation methods or the use of special functions.

Periodic forced oscillations

[21] An alternative way in which a flow gives rise to a map is in non-autonomous are periodically forced oscillations.

Consider a system

$$\dot{x} = f(x, t) \qquad (x, t) \in \mathbb{R}^n \times \mathbb{R}$$

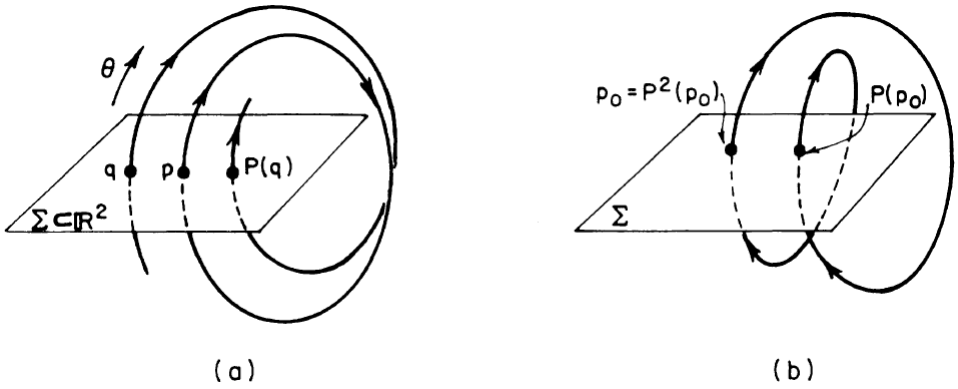

Figure 15: he Poincaré map for forced oscillations. (a) A periodic orbit of period T and the fixed point p = P(p); (b) a subharmonic of period 2T. Image from [21]

where $f(,t) = f(,t+T)$ is periodic of period T in t. The system can be rewritten as:

$$\begin{matrix} \dot{x} = f(x,\theta) \\ \dot{\theta} = 1 \end{matrix} \quad (x,\theta) \in \mathbb{R}^n \times S^1 \tag{2.8.2}$$

The phase space is the manifold $\mathbb{R}^n \times S^1$, where the circular component $S^1 = \mathbb{R}(modT)$ reflects the periodicity of the vector field f in θ. For this problem we can define a global cross section:

$$\{\Sigma = (x,\theta) \in \mathbb{R}^n \times S^1 | \theta = \theta_0\}$$

Since all solutions cross Σ transversely, the Poincaré Map $P : \Sigma \to \Sigma$, if defined globally, is given by:

$$P(x_0) = \pi \circ \phi_T(x_0, \theta_0)$$

where $\theta_t : \mathbb{R}^n \times S^1$ is the flow of (2.8.2) and π denotes the projection onto the first factor. Note that the time T is the same for all $x \in \Sigma$. That is, $P(x_0) = x(x_0, T + \theta_0)$ where $x(x_0, t)$ is the solution of (2.8.2) based at $x(x_0, \theta_0) = x_0$. The Poincaré map for forced oscillations is illustrated in Figure 15.

The Poincaré map can also be obtained as a discrete dynamical system arising from the flow $\psi(x,t)$ of the time-dependent vector field of $\dot{x} = f(x,t)$. Since f is $T - periodic$, we have that $\psi(x, nT) \equiv \psi_T^n(x)$ and the map $P(x_0) = \psi_T(x_0)$ is an example of a discrete dynamical system.

It is important to note that P may not be globally defined but is usually defines for some subset $U \subset \Sigma$ such that $P : U \to \Sigma$.

Again, it is clear that a fixed point p of P corresponds to a periodic orbit of period T for the flow. Thus, a periodic point of period $k > 1$ ($P^k(p) = P(P(P(...(p)...))) = p$ but $P^J(p) \neq p$ for$j = 1 \div (k-1)$) corresponds to a subharmonic of period kT and such periodic points must always come in sets of k : $p_0, ..., p_{k-1}$ such that $P(p_i) = p_{i+1}$, $i = 0 \div (k-2)$ and $p_0 = P(p_{k-1})$. This also applies for the autonomous case.

Poincaré Sections

[22] We have seen that a Poincaré Map has only one intersection between a periodic orbit γ and a hypersurface Σ. We consider a **Poincaré section** the points of intersection when Σ has not been shrinked.

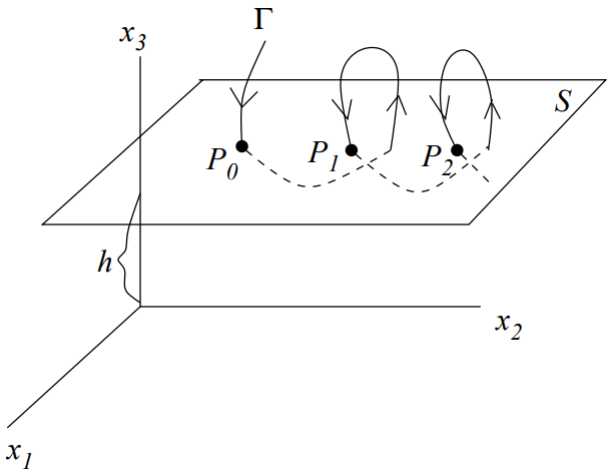

Figure 16: Poincaré section of a 3D-fow. Image from [22]

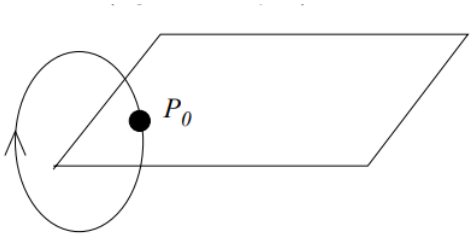

Figure 17: Poincaré map for a periodic orbit. Image from [22]

For example, with a 3D flow, instead of studying it directly we can consider its intersection with a plane, as can be seen in Figure 16.

In this case, the points of intersection correspond with $\{\dot{x_3} < 0 | x_3 \in \Gamma\}$ and the height h is chosen so that Γ continually crosses Σ. The Poincaré section P is $P = \{P_0, P_1, P_2\}$ and is a continuous mapping T of the plane Σ into itself: $P_{k+1} = T(P_k) = T(T(P_{k-1}))$.... Thus, we have that every point determines the next one.

The main purpose of the Poincaré section is to reduce a continuous flow to a discrete-time mapping though the time interval from point to point does not have to be constant. It is useful because some geometric properties of the flow are conserved in the Poincaré section, such as dissipation or attraction, reducing the study of the stability of a periodic orbit to the sudy of a fixed point, as we have already seen.

We classify three types of flow:

- **Periodic**: the flow is a closed orbit.

  P_0 is a fixed point of the Poincaré Map: $P_0 = T(P_0) = T^2(P_0)$... as can be seen in Figre 17.

  We can analyze the stability: to first order a Poincaré Map can be described by a matrix M [7] defined in a neighbourhood of P_0:

$$M_{ij} = \left.\frac{\partial T_i}{\partial x_j}\right|_{P_0}$$

[7] M is the Floquet Matrix

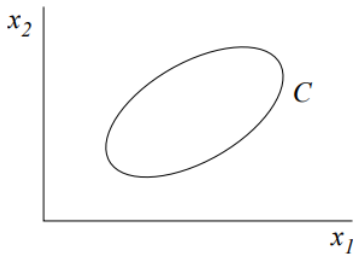

Figure 18: Poincaré section of a quasiperiodic flow with irrational ratio. Image from [22]

M describes how a point $P_0 + \delta$ moves after one intersection of the Poincaré Map. The Taylor expansion about the fixed point is:

$$T_i(P_0 + \delta) \simeq T_i(P_0) + \left.\frac{\partial T_i}{\partial x_1}\right|_{P_0} \cdot \delta_1 + \left.\frac{\partial T_i}{\partial x_2}\right|_{P_0} \cdot \delta_2 \qquad i = 1, 2$$

and, knowing that $T(P_0) = P_0$, we have

$$T(P_0 + \delta) \simeq P_0 + M\delta$$

Therefore,

$$T(T(P_0 + \delta)) \simeq T(P_0 + M\delta) \simeq T(P_0) + M^2\delta \simeq P_0 + M^2\delta$$

By induction it is straight forward to see that

$$T^m(P_0 + \delta) = P_0 + M^m\delta$$

holds and thus, the stability depends on the properties of M. We can assume, if not directly, we can make the necessary transformations to make the following hold, that δ is an eigenvector of M. Then,

$$M^m\delta = \lambda^m\delta$$

where λ is the corresponding eigenvalue. Therefore, a periodic map is unstable if one of the eigenvalues of M crosses the unit in the complex plane.

- **Quasiperiodic flows**: consider a 3D flow with two fundamental frequencies: f_1 and f_2. The flow is like a torus. The points of intersection of the flow with Σ are a closed curve C. The form of the resulting Poincaré section depends on the ratio $\frac{f_1}{f_2}$:
  - Irrational $\frac{f_1}{f_2}$: the closed curve C appears continuous, as can be seen in Figure 18.
    The trajectory on the torus T^2 never repeats itself exactly. The curve is not traversed continuously but $T(C) =$ 'finite shift along' C.
  - Rational $\frac{f_1}{f_2}$: there are finite number of intersections (points) along C and the trajectory repeats itself after n_1 revolutions and n_2 rotations. The Poincaré section is periodic with period

    $$\frac{n_1}{f_1} = \frac{n_2}{f_2} \tag{2.8.3}$$

    where n_1 is the number of points contained, that is, $P_i = T^{n_1}(P_i)$. A representation can be seen in Figure 19.

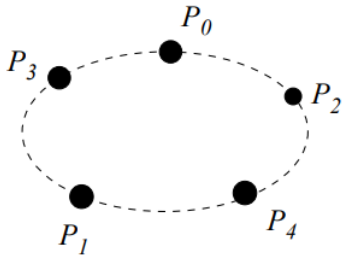

Figure 19: Poincaré section of a quasiperiodic flow with rational ratio. Image from [22]

- **Aperiodic flows**: such flows may no longer lie on reasonable simple curves and can even be point clouds. In these cases, it becomes useful to define a coordinate x that falls roughly along this curve and study the iterates. This is what we have already seen, first return maps. Such maps are of the form

$$x_{k+1} = f(x_k) \tag{2.8.4}$$

where iterations converge to $x = x^*$ which is where the identity map $x_{k+1} = x_k$ intersects $f(x)$. Thus, x^* is a fixed point of f and its stability is determined by $|f'(x^*)|$.

Summary

Consider an n-dimensional continuous vector field and an $(n-1)$ dimensional surface Σ chosen so that the flow is always transverse to Σ. Let the successive intersections in a given direction of the solution $x(t)$ with Σ be denoted by x_i. The Poincaré Map $x_{i+1} = g(x_i)$ determines the $(i+1)$-th intersection of the trajectory with Σ from the i-th intersection.

A periodic orbit of an autonomous vector field corresponds to a fixed point x_j of this Poincaré Map as $g(x_j) = x_j$. The stability of those orbits correspond to the stability of the fixed point of the map, that can be easily described considering its linearization:

$$\xi_{i+1} = Dg(x_j)\xi_i$$

If all eigenvalues of Dg have modulus less than unity, then x_j (and the corresponding periodic orbit) is asymptotically stable. If any eigenvalues of Dg have modulus greater than unity, then x_j (and the corresponding periodic orbit) is unstable. The stability properties of a periodic orbit are independent of the cross section Σ. If x_j is stable then it is an attractor of the Poincaré Map and the corresponding periodic orbit is an attractor of the vector field.

Since the definition of the Poincaré Map relies on knowledge of the flow of the differential equation, Poincaré maps cannot be computed unless general solutions of these equations are available. However, perturbation and averaging methods can be used to approximate the map in appropriate cases.

2.9 Limit Cycles

2.9.1 Limit cycles

We consider a two-dimensional dynamical system such:

$$\dot{x}(t) = f(x(t)) \qquad f : \mathbb{R}^n \to \mathbb{R}^n \tag{2.9.1}$$

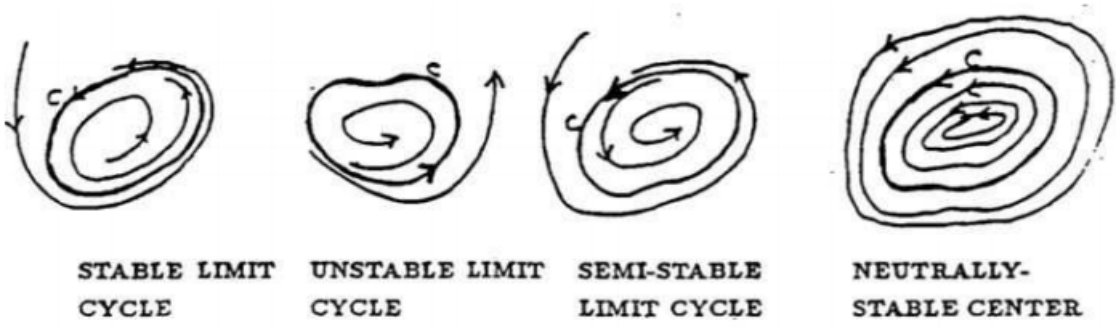

Figure 20: Type of limit cicles. Image from [23]

With f smooth function.

We have seen that a trajectory of the system is a function $x(t)$ with values in $\mathbb{R}^n$ which satisfies the differential equation. Such trajectory is called closed (or periodic) if it is not constant but returns to its starting point. An orbit is the image of a trajectory and a closed orbit is the image of a closed trajectory. Thus, a limit cycle is a cycle which is the limit set of some trajectory.

More intuitively, consider a dynamical system in $\mathbb{R}^2$ that has a trajectory which traces out a closed curve C. If this happens, the solution $x(t) = (x(t), y(t))$ will be geometrically realized by a point which goes round and round C with a certain period T. Thus, if there is such a closed curve, the nearby trajectories must behave something like C. The possibilities are (Figure 20):

- **Stable limit cycle**: the trajectories spiral in toward C.
- **Unstable limit cycle**: the trajectories spiral away from C.
- **Semi-stable limit cycle**: the trajectories both spiral towards and away from the curve C.

A last possibility for the behaviour of the trajectories around a closed curve C is that they also are closed curves. Then the curve C is not a limit cycle but a neutrally stable center, since it does not fit the idea of a limit cycle being where trajectories end up.

The main tool used to show that a planar dynamical system has stable limit cycle is the Poincaré-Bendixson theorem.

2.9.2 Poincaré-Bendixson theorem

Before stating the theorem, some fundamental concepts need to be list. Let $\dot{x}(t) = V(x)$ be a dynamical system and consider a trajectory $\gamma : t \to x(t)$. We have defined a positive limit point as a point for which exists a sequence $\{t_i\}_{i\geq 1}$ such that $n \to \infty$ $\lim_{n\to\infty} x(t_n) = a$, and it is been defined the $\omega - limit$ set as the set of all the positive limit points of that trajectory. The importance of the w-limit set lies in the fact that trajectories in a bounded region of the plane will spiral inward to $\omega - limit$ set. The following theorem is a necessary previa for our purpose.

Theorem 2.9.1. *[24] The sets $\alpha(\gamma)$ and $\omega(\gamma)$ [8] are closed and invariant. If γ^+ (forward part of γ) is bounded then $w(\gamma)$ is compact, connected and non-empty. Moreover, the distance between $x(t)$ and $w(\gamma)$ goes to zero as $t \to \infty$.*

[8] $\alpha - limit$ set is the set of all negative limit points.

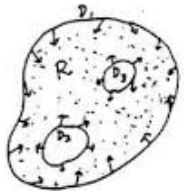

Figure 21: Illustration of the hypotheses of the Poincaré-Bendixson Theorem. Image from [23]

Using the concept of $\omega - limit$ set (and $\alpha - limit$ set) we can formally define limit cycles:

Definition 2.9.2. A limit cycle γ of a dynamical system in the plane is a periodic orbit which is the $\alpha-$ or $w - limit$ set of a trajectory γ' other than γ. If a limit cycle γ is the $\omega - limit$ set of every other trajectory in a neighborhood of γ, γ is said to be an stable limit cycle. Likewise, if γ is the $\alpha - limit$ set of neighbouring trajectories, γ is said to be an unstable limit cycle.

Theorem 2.9.3. Poincaré-Bendixson *[16].Let R be a region of the plane closed and bounded (ie, compact). Consider a dynamical system $\dot{x} = V(x) in R$ where the vector field $V \in e^1$ at least. Assume that R has no fixed points of V and that there exists a trajectory γ of V starting in R which stays in R for all future times. Then, either γ is a closed orbit or v asymptotically approaches a closed orbit; ie, there exists a limit cycle in R.*

More formally, if γ^+ is contained in a compact subset of the plane which contains no fixed points, $\omega(\gamma)$ will be the desired periodic orbit.

An alternative and more straight-forward statement of the theorem would be: "A non-empty compact $\omega-$ or $\alpha - limit$ set of a planar flow, either contains at least one equilibrium point or it is a limit cycle".

The theorem strongly appeals to intuition, the hypotheses are illustrated in the Figure 21.

If we start on one of the boundary curves, the solution will enter R, since the velocity vector points into the interior of it. As time goes on, the solution can never leave R, the only thing it can do as $t \to \infty$ is either approach a critical point, which is not there by hypothesis, or spiral in towards a closed trajectory. Thus there is a limit cycle inside R.

The hard part of the Poincaré-Bendixson Theorem consists of finding a suitabe trajectory γ. However, there are a number of special cases in which this is easier in practice: define a trapping region to be any region R of the plane which is positively invariant under the flow of $V : \phi_t(R) \subset R \ \forall t > 0$. Then, if R is a trapping region every trajectory of V starting in R stays in it for all future times. To check that R is a trapping region is enough to verify that on the boundary of R, V is everywhere pointing inward. Practically speaking, one proceeds by construction an annular region R in the plane so that on the boundary of R the vector field points into R.

Proposition 2.9.4. *[16] R will always be annular, ie it will contain at least one hole.*

Proof. We will use index theory. Denote the outer boundary of R, C: since the vector field is pointing inward on C, the index $I_c = +1$. Hence C has to enclose a given number of fixed points with total index 1. These fixed points have to be excised from R so the Poincaré-Bendixson Theorem can be used, which means that the domain cannot be simply connected. □

Note that there exists a time-reversed version of the Poincaré-Bendixson Theorem, in the sense that if the backward trajectory $\gamma^- = \{x(t), y(t)) | t \leq 0\}$ is contained in a compact subset R of the plane which

contains no fixed points, then $\alpha(\gamma)$ is a limit cycle in R. If an annular region such that the vector field points outwards of it, then this version of the theorem can be applied.

The theorem sets that in two dimension systems, the only possible asymptotic behaviours for non-conservative systems are stationary solutions (fixed points) and periodic solutions (limit cycles) [25]. In fact, limit cycles can only exist in non-conservative systems because for conservative ones, closed orbits correspond to centers and there are an infinity of then nested into each other. It is also important to mention that the amplitude of closed orbits is fixed by the initial condition, while in the case of limit cycles, the form and amplitude of the oscillation have nothing to do with the initial condition.

Proposition 2.9.5. *[23]* **Critical point criterion**. *A closed trajectory has a critical point in its interior.*

If we turn this statement around, we see that it is a criterion for non-existence: it says that if a region R is simply connected (ie, it has no holes) and has no critical points, then it cannot contain only limit cycles. For if it did, the criterion says there would be a critical point inside the limit cycle, and this point would also be in R since it has no holes. It is important to remark the difference between this theorem, which says that limit cycles enclose regions which do contain critical points, while the Poincaré-Bendixson Theorem seems to imply that limit cycles tend to be in regions without critical points. The difference is that these latter regions always contain a hole, so the critical points are in there.

Limitations of the Poincaré-Bendixson Theorem. The theorem essentially rules out chaos in the plane, as we will see further on. This turns out to be a highly non-generic result which does not hold for other configuration spaces or other types of dynamical systems, such as discrete ones, or higher order systems.

3. Bifurcations

Dynamical systems usually have parameters present in the defining systems of equations and as these parameters may vary, changes can occur in the qualitative structure of the solutions for certain parameter values. These changes are called bifurcations and the parameters values are called bifurcation values.

In parameter regions consisting of structurally unstable systems the detailed changes in the topological equivalence class of a flow can be exceedingly complicated. Therefore, we will focus on bifurcations of individual equilibria and periodic orbits, a part of the theory which is quite complete. Since the analysis of such bifurcation is generally performed by studying the vector field near the bifurcating (degenerate) equilibrium point or closed orbit, and bifurcation solutions are found in a neighbourhood of that limit set, these bifurcations as considered local. Global bifurcations, are those characterized by a lack of transversality between the stable and unstable manifolds of periodic orbits and equilibria will not be treated because are out of the scope of this text.

3.1 Bifurcation problems

3.1.1 Definition

[26] Poincaré firsts describes the splitting of equilibrium solutions in a family of differential equations as bifurcation. Let

$$\dot{x} = f_\mu(x) \qquad x \in \mathbb{R}^n \qquad \mu \in \mathbb{R}^k \tag{3.1.1}$$

be a system of differential equations depending on $\mu \in \mathbb{R}^k$. Then, the equilibrium solutions of (3.1.1) are given by $x^* \in \mathbb{R}^n$ that satisfy $f_\mu(x^*) = 0$. As μ varies, the Implicit Function Theorem implies that these equilibria are described by smooth functions of μ away from those points at which $D_x f_\mu$ has a zero eigenvalue. The graph of each of these functions is a branch of equilibria of the system (3.1.1).

At an equilibrium point (x_0, μ_0) where $D_x f_\mu$ has a zero eigenvalue, several branches of equilibria may come together and the point is considered a bifurcation point.

Bifurcations of equilibria produce changes in the topological type of a flow, but those are not the only kinds of changes that can happen in the topological equivalence class of flows. Thus, the more formal definition of bifurcation is:

Definition 3.1.1. A value μ_0 of (3.1.1) for which its flow is not structurally stable is a bifurcation value of μ.

This definition leads to very difficult technical questions and not all of them have relevance for applications of the theory. Because of this, we will examine only some of the qualitative features of a system but we will not only deal with bifurcations of equilibria. Another remark on the definition to be made is that a point of bifurcation does not need to represent a change in the topological equivalence class of a flow. However, arbitrary perturbations do give topologically distinct flows.

Given a system (3.1.1) an important and useful tool to study is the bifurcation diagram. It shows in the (x, μ) product space the invariant set of the system. These invariant sets can be fixed points; periodic orbits are often represented in terms of some measure of their amplitude. Another option is to draw the

bifurcation set, the place in the $\mu - space$ that corresponds to systems for which structural stability breaks down in specific ways.

The main interest is to identify kinds of bifurcations that appear in different problems. It would be desirable to have a classification of them that enlisted characteristics of each one. For example, parts of a classification by the number of parameters in the problem, the dimension of the phase space and symmetries or other special properties of the system, has been developed for global bifurcations but that has not been extended to local bifurcations.

The classification schemes are based in the theory of transversality in differential topology. The transversality theorem implies that when two manifolds of dimensions k and l meet in a n-dimensional space, then (in general) their intersection will be a manifold of dimensions $(k + l - n)$. If $k + l < n$ then one does not expect intersections at all[9]. The dimension formula can be expressed also in terms of **codimension**: the codimension of an l-dimensional submanifold of n-space is $(n - l)$. Then intersection of two submanifolds Σ_1, Σ_2 generally satisfies $(n - l) + (n - k) = 2n - (l + k) = n - (l + k - n)$. Therefore, the codimension of $\Sigma_1 \cap \Sigma_2$ is the sum of the codimensions if the intersection is transversal. To apply this to bifurcation theory we do it the following way: the goal is to study bifurcations that occur in general in k-parameter families (3.1.1). We get to this by formulating a collection of transversality conditions that are met by most families at bifurcation value μ_0. At μ_0, some of the conditions for structural stability will be violated and it will determine the type of bifurcation.

Example[10]: Consider a two parameter system:

$$\dot{x} = f_\mu(x), \qquad x \in \mathbb{R}^n, \mu \in \mathbb{R}^k$$

with a bifurcation value μ_0 at which f_μ has a nonhyperbolic equilibrium p. It can be studied the linearization of f_μ at p and the way the vector field changes for μ near μ_0. Transversality leads us to believe that the set of equilibria of the system in the (x, μ) space will form a smooth two-dimensional surface M. By checking linearizations of f_μ at the equilibria in M, a transversality condition that can be stated is that no linearization of f_μ has a zero eigenvalue of multiplicity greater than two, and that any equilibrium which does, has a Jordan normal form with the block $\begin{bmatrix} 0 & 1 \\ 0 & 0 \end{bmatrix}$. To state this, the map of M into the space of matrices nxn which associates to $(x, \mu) \in M$ the Jacobian derivative $D_x f \mu$ at (x, μ) needs to be defined. In this space, there are submanifolds which correspond to various combinations of eigenvalues on the imaginary axis. Because M has dimension two its image under the map will generally meet only those submanifolds of matrices whose codimension is at most two. The set of matrices with a Jordan form having just one block $\begin{bmatrix} 0 & 1 \\ 0 & 0 \end{bmatrix}$ forms a submanifold of codimension two. We can list the normal forms of the Jacobian derivatives $D_x f \mu$ evaluated at bifurcation points (x_0, μ_0) of codimensions one and two:

- Codimension one
  - Simple zero eigenvalue: $D_x f_\mu = \begin{bmatrix} 0 & 0 \\ 0 & A \end{bmatrix}$
  - Simple pure imaginary pair: $D_x f_\mu = \begin{bmatrix} \begin{bmatrix} 0 & -\omega \\ \omega & 0 \end{bmatrix} & 0 \\ 0 & A \end{bmatrix}$

[9] Stated as in chapter 3 of Guckenheimer and Holmes, 1983
[10] Extracted from chapter 3 of Guckenheimer and Holmes, 1983

- Codimension two
  - Double zero nondiagonalizable: $D_x f_\mu = \begin{bmatrix} \begin{bmatrix} 0 & 1 \\ 0 & 0 \end{bmatrix} & 0 \\ 0 & A \end{bmatrix}$
  - Simple zero + pure imaginary pair: $D_x f_\mu = \begin{bmatrix} \begin{bmatrix} 0 & -\omega & 0 \\ \omega & 0 & 0 \\ 0 & 0 & 0 \end{bmatrix} & 0 \\ 0 & A \end{bmatrix}$
- Two distinct pure imaginary pairs: $D_x f_\mu = \begin{bmatrix} \begin{bmatrix} 0 & -\omega_1 & 0 & 0 \\ \omega_1 & 0 & 0 & 0 \\ 0 & 0 & 0 & -\omega_2 \\ 0 & 0 & \omega_2 & 0 \end{bmatrix} & 0 \\ 0 & A \end{bmatrix}$

In each case, A is a matrix $(n-1)x(n-1)$ or $(n-2)x(n-2)$ or what is appropriate, all of whose eigenvalue have non-zero real parts.

The codimension of a bifurcation will be the smallest dimension of a parameter space which contains the bifurcation in a persistent way. An unfolding of a bifurcation is a family which contains the bifurcation in a persistent way.

3.1.2 Center Manifolds

For the system $\dot{x} = f(x)$ near a fixed point x^* we have seen by Hartman's Theorem that if none of the eigenvalues of the Jacobian $Df(x^*)$ has a real part zero, then the behaviour is determined by its linearized system $\dot{y} = Df(x^*)y$ with $y = x - x^*$. If there are eigenvalues with zero real parts, then the study of the flow can be quite complicated, nonlinear terms are expected to play a role and the behaviour could change accordingly. Since stability, and the lack of it, of fixed points is indicated precisely by the real part of the eigenvalues, we are going to see how these eigenvalues pass the imaginary axis, as the parameter changes.

We know, by the Stable Manifold Theorem that the structure of the system near a hyperbolic fixed point does not change when nonlinear terms are added. However, if there is any eigenvalue with zero real part, we expect some qualitative changes in the property when certain parameter changes, which points out the importance of the following theorem that is illustrated in Figure 22:

Theorem 3.1.2. Centre Manifold Theorem *[27]: Given $\dot{x} = f(x), x \in \mathbb{R}^n, f \in C^r$ and suppose $f(0) = 0$. Suppose $Df(0)$ has eigenvalues in sets σ_u with $Re(\lambda) > 0$, σ_s with $Re(\lambda) < 0$ and σ_c with $Re(\lambda) = 0$; and corresponding generalized linear eigenspaces E^u, E^s and E^c respectively. Then there exists unstable and stable manifolds W^u, W^s of the same dimension as E^u, E^s and tangential to E^s and E^u at $x = 0$; and an invariant centre manifold W^c tangential to E^c at $x = 0$* [11].

In general, locally $\mathbb{R}^n = W^c \oplus W^u \oplus W^s$ with the approximate governing equations on each manifold:

$$\begin{array}{lll} \dot{x} = g(x) & \text{on} & W^c \\ \dot{y} = By & \text{on} & W^s \text{ (stable directions)} \\ \dot{z} = Cz & \text{on} & W^u \text{ (unstable directions)} \end{array}$$

[11] The full proof was first published by Kelley at 1968

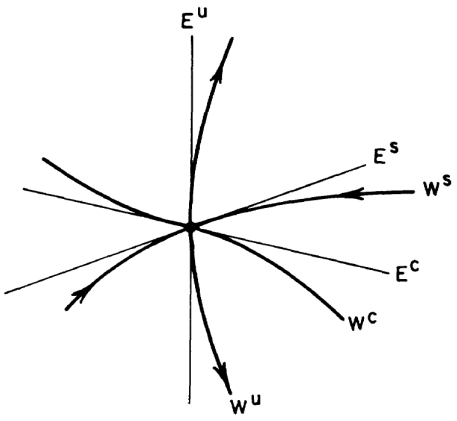

Figure 22: Behaviour on W^c depends on nonlinear terms, behaviour off W^c is dominated by exponential contraction in the E^s direction. Image from [27]

where $g(x)$ is quadratic (or higher order) in x, all eigenvalues of B have negative real parts, and all eigenvalues of C have positive real parts.

The dynamics on W^c depend on nonlinear terms, is usually much slower and determines the dynamics of the whole system in the long term.

Now we want to approximate or compute the center manifold [28]. Suppose that after a change of coordinate, the hyperplane $(x, 0)$ is spanned by E^c and $(0, y)$ by E^s, then the center manifold is tangential to $y = 0$ at $(0, 0)$ and we can assume that

$$W^c = \{(x, y)|y = h(x),\ h(0) = 0,\ Dh(0) = 0\}$$

In this coordinate, th system can be written as

$$\dot{x} = Ax + f_1(x, y)\ ,\ \dot{y} = C_y + f_2(x, y)$$

with A with all eigenvalues with real part zero and C with non-zero real part eigenvalues. Also, f_i, contains only nonlinear terms. So, on the center manifold W^c, $\dot{x} = Ax + f_1(x, h(x))$ and $\dot{y}$ can be calculated on W^c in two ways: directly from the $\dot{y}$ equation or by differentative $y = h(x)$ as:

$$\dot{y} = Ch(x) + f_2(x, y) \text{ and } \dot{y} = \frac{d}{dt}h(x) = Dh(x)\dot{x} = Dh(x)[Ax + f_1(x, h(x))]$$

Expanding h as a Taylor series (note that the constant and linear terms vanish) the two equations for $\dot{y}$ provide two different polynomials and the coefficients of different monomials can be equaled to determine the coefficients of the Taylor expansion.

To summarize, for a specific problem the general procedure to calculate the center manifold is:

1. Change the system into normal form, so that the linearized system is a diagonal matrix.
2. Identify the center manifold E^c of the linearized system, which is the linear space spanned by the eigenvectors associated with the zero eigenvalues.
3. Parameterize the center manifold: it is easier to start with E^c and then go on with W^c.

4. Determine the coefficients in the parameterization by differentiation on both sides.

As we have dealt with it, the center Manifold Theorem does not allow working with parameters. To include their effect and hence to treat bifurcations, we extend the idea of center manifold with the apparently trivial equation $\dot{\mu} = 0$:

$$\begin{aligned} \dot{x} &= Ax + f_1(x, y, \mu) \\ \dot{y} &= Cy + f_2(x, y, \mu) \\ \dot{\mu} &= 0 \end{aligned}$$

Thus, we can parameterize the center manifold as $y = h(x, \mu)$. Also, we add one more dimension and we can work in a neighbourhood of both $(x, y) = (0, 0)$ in phase space and $\mu = 0$ in parameter space, where $\mu = 0$ is the value at which the bifurcation occurs. The Center Manifold Theorem gives the motion on the stable and unstable manifolds, W^s and W^u in y, and there is a $n_c + 1$ dimensional manifold (where n_c is the dimension of x) valid for $|x|$ and $|\mu|$ small [29].

If coordinates are chosen so that the central motion is in normal form, the extended centre manifold can be parameterized by $y = h(x, \mu)$ with $h(0, 0) = 0$ and $Dh(0, 0) = 0$. Then $\dot{x} = Ax + f_1(x, h(x, \mu), \mu)$ typical behaviour is sketched in the (x, μ) plane in bifurcation diagrams. By convention, dotted lines are used to show unstable solutions and continuous lines for stable ones.

3.1.3 Normal Forms

We want to explore the idea of introducing successive coordinate transformations to simplify the analytic expression of a bifurcation problem [12] [30]. Suppose we have a system:

$$\dot{x} = f(x) \tag{3.1.2}$$

with an equilibrium at $x^* = 0$. We want to find $x = h(y)$ with $h(0) = 0$ that transforms (3.1.2) in something as simple as possible. In the y-coordinates, we have

$$Dh(y)\dot{y} = f(h(y)) \qquad \text{or} \qquad \dot{y} = (Dh(y))^{-1} f(h(y)) \tag{3.1.3}$$

We expect (3.1.3) to be linear; formally it would mean trying to find a sequence of coordinate transformations by iterating to remove terms of increasing degree from the Taylor series at the origin. The normal form procedure systematizes these calculations without, however, giving the strongest results in all classes. When the procedure is applied to a hyperbolic equilibrium, one gets the formal part of Hartman's linearization Theorem.

Assume that $Df(0)$ has distinct eigenvalues $\lambda_1, ..., \lambda_n$ and that an initial linear change of coordinates has diagonalized $Df(0)$. Then (3.1.2) becomes

$$\begin{aligned} \dot{x}_1 &= \lambda_1 x_1 + g_1(x_1, ..., x_n) \\ \dot{x}_2 &= \lambda_2 x_2 + g_2(x_1, ..., x_n) \\ &\vdots \\ \dot{x}_n &= \lambda_n x_n + g_n(x_1, ..., x_n) \end{aligned} \qquad \text{or} \qquad \dot{x} = \Lambda x + g(x) \tag{3.1.4}$$

[12] This has been used in the previous section, now we want to 'formalize' the work.

where g_i vanish to second order at the origin. We would like to find a coordinate change h of the form identity plus higher order terms, which has the same property of (3.1.3): non-linear terms vanish to higher order than those of g. If k is the smallest degree of a non-vanishing derivative of g_i, we seek h of the form

$$x = h(y) = y + P(y)$$

with P a polynomial of degree k, so that the lowest degree of the nonlinear terms in the transformed equation (3.1.3) is $k+1$. Thus,

$$\dot{y} = (I + DP(y))^{-1} f(y + P(y))$$

We would like to expand this expression, retaining only terms of degree k and lower. If the terms of degree k of g_i are g_i^k, we have:

$$\dot{y} = \lambda_i y_i + \lambda_i P_i(y) + g_i^k(y) - \sum_{j=1}^{n} \frac{\partial P_i}{\partial y_i} \lambda_j y_j$$

Knowing that $(I + DP)^{-1} = I - DP$, modulo terms of degree k and higher. Thus, we are seeking for P that satisfies:

$$-g_i^k(y) = \lambda_i P_i(y) - \sum_j \frac{\partial P_i}{\partial y_j} \lambda_j y_j = \lambda_i P_i(y) - \sum_j a_j \lambda_j P_i = (\lambda_i - \sum_j a_j \lambda_j) P_i$$

So, P can be found if none of the sums $\lambda_i - \sum_j a_j \lambda_j$ is zero when a_n are non-negative integers with $\sum_{j=1}^{n} a_j = k$. If there is no equation $\lambda_i - \sum_j a_j \lambda_j = 0$ which is satisfied for non-negative integers a_j with $\sum_j a_j \geq 2$, then the equation can be linearized to any desired algebraic order.

For bifurcation theory, we focus in equilibria with zero real part eigenvalues. There, the linearization problem cannot be solved and there are non-linear resonance terms in f which cannot be removed by coordinate changes. We need to remember that the solvability depends only on the linear part of the vector field and that the problem can be reduced to a sequence of linear equations to be solved. The result is a Taylor series for the vector field with only the essential resonant terms.

Let's demote $L = Df(0)x$ the linear part of (3.1.2) at $x = 0$, then L induces a map $ad\ L$ on the linear space H_k of vector fields whose coefficients are homogeneous polynomials of degree k [30]. The map is defined:

$$ad\ L(y) = [Y, L] = DLY - DYL$$

where $[.,.]$ is:

$$[Y, L]^i = \sum_{j=1}^{n} \left(\frac{\partial L^i}{\partial Y_j} y^j - \frac{\partial Y^i}{\partial y_j} L^j \right)$$

Theorem 3.1.3. *[30] Let $\dot{x} = f(x)$ be a C^r system of differential equations with $f(0) = 0$ and $Df(0)x = L$. Choose a complement G_k for ad $L(H_k)$ in H_k, so that $H_k = ad\ L(H_k) + G_k$. Then there is an analytic change of coordinates in a neighbourhood of the origin which transforms the system $\dot{x} = f(x)$ to $\dot{y} = g(y) = g^{(1)}(y) + ... + g^{(r)}(y) + R_r$ with $L = g^{(1)}(y)$ and $g^{(k)} \in G_k$ for $2 \leq k \leq r$ and $R_r = o(|y|^r)$.*

Proof. We use induction and assume that $\dot{x} = f(x)$ has been transformed so that the terms of degree smaller than s lie in the complementary subspace G_i, $2 \leq i < s$. We then introduce a coordinate transformation

of the form $x = h(y) = y + P(y)$, where P is a homogeneous polynomial of degree s whose coefficients are to be determined. Substitution then gives the equation

$$(I + DP(y))\dot{y} = f^{(1)}(y) + f^{(2)}(y) + ... + f^{(s)}(y) + Df(0)P(y) + o(|y|^s)$$

The terms of degree smaller than s are unchanged by this transformation, while the new terms of degree s are

$$f^{(s)}(y) + DLP(y) - DP(y)L = f^{(s)}(y) + ad\ L(P)(y)$$

where $L(y) = f^{(1)}(y)$. Clearly a suitable choice of P will make

$$f^s(y) + ad\ L(P)(y)$$

lie in G_s as desired. □

The proof, that can be found at Guckenheimer and Holmes, can be used to implement the calculations of normal forms in examples. We have neglected higher order terms because we do not just want to derive the normal forms of vectors fields with specific linear parts L but general non-linear points. However, the successive transformations introduce additional higher-order terms at each stage, all of which must be retained if specific coefficients of the terms in a given normal form are to be computed.

3.2 Local Bifurcations

3.2.1 Equilibria bifurcations

We will start dealing with the simple bifurcation of equilibria which depends on a single parameter.

The saddle-node

Consider a system of equations

$$\dot{x} = f_\mu(x) \tag{3.2.1}$$

$x \in \mathbb{R}^n$ and $\mu \in \mathbb{R}$ and f_μ smooth. Suppose that there is an equilibrium at (x_0, μ_0) that has a zero eigenvalues for the linearization. Usually, this eigenvalue will be simple and the center manifold theorem let us reduce the study of the bifurcation problem to one which has $x \in \mathbb{R}$. Moreover, we can find a two-dimensional center manifold $\Sigma \subset \mathbb{R}^n \times \mathbb{R}$ passing through (x_0, μ_0) such that:

1. The tangent space of Σ at (x_0, μ_0) is spanned by an eigenvector of eigenvalue 0 for $Df_{\mu_0}(x_0)$ and a vector parallel to the μ-axis.
2. For any $r < \infty$, $\Sigma \in C^r$ if restricted to a small enough neighbourhood of (x_0, μ_0).
3. The vector field of (3.2.1) is tangent to Σ.
4. There is a neighbourhood U of (x_0, μ_0) in $\mathbb{R}^n \times \mathbb{R}$ such that all trajectories contained entirely in U for all time lie in Σ.

If we restrict (3.2.1) to Σ, we get a one-parameter family of equations of the one-dimensional curves Σ_μ in Σ obtained by fixing μ. This one-parameter family is our reduction of the bifurcation problem. We can also formulate the tranversality conditions for the system, when $n = 1$:

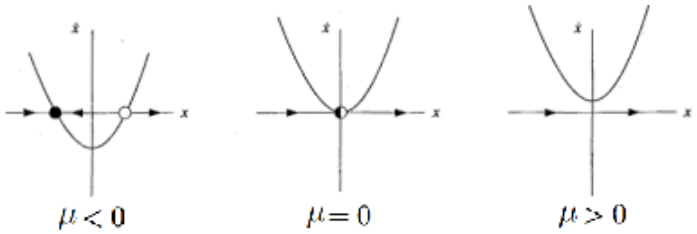

Figure 23: Phase portraits for $x = \mu + x$. Image from [31]

a) $\left.\frac{\partial f_{\mu_0}}{\partial \mu}\right|_{x_0} \neq 0$ The implicit function theorem then implies that the equilibria of the system form a curve which will be tangent to the line $\mu = \mu_0$.

b) $\left.\frac{\partial^2 f_{\mu_0}}{\partial x^2}\right|_{x_0} \neq 0$ This means that the curve of equilibria has a quadratic tangency with $\mu = \mu_0$ and locally dies to one side of this line.

Besides these two condition, we have established that f also satisfies:

c) $f(x_0, \mu_0) = 0$

d) $\left.\frac{\partial f_{\mu_0}}{\partial x}\right|_{x_0} = 0$

With this, we can conclude that the local phase portraits are topologically equivalent to:

$$\dot{x} = \pm(\mu - \mu_0) \pm (x - x_0)^2$$

Bifurcation diagram

The saddle-node bifurcations are the basic mechanism by which fixed points are created and destroyed. As μ is varied, two fixed points move towards each other and collide, mutually annihilating. If we consider the problem: $\dot{x} = \mu + x^2$ we can plot the phase portraits ($\dot{x}$ vs x) depending on the value of μ23: the fixed points are the solutions of $\dot{x} = 0$

$$x^* = \begin{cases} 0 & \mu = 0 \\ \pm\sqrt{-\mu} & \mu < 0 \end{cases}$$

Thus, we have:

The bifurcation diagram for the saddle-node bifurcation $\dot{x} = \mu + x^2$ is sketched in Figure **??**.

The transcritical

Saddle-node bifurcations are important because all bifurcations of one-parameter families at equilibrium with a zero eigenvalue can be perturbed to them. Thus, one expects that all the zero eigenvalues bifurcations will be saddle-nodes. If they are not, it is often because the formulation restricts the context in order to prevent them from occurring. The transcritical bifurcation is a way to avoid a saddle-node by manipulating the setting of the problem.

It is usually assumed that there is a trivial solution from which bifurcation is to occur, and therefore $f_\mu(x_o) = 0$, $\forall \mu$ so that x_0 is an equilibrium for all parameters values. Since saddle-node families contain parameter values for which there are no equilibria near the point of bifurcation, the situation is qualitatively different. The appropriate transversality conditions for the system are:

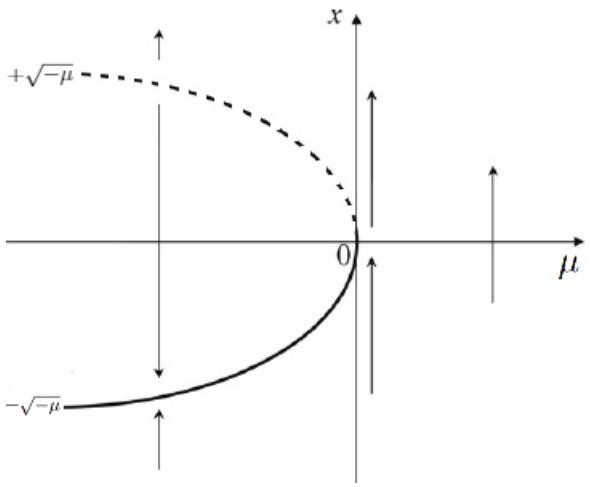

Figure 24: Bifurcation diagram for a saddle-node bifurcation. Image from [32]

a) $\left.\frac{\delta^2 f_{\mu_0}}{\partial \mu \delta x}\right|_{x=0} \neq 0$

b) $\left.\frac{\partial^2 f_{\mu_0}}{\delta x^2}\right|_{x_0} \neq 0$

Besides these two condition, we have established:

c) $f(0, \mu) = 0$

d) $\left.\frac{\partial f_{\mu_0}}{\partial x}\right|_{x_0} = 0$

With this, we can conclude that the local phase portraits are topologically equivalent to:

$$\dot{x} = \mu x \pm x^2$$

Bifurcation diagram

The transcritical bifurcation is the basic mechanism by which fixed points are never destroyed and exchange stability when they cross the bifurcation point. That is, both before and after the bifurcation, there is an stable fixed point and an unstable one. Where they collide, they switch stabilities and the stable becomes the unstable one and vice versa.

If we consider the problem:

$$\dot{x} = \mu x - x^2$$

we can plot the phase portraits depending on the value of μ (Figure 25): the fixed points are the solutions to $\dot{x} = 0$.

$$x^* = \begin{cases} 0 & \forall \mu \in \mathbb{R} \\ \mu & \forall \mu \in \mathbb{R} \end{cases}$$

Thus, we have:

The bifurcation diagram for the transcritical bifurcation $\dot{x} = \mu x - x^2$ is:

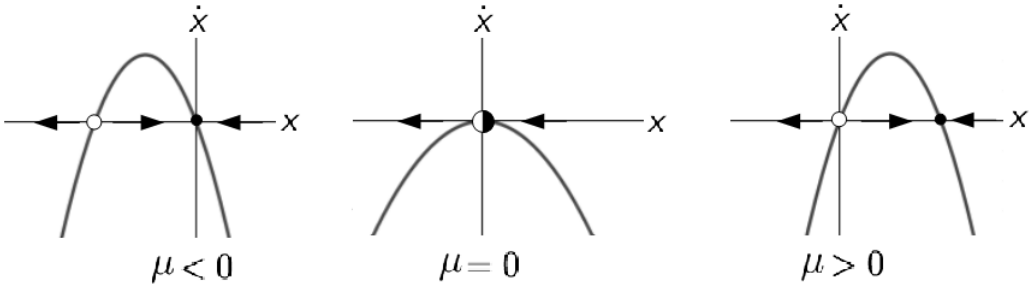

Figure 25: Phase portrait for $\dot{x} = \mu x - x$. Image from [33]

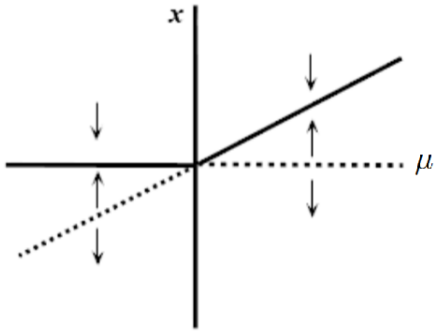

Figure 26: Bifurcation diagram for a transcritical bifurcation. Image from [34]

The Pitchfork

Systems that include symmetries do not have saddle-node bifurcations. In one dimension, a differential equation is symmetric with respect to x if $f(-x) = -f(x)$. Thus, the equivariant vector fields are those that have f_μ as an odd function of x and all of them have an equilibrium at 0.

The transcritical bifurcation cannot happen in these systems because f_μ cannot satisfy $\frac{\partial^2 f_{\mu_0}}{\partial x^2} \neq 0$, but if we replace this by the condition $\frac{\partial^3 f_{\mu_0}}{\partial x^3} \neq 0$ we get the pitchfork bifurcation: at the point of bifurcation the stability of the trivial equilibrium changes and a new pair of equilibria appear. We can state the appropriate transversality conditions:

a) $\left.\frac{\partial^2 f_{\mu_0}}{\partial x \delta \mu}\right|_{x=0} \neq 0$

b) $\left.\frac{\partial^3 f_{\mu_0}}{\partial x^3}\right|_{x=0} \neq 0$

Besides these two condition, we have established:

c) $f(-x, \mu) = -f(x, \mu)$

d) $\left.\frac{\partial f_{\mu_0}}{\partial x}\right|_{x=0} = 0$

With this, we can conclude that the local phase portraits are topologically equivalent to:

$$\dot{x} = \mu x \pm x^3$$

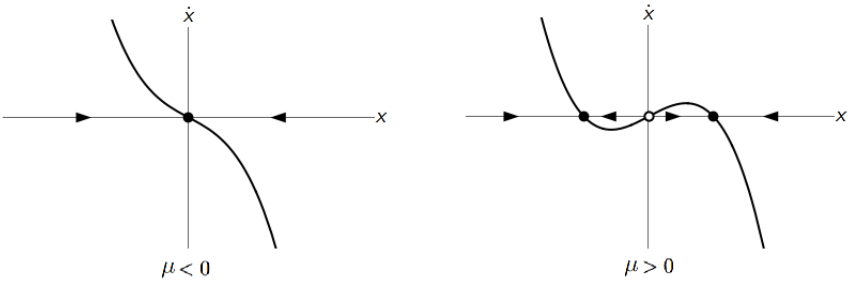

Figure 27: Phase portraits for $\dot{x} = \mu x - x^3$. Image from [33]

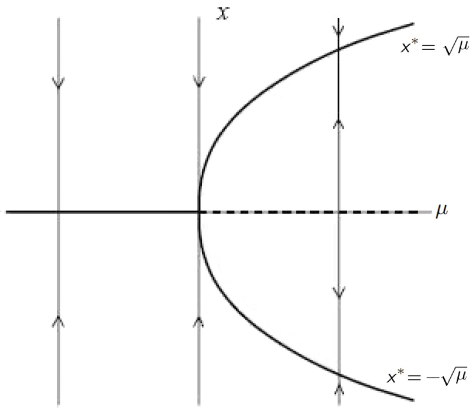

Figure 28: Bifurcation diagram for a supercritical Pitchfork bifurcation. Image from [35]

Bifurcation diagram The pitchfork bifurcation is the mechanism for problems with a symmetry and with fixed points that either appear or disappear in pairs. Depending on the sign of the cubic term, the bifurcation can be called supercritical (if the cubic term is negative) and the effect is stabilizing; or it can be called subcritical if the cubic term is positive and, therefore, destabilizing.

If we consider the problem:

$$\dot{x} = \mu x - x^3$$

We can plot the phase portraits depending on the value of μ (Figure 27): the fixed points are the solutions to $\dot{x} = 0$

$$x^* = \begin{cases} 0 & \forall \mu \in \mathbb{R} \\ \pm\sqrt{\mu} & \forall \mu > 0 \end{cases}$$

Thus, we have:

The bifurcation diagram for the Pitchfork bifurcation $\dot{x} = \mu x - x^3$ is sketched in Figure 28.

Hopf bifurcations

Consider now a system $\dot{x} = f_\mu(x)$ with a parameter value μ_0 and an equilibrium $p(\mu_0)$ at which Df_{μ_0} has a simple pair of pure imaginary eigenvalues, $\pm i\omega$, $\omega > 0$, and no other eigenvalues with zero real part.

Because the Df_{μ_0} is invertible, we can use the Implicit function Theorem to assure that for each μ near μ_0 there will be an equilibrium $p(\mu)$ near $p(\mu_0)$ which varies smoothly with μ. However, the dimensions

of stable and unstable manifolds of $p(\mu)$ can change if the eigenvalues of $Df(p(\mu))$ cross the imaginary axis at μ_0. This qualitative change in the local flow needs to be in phase portraits and fixed points are not useful to do so.

We want to understand what goes on in a bifurcation problem involving an equilibrium that has pure imaginary eigenvalues. We can do it by studying linear systems that have the same change, for example:

$$\begin{aligned} \dot{x} &= \mu x - \omega y \\ \dot{y} &= \omega x + \mu y \end{aligned}$$

that has solutions

$$\begin{pmatrix} x(t) \\ y(t) \end{pmatrix} = e^{\mu t} \begin{pmatrix} \cos \omega t & -\sin \omega t \\ \sin \omega t & \cos \omega t \end{pmatrix} \begin{pmatrix} x_0 \\ y_0 \end{pmatrix}$$

We can study the solutions depending on the parameter:

- $\mu < 0$: solutions spiral into origin
- $\mu = 0$: solutions are periodic
- $\mu > 0$: solutions spiral away from the origin

Using the normal form theorem we can change the system and get the Taylor series of degree 3, that expressed in polar coordinates is:

$$\begin{aligned} \dot{r} &= (d\mu + ar^2)r \\ \dot{\theta} &= (\omega + c\mu + br^2) \end{aligned}$$

where there are periodic orbits from the nonzero solutions of $\dot{r} = 0$. If a and d are not zero, these solutions lie along the parabola $\mu = \frac{-ar^2}{d}$ meaning that the surface of periodic orbits has a quadratic tangency with its tangent plane $\mu = 0$ in $\mathbb{R}^2 \times \mathbb{R}$.

Theorem 3.2.1. *[36] Suppose that the system $\dot{x} = f_\mu(x)$, $x \in \mathbb{R}^n$, $\mu \in \mathbb{R}$ has an equilibrium (x_0, μ_0) at which the following properties are satisfied:*

1. *$D_x f_{\mu_0}(x_0)$ has a simple pair of pure imaginary eigenvalues and no other eigenvalues with zero real parts.*
2. *$\frac{\partial}{\partial \mu}(Re(\lambda(\mu)))\Big|_{\mu=\mu_0} = d \neq 0$*

Then (1) implies that there is a smooth curve of equilibria $(x(\mu), \mu)$ with $x(\mu_0) = x_0$. The eigenvalues $\lambda(\mu)$, $\bar{\lambda}(\mu)$ of $D_x f_{\mu_0}(x(\mu))$ which are imaginary at $\mu = \mu_0$ vary smoothly with μ. If, moreover, (2) holds, then there is a unique 3-Dimensional center manifold passing through (x_0, μ_0) in $\mathbb{R}^2 \times \mathbb{R}$ and a smooth system of coordinates for which the Taylor expansion of degree 3 on the center namifold is given by:

$$\begin{aligned} \dot{x} &= (d\mu + a(x^2 + y^2))x - (w + c\mu + b(x^2 + y^2))y \\ \dot{y} &= (\omega + c\mu + b(x^2 + y^2))x + (d\mu + a(x^2 + y^2))y \end{aligned}$$

If $a \neq 0$, there is a surface of periodic solutions in the center manifold which has quadratic tangency with the eigenspace $\lambda(\mu_0)$, $\bar{\lambda}(\mu_0)$ agreeing to second order with the the paraboloid $\mu = -(\frac{a}{d})(x^2 + y^2)$

If $a < 0$, then these periodic solutions are stable limit cycles; while, if $a > 0$, the periodic solutions are repelling.

For large systems, the computation of the normal form and the cubic coefficient, that determines the stability, can be a hard task. In a two-dimensional system of the form

$$\begin{pmatrix}\dot{x}\\ \dot{y}\end{pmatrix} = \begin{pmatrix}0 & -\omega\\ \omega & 0\end{pmatrix}\begin{pmatrix}x\\ y\end{pmatrix} + \begin{pmatrix}f(x,y)\\ g(x,y)\end{pmatrix}$$

with $f(0) = g(0) = 0$ and $Df(0) = Dg(0) = 0$, the normal form calculation yields [36]:

$$a = \frac{1}{16}[f_{xxx} + f_{xyy} + g_{xxy} + g_{yyy}] + \frac{1}{16w}[f_{xy}(f_{xx} + f_{yy}) - g_{xy}(g_{xx} + g_{yy}) - f_{xx}g_{xx} + f_{yy}g_{yy}]$$

when using this formula on systems of dimension greater than two, the quadratic terms that appear in the center manifold calculations can affect the value of a. The value cannot be found by just projecting the system of equations onto the eigenspace of $\pm i\omega$, but it must approximate the center manifold at least to quadratic terms.

Supercritical Hopf bifurcation

The simplest case with a bifurcation with two purely imaginary eigenvalues, the center manifold at $\mu = 0$ is two dimensional and the extended center manifold is three dimensional. The canonical example is a supercritical Hopf bifurcation given by:

$$\begin{aligned}\dot{x} &= \mu x - \omega y - x(x^2 + y^2)\\ \dot{y} &= \omega x - \mu y - y(x^2 + y^2)\end{aligned}$$

that in polar coordinates is

$$\begin{aligned}\dot{r} &= \mu r - r^3\\ \dot{\theta} &= \omega + br^2\end{aligned}$$

There are three parameters:

1. μ: controls the stability of the fixed point at the origin.
2. ω: gives the frequency of the infinitesimal oscillations.
3. b: determines the dependence of frequency on amplitude for layer amplitude oscillations.

The phase portraits look like the ones of the Figure 29, depending on the value of μ: when $\mu < 0$ the origin is a stable spiral whose sense of rotation depends on the sign of ω. For $\mu = 0$ the origin is still a stable spiral but a very weak one. Finally, for $\mu > 0$ there is an unstable spiral at the origin and a stable circular limit cycle at $r = \sqrt{\mu}$.

The behaviour of the eigenvalues during the bifurcation is studied with the Jacobian of the system in Cartesian coordinates, which is $\begin{pmatrix}\mu & -\omega\\ \omega & \mu\end{pmatrix}$ and has eigenvalues $\mu \pm i\omega$. As the parameter is varied, a stationary point changes its stability and a periodic orbit is created with the opposite stability.

The bifurcation diagram for a supercritical Hopf bifurcation is sketched in figure 30.

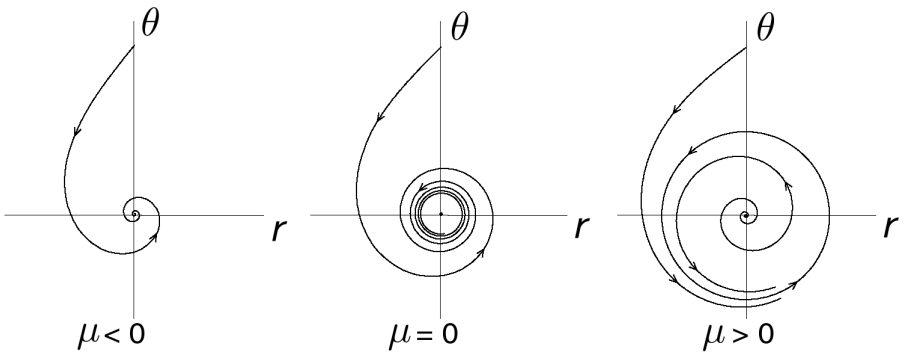

Figure 29: Supercritical Andronov-Hopf bifurcation in the plane. Image from [37]

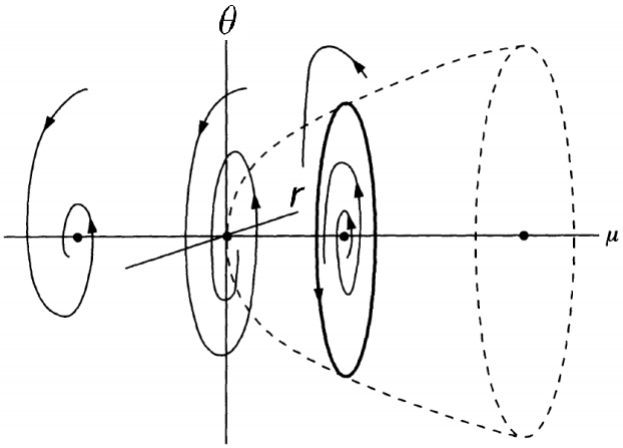

Figure 30: Hopf bifurcation: when μ increases, the stable focus becomes unstable, and a periodic solution called limit cycle appears. Image from [38]

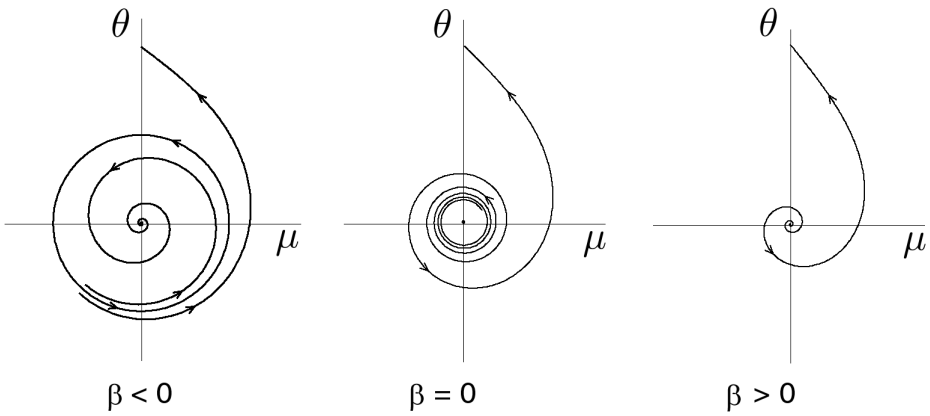

Figure 31: Subcritical Andronov-Hopf bifurcation in the plane. Image from [37]

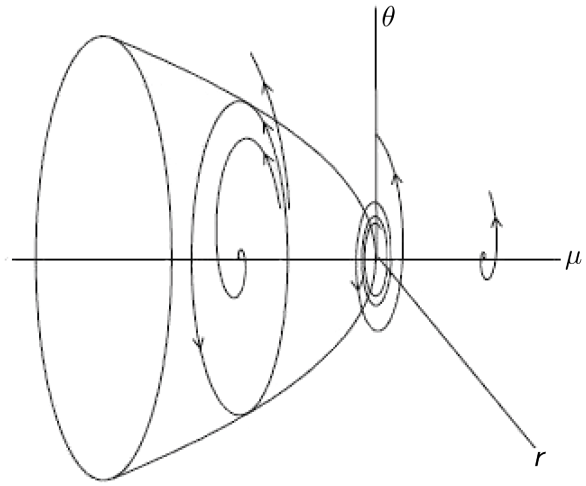

Figure 32: Supercritical Hopf bifurcation. Image from [39]

Subcritical Hopf bifurcation

The subcritical case is more dramatic because after the bifurcation, the trajectories jump to a distant attractor, that can be a fixed point, a limit cycle, infinity or (in 3 and higher dimensions) a chaotic attractor. Consider the system:

$$\begin{aligned} \dot{r} &= \mu r + r^3 - r^5 \\ \dot{\theta} &= \omega + br^2 \end{aligned}$$

The cubic term is destabilizing and makes trajectories go away from the origin. The phase portraits, depending on the value of μ, are like the ones in Figure 31. For $\mu < 0$ there are two attractors, a stable limit cycle and a stable fixed point at the origin; between them lies an unstable cycle. As μ increases, the unstable cycle closes around the fixed point until $\mu = 0$, when a bifurcation occurs and the unstable cycle shrinks to zero amplitude and engulfs the origin, rendering it unstable. For $\mu > 0$, the large-amplitude limit cycle becomes the only attractor and the origin is a repellor.

The bifurcation diagram for a subcritical Hopf bifurcation can be seen in Figure 32.

Degenerate Hopf bifurcation

Given that linearization does not provide a distinction between subcritical and supercritical Hopf bifurcation because in both cases a pair of eigenvalues moves from the left to the right half-plane, and that the analytical criterian can be to difficult to use; a quick way to know which type of bifurcation we are dealing with is to use numeric methods.

If a small, attracting limit cycle appears immediately after the fixed point goes unstable, and if its amplitude shrinks back to zero as the parameter is reversed, the bifurcation is most likely supercritical.

Also, a degenerate case of Hopf bifurcation can happen: this degenerate case typically arises when a non-conservative system becomes conservative at the bifurcation point. Then the fixed point becomes a nonlinear center, rather than the weak spiral that happens at a Hopf bifurcation.

3.2.2 Periodic orbits and Map bifurcations (codimension one)

We will deal with the simplest bifurcations of periodic orbits. It is important to remark that when dealing with them, the computations are way more difficult because before an extensive analysis of the bifurcation itself can be done, the equations have to be integrated near the periodic orbit to find the Poincaré return map. In this brief study, the aim is to focus on the geometric aspects of these bifurcations.

There are three ways in which a fixed point p of a discrete mapping $f : \mathbb{R}^n \to \mathbb{R}^n$ may fail to be hyperbolic:

- $Df(p)$ has an eigenvalue $+1$.
- $Df(p)$ has an eigenvalue -1.
- $Df(p)$ has a pair of complex eigenvalues λ, $\bar{\lambda}$ with $|\lambda| = 1$.

Map bifurcation

The bifurcation theory for fixed points with eigenvalue 1 is completely analogous to the bifurcation theory for equilibria with eigenvalue 0. The generic one parameter family has a two-dimensional center manifold on which it is topologically equivalent to the saddle-node family defined by the map: $f_\mu(x) = x + \mu \pm x^2$. If constraint conditions are added, the resultant bifurcation is topologically equivalent to $f_\mu(x) = (1+\mu)x \pm x^2$, the transcritical bifurcation. If the problem has a symmetry, we get the equivalent for the Pitchfork equations, defined by the map: $f_\mu(x) = (1+\mu)x \pm x^3$. The behaviour can be seen in the Figure 33, Figure 44 and Figure 35.

Although bifurcation diagrams of the three bifurcations look the same as their analogous for differential equations, two remarks should be make:

1. Bifurcations are only local for maps, because convergency does not work the same way.
2. Another bifurcation could happen along the stable fixed point as μ further increases or decreases.

Period doubling bifurcation

Bifurcations with eigenvalue -1 do not have an analogue for equilibria, are associated with flip or period doubling bifurcations. We can use the center manifold theorem to reduce the problem to one-dimensional

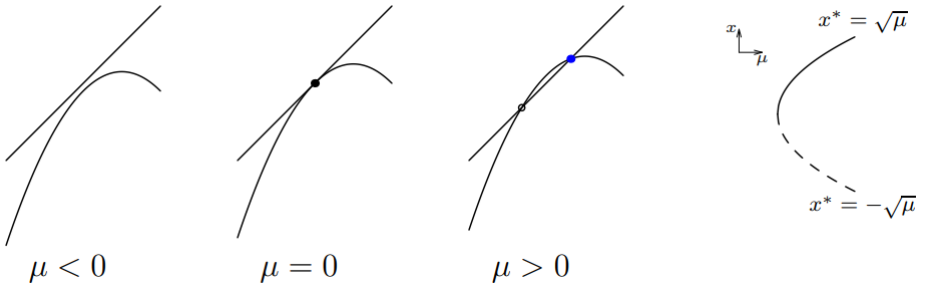

Figure 33: Saddle-node (tangential) bifurcation. Image from [40]

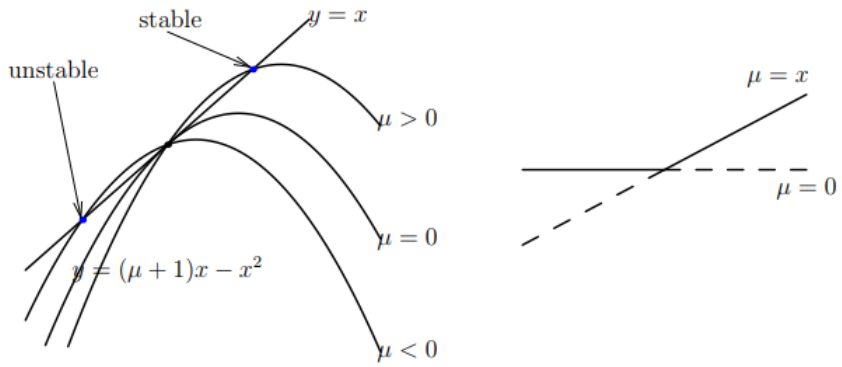

Figure 34: Transcritical bifurcation. Image from [40]

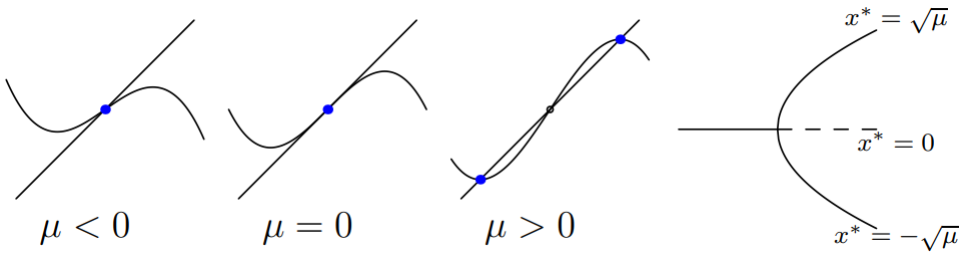

Figure 35: Pitchfork bifurcation. Image from [40]

mappings f_μ where $\mu \in \mathbb{R}$. If 0 is an equilibrium of eigenvalue -1 of $f_{\mu_0} : \mathbb{R} \to \mathbb{R}$, then the Taylor expansion is:

$$f_{\mu_0}(x) = -x + a_2x^2 + a_3x^3 + R_3(x) \qquad \text{with } R_3(x) = o(|x^3|)$$

We know, by the Implicit function theorem, that there is a smooth curve $(x(\mu), \mu)$ of fixed points in the plane that passes through $(0, \mu_0)$. Thus, besides a change of stability, there are changes in the dynamical behaviour that need to be dealt with. If we compose f_{μ_0} with itself

$$f^2_{\mu_0}(x) = x - (2a_2^2 + 2a_3)x^3 + \tilde{R}_3(x)$$

It is clear that $f^2_{\mu_0}$ has eigenvalue $+1$ and we expect fixed points of f^2_μ near $(0, \mu_0)$ which are not fixed points of f_μ. These points are periodic orbits of period 2. Also, because $f^2_{\mu_0}(x)$ has no quadratic term we expect the bifurcation to behave like a pitchfork bifurcation. However, the new orbits that appear are not fixed points but period two orbits. We can sum up this reasoning in the following theorem:

Theorem 3.2.2. *[41] Let $f_\mu : \mathbb{R} \to \mathbb{R}$ be a one-parameter family of mappings such that f_{μ_0} has a fixed point x_0 with eigenvalue -1. Assume*

$$(\frac{\partial f}{\partial \mu}\frac{\partial^2 f}{\partial x^2} + 2\frac{\partial^2 f}{\partial x \partial \mu}) = \frac{\partial f}{\partial \mu}\frac{\partial^2 f}{\partial x^2} - (\frac{\partial f}{\partial x} - 1)\frac{\partial^2 f}{\partial x \partial \mu} \neq 0 \qquad \text{at } (x_0, \mu_0) \tag{3.2.2}$$

$$a = (\frac{1}{2}(\frac{\delta^2 f}{\delta x^2})^2 + \frac{1}{3}(\frac{\delta^3 f}{\delta x^3})) \neq 0 \qquad \text{at } (x_0, \mu_0) \tag{3.2.3}$$

Then there is a smooth curve of fixed points of f_μ passing through (x_0, μ_0), the stability of which changes at (x_0, μ_0). There is also a smooth curve γ passing through (x_0, μ_0) so that $\gamma - \{(x_0, \mu_0)\}$ is a union of hyperbolic period 2 orbits. The curve γ has quadratic tangency with the line $\mathbb{R} \times \mu_0$ at (x_0, μ_0).

The quantity (3.2.2) is the μ-derivative of f' along the curve of fixed points and it is the non-degeneracy condition. In (3.2.3) the sign of a determines the stability and direction of bifurcation of the orbits of period 2. If $a > 0$, the orbits are stable, otherwise they are unstable.

Thus, a normal form for a period doubling bifurcation would be

$$f_\mu(x) = -(1 + \mu)x + x^3 \tag{3.2.4}$$

A representation of f_μ, f^2_μ and the bifurcation diagram can be found in Figure 36.

A final remark needs to be made about the relationship of a return map P with eigenvalue -1 at an equilibrium p, to the continuous flow around the corresponding orbit. The trajectories of P alternate from one side of p to the other along the direction of the eigenvector to -1. This means that the two-dimensional center manifold for the periodic orbit is like a Mobius band around its center line. This means that is not possible to have period doubling bifurcations in orientable two-dimensional manifold, but in flows of dimension 3 and higher.

A period doubling bifurcation corresponds to the creation or destruction of a periodic orbit with double the period of the original orbit. As in the case of Pitchfork bifurcations, it can be classified in whether the bifurcation creates or destroys the periodics orbits: for a continuous family f_μ, a period-doubling is a bifurcation by which a τ-periodic orbit $O_{0,\mu}$ looses its stability as the parameter μ crosses the critical value μ_c of μ and at which point either:

- a stable 2τ-periodic orbit emerges: we have a supercritical period doubling bifurcation.

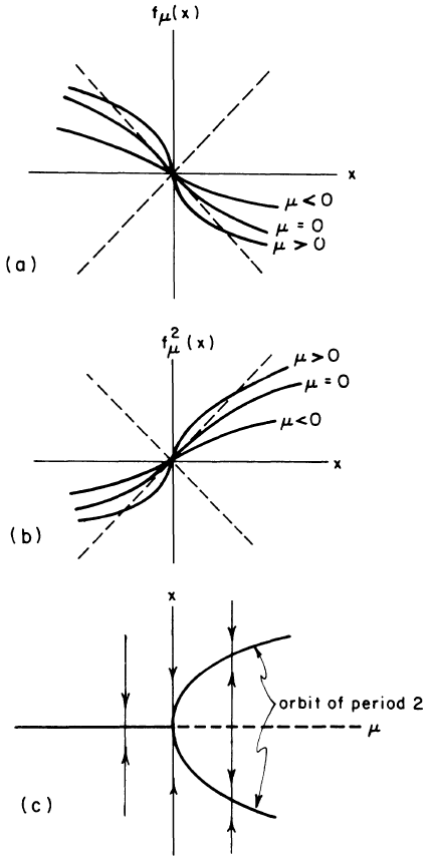

Figure 36: The flip bifurcation for equation (3.2.4). (a) Graphs of $f\mu(x)$; (b) graphs of $f_\mu^2(x)$; (c) the bifurcation diagram. Image from [41]

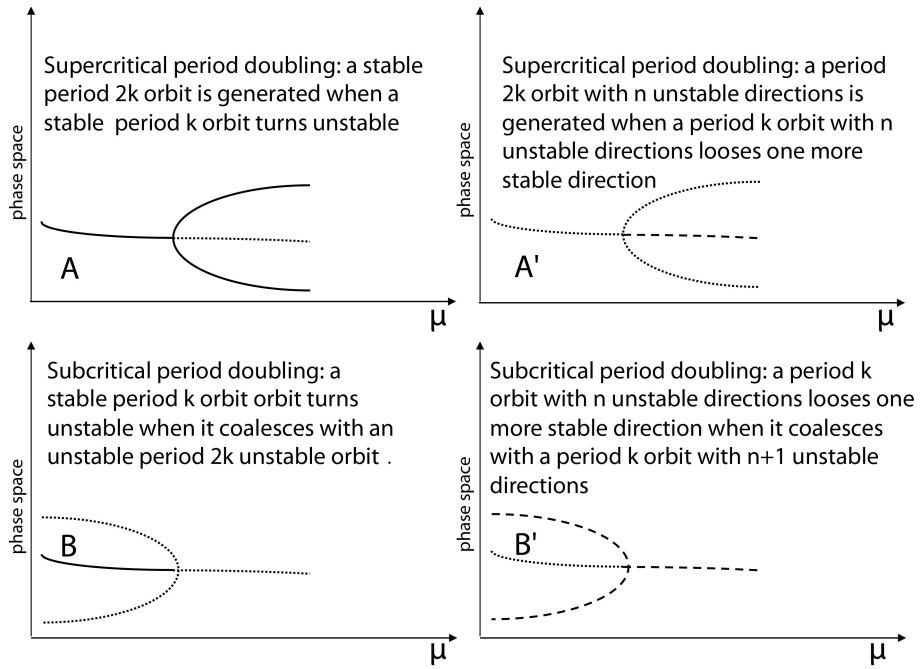

Figure 37: Period doubling for maps: evolution with parameters with continuous lines representing stable orbits and bigger gaps between dots meaning less dimensions of stability. Image from [42]

- an unstable 2τ-periodic orbit coalesces with $O_{0,\mu}$ and is destroyed: we have a subcritical period doubling bifurcation.

In a geometric point of view, for period doubling, the characterization of the bifurcation is that the parameter-dependent eigenvalue crosses the unit circle at -1 along the real line. In dimension 1, $\lambda_\mu = f'_\mu(x_0)$ is the only eigenvalue of the linearized map at x_0 and crosses -1 from above so that $|\lambda_\mu|-1$ increases and x_0 becomes more repelling. In greater dimensions, an eigenvalue of the linearized map crosses -1 from above. Then, if all the other eigenvalues of the linearized map at x_0 have norm different than one, for μ close enough to μ_c, there is a μ-dependent one-dimensional center manifold.

One dimensional case

For a map in one dimension, in the neighbourhood of $(O_0, \mu_c = (0, 1)$ the generic normal form for the bifurcation is:

$$f_\mu = -\mu x \pm x^3$$

when the sign is $+$, the bifurcation is supercritical; when is $-$, the bifurcation is subcritical. This normal form is valid if f_μ is invertible on the corresponding interval. In particular, the formula cannot contain the next period doubling in a meaningful way. The bifurcation diagrams are sketched in Figure 37, Figure 38.

In dimension 1, the center manifold is simply the local part of the full phase space near the bifurcating orbit. It only remains to compute the criticality type, that is, whether the bifurcation is supercritical or subcritical. As we have seen before, by using the Taylor expansion of degree 3, we can obtain a formula for the quantity a, that defines the stability and direction of bifurcation. In dimension 1,

$$a = \frac{1}{2}f''(x)^2 + \frac{1}{3}f'''(x)$$

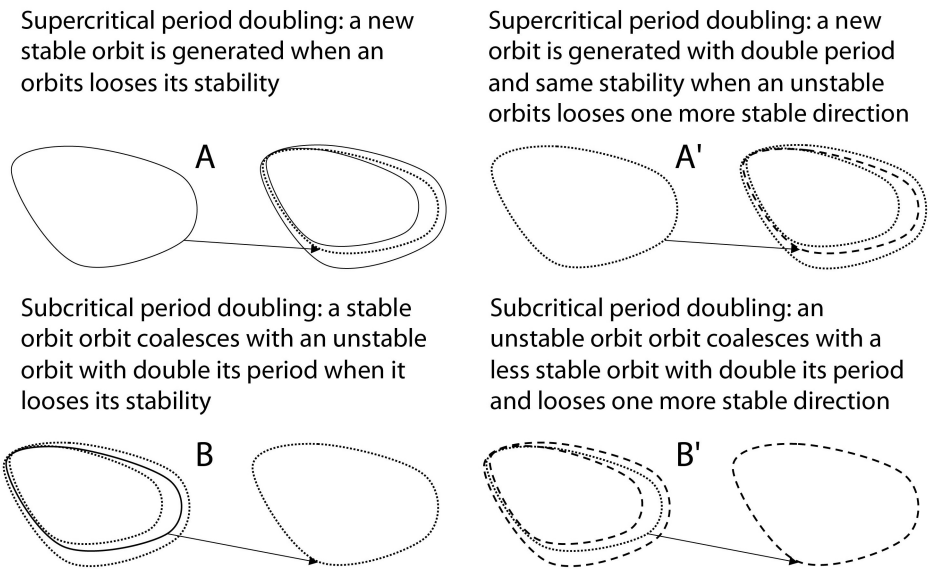

Figure 38: Period doubling for differential equations: description for two parameters, one below, one above the bifurcation with continuous lines representing stable orbits and bigger gaps between dots meaning fewer dimensions of stability. Image from [42]

and if it is positive, the bifurcation is supercritical. Otherwise, the bifurcation is subcritical, if $a \neq 0$. When $a = 0$, higher order terms are necessary to determine stability.

Bifurcation diagram

When the quantity $a = 0$ we can have that the bifurcation is marginal for all orders, in which case, if not flat term breaks the degeneracy, the fixed point $x_0 = f_{\mu_c}(x_0)$ is the common end point of two segments of period two that are exchanged by f_{μ_c}.

We plot three options of period doubling bifurcation, including the marginal case in Figure 39.

It is important to remark that the bifurcation theory regarding period doubling is only local and it can hardly be extended globally.

Secondary Hopf bifurcation

The last option we have in bifurcations of periodic orbits are those that have a pair of conjugate complex eigenvalues with unit modulus. Even though there are quite some similarities with Hopf bifurcations, we can find quasiperiodic behaviour and more subtle analysis is needed to understand this. First, a remark about polar coordinate transformation needs to be made.

Consider the transformation $f : \mathbb{R}^2 \to \mathbb{R}^2$, where the origin is an equilibrium and $Df(0)$ is the matrix:

$$\begin{pmatrix} cos2\pi\theta & -sin2\pi\theta \\ sin2\pi\theta & cos2\pi\theta \end{pmatrix}$$

Our purpose is to find the normal form for the bifurcation and to do so we need to simplify the higher order terms of the Taylor series of f. If we use the transformation and see (x, y) as complex, then the eigenvectors of $Df(0)$ are $\begin{pmatrix} 1 \\ -i \end{pmatrix}$ and $\begin{pmatrix} 1 \\ i \end{pmatrix}$ with eigenvalues $e^{2\pi i\theta}$ and $e^{-2\pi i\theta}$ and coordinates z and $\bar{z}$,

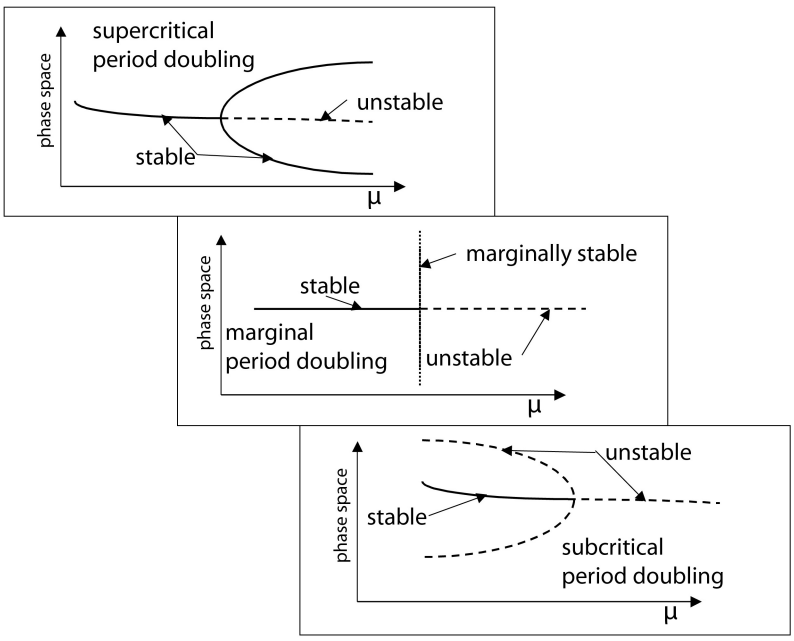

Figure 39: Period doubling from supercritical to subcritical through the degenerate marginal case that can provide all configuration by deformation of the period doubling orbits curve: only the most three basic cases have been represented here. Image from [42]

respectively. It can be shown that when θ is irrational, the normal forms of f are analogues of the normal forms for the Hopf bifurcation for flows [13]. However, if θ is rational then there are additional resonant terms and the denominator of θ determines the lowest degree at which these terms can appear. The bifurcation structures associated with fixed points that are the third and fourth roots of unity are special and will not be considered in the following theorem because their study is way more complex than the aim of this paper. If we leave those roots apart, we can state the following analysis of Hopf bifurcations for periodic orbits, also known as secondary Hopf bifurcations.

Theorem 3.2.3. *Let f_μ:$\mathbb{R}^2 \to \mathbb{R}^2$ be a one parameter family of mappings which has a smooth family of fixed points $x(\mu)$ at which the eigenvalues are complex conjugates$\lambda(\mu)$, $\bar{\lambda}(\mu)$. Assume:*

$$|\lambda(\mu_0)| = 1 \qquad \textit{but } \lambda^j(\mu_0) \neq 0 \qquad \textit{for } j = 1, 2, 3, 4 \tag{3.2.5}$$

$$\frac{d}{d\mu}(|\lambda(\mu_0)|) = d \neq 0 \tag{3.2.6}$$

Then there is a smooth change of the coordinates h so that the expression of $hf_\mu h^{-1}$ in polar coordinates has the form

$$hf_\mu h^{-1}(r, \theta) = r(1 + d(\mu - \mu_0) + ar^2), \theta + c + br^2) + \textit{higher-order terms} \tag{3.2.7}$$

(Note: λ complex and 3.2.6 imply $|arg(\lambda)| = c$ and d are nonzero). If, in addition

$$a \neq 0$$

[13] The demonstration of this can be seen in section 3.5 of Guckenheimer and Holmes, 1983.

Then there is a two-dimensional surface Σ (not necessarily infinitely differentiable) in $\mathbb{R}^2 \times \mathbb{R}$ having quadratic tangency with the plane $\mathbb{R}^2 \times \mu$ which is invariant for f. If $\Sigma \bigcap (\mathbb{R}^2 \times \mu)$ is larger than a point, then it is a simple closed curve.

The theorem is very similar to the one for Hopf bifurcations of equilibria, here the sign of a and d also determine the direction and stability of the bifurcating periodic orbits. A general read would say that something that resembles the limit cycles of the Hopf theorem, appear in the phase portrait of f_μ. These are simple closed curves which bound the basin of attraction or repulsion of a fixed point. Also, if $b \neq 0$, there is a complicated pattern of periodic and quasiperiodic behaviour inside Σ. To be able to study this, global bifurcations need to be examined, and that is not in the goal of the paper.

A stability formula, giving an expression for the coefficient a in the normal form (3.2.7) can be obtained in the same way as for flows [41]. Assuming that the bifurcating system (restricted to the center manifold) is in the form

$$\begin{pmatrix} x \\ y \end{pmatrix} \longmapsto \begin{bmatrix} \cos c & -\sin c \\ \sin c & \cos c \end{bmatrix} \begin{pmatrix} x \\ y \end{pmatrix} + \begin{pmatrix} f(x,y) \\ g(x,y) \end{pmatrix}$$

with eigenvalues λ, $\bar{\lambda} = e^{\pm ic}$, one obtains

$$a = -Re\left[\frac{(1-2\lambda)\bar{\lambda}^2}{1-\lambda}\xi_{11}\xi_{20}\right] - \frac{1}{2}|\xi_{11}|^2 - |\xi_{02}|^2 + Re(\bar{\lambda}\xi_{21})$$

where

$$\begin{aligned} \xi_{20} &= \tfrac{1}{8}[(f_{xx} - f_{yy} + 2g_{xy}) + i(g_{xx} - g_{yy} - 2f_{xy})] \\ \xi_{11} &= \tfrac{1}{4}[(f_{xx} + f_{yy}) + i(g_{xx} + g_{yy})] \\ \xi_{02} &= \tfrac{1}{8}[(f_{xx} - f_{yy} + 2g_{xy}) + i(g_{xx} - g_{yy} + 2f_{xy})] \end{aligned}$$

and

$$\xi_{21} = \frac{1}{16}[(f_{xxx} + f_{yyy} + g_{xxy} + g_{yyy}) + i(g_{xxx} + g_{xyy} - f_{xxy} - f_{yyy})]$$

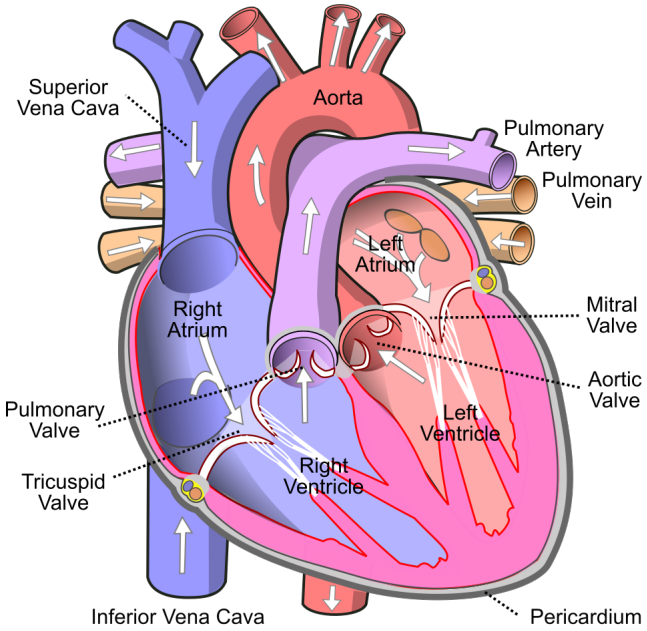

Figure 40: Diagram of the human heart showing the valves, arteries and veins. The white arrows show the normal direction of blood flow. Image from [44]

Stability of intracellular calcium in cardiac myocytes

4. Stability of intracellular calcium in cardiac myocytes

4.1 Introduction

The heart is a hollow muscular organ located in the thoracic cavity wrapped in a sac: the pericardium. The inside of the heart is formed by four cavities, two auricles and two ventricles, and it has four valves, two atrio-ventricular valves and two sigmoid valves (Figure 40). The heart wall is made of three layers: the inner endocardium, the middle myocardium and the outer epicardium. The right cavities pump the blood from the systemic circulation to the pulmonary circulation, and the left ones pump the blood from the other direction, this is possible because the myocardium, that is the cardiac muscle, allows the contractions of the auricles and ventricles. This contractions need to have a specific sequence and with an appropriate interval in order to keep the heart working properly. This coordination is achieved by the conduction system of the heart that is able to create and transmit electric impulses that control this activity. Anomalies of this conduction can be the cause of serious health problems that can end up in arrhythmias and even death. [43]

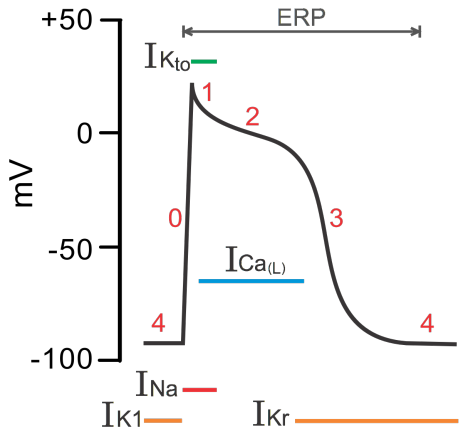

Figure 41: Action potential of a contractile cardiac cell. Image from [46]

4.1.1 Cardiac electrophysiology

Cardiac myocytes are the most common cells on the heart wall and are about 80-100 μm long and have a diameter of 10 to 20 μm. They are encapsuled by a thin membrane. The outer membrane encapsules a small volume that is known as the intracellular space and where there is a compartment called sarcoplasmic reticulum (SR). In the cell membrane there ion channels that allow only specific ions to pas through, and only under certain conditions [45]. Cardiac myocytes have a resting potential and the property of excitability, and typically require an impulse from another myocardial cell to depolarize. The action potential of contractile cells is divided into several phases [46] as it can also be seen in Figure 41:

- **Phase 4**: the membrane remains essentially at rest at about -90 mV until excited. Leaky potassium channels, I_K, maintain the cell at resting potential trough the outward movement of potassium ions.
- **Phase 0**: Depolarisation occurs in an adjacent cell and the threshold potential is met. Fast voltage-gated sodium channels, I_{Na} open and sodium ions enter the cell rapidly.
- **Phase 1**: The first stage of repolarisation, potassium ions leave the cell via trancient K^+ channels, I_{Kto}.
- **Phase 2**: inward movement of calcium ions via voltage gated L-type channels, I_{CaL} prolongs repolarisation.
- **Phase 3**: Completion of repolarisation. Outward movement of potassium ions via I_k channels returns the membrane to its resting potential.

Besides excitability, which we have seen as action potential, cardiac myocytes have another three physiological properties: refractoriness, conductivity and automatism. Refractoriness, in this context, is the time needed after each beat for the heart to regain its ability to become excitable again. It starts with phase 0 and ends with phase 3. Automatism is the feature that some specialized heart cells have to excite themselves in a rhythmic way. These cells, that are not myocytes but autorhythmic cells, have a higher resting potential (-70mV) that it is not stable during phase 4. Finally, conductivity is the property that cardiac myocytes have to channel the spur coming from the surrounding autorhythmic cells to close structures around them [43].

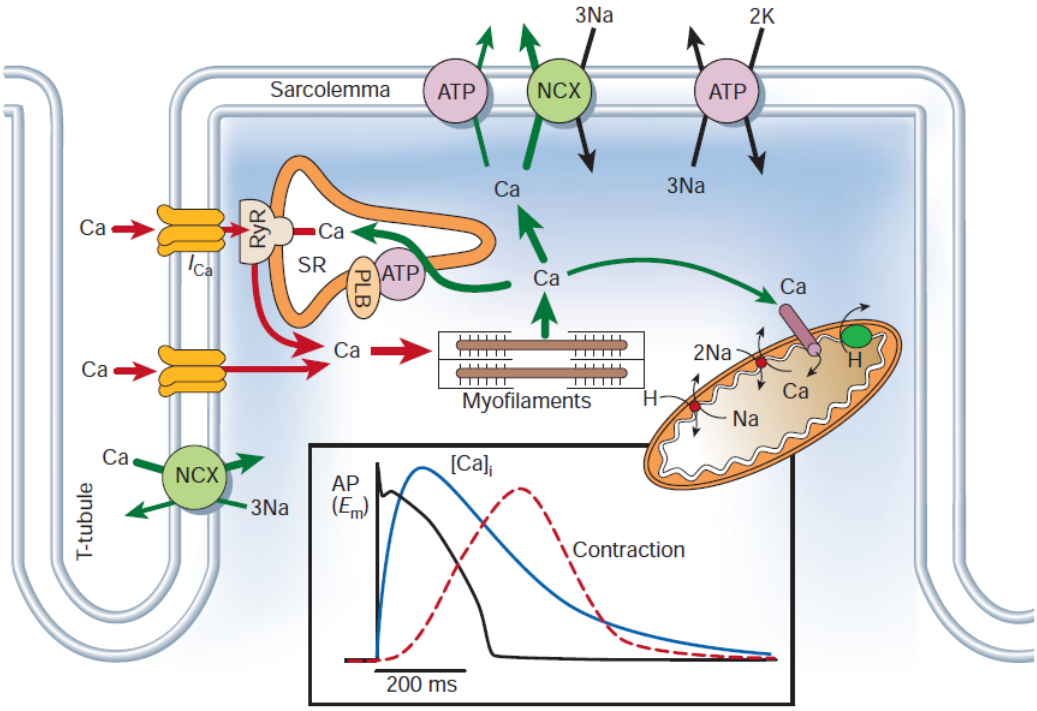

Figure 42: Ca^{2+} transport in ventricular myocytes. Inset shows the time course of an action potential, Ca^{2+} transient and contraction measured in a rabbit ventricular myocyte at $37°C$. NCX, Na^{+}/Ca^{2+} exchange; ATP, ATPase; PLB, phospholamban; SR, sarcoplasmic reticulum. Image from [47]

4.1.2 Calcium and contraction

Cardiac excitation-contraction coupling is the process from the electrical excitation of the myocyte to the contraction of the heart, that travels from the sino atrial node along the atria and ventricles and propels blood out. Ca^{2+} is essential in cardiac electric activity and is the direct activator of the myofilament that cause contraction. During the cardiac action potential, calcium ions enter the cell the depolarization-activated Ca^{2+} channels as inward Ca^{2+} current, I_{Ca}, which contributes to the action potential plateau as can be seen in the figure below:

Ca^{2+} entry triggers Ca^{2+} release from the sarcoplasmic reticulum (SR). The change in the concentration of calcium at the SR affects the opening probabilities of the calcium sensitive ryanodine receptors (RyR2), that when are opened, release calcium from the SR into the cytosol. The combination influx and release raises the free intracellular Ca^{2+} concentration ($[Ca^{2+}]_i$), allowing it to bind to the myofilament protein troponin C, which then switches on the contractile machinery. For relaxation to occur, $[Ca^{2+}]_i$ must decline, allowing Ca^{2+} to dissociate from troponin. This requires Ca^{2+} transport out of the cytosol by four pathways involving SR Ca^{2+}-ATPase, sarcolemmal Na^{+}/Ca^{2+} exchange, sarcolemmal Ca^{2+}-ATPase or mitochondrial Ca^{2+} uniport. Either the RyR2 channels get inactivated or the calcium levels close to the RyR2 decrease. Eventually, the concentration of calcium returns to its basal value, ready to produce another transient. [47]

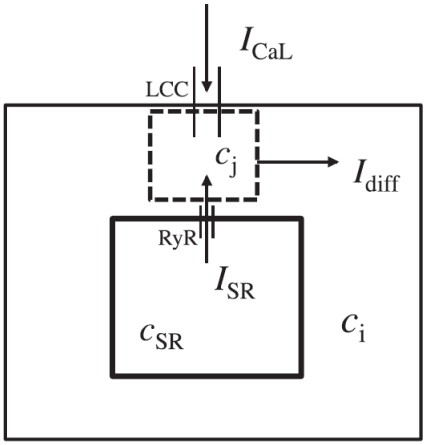

Figure 43: Calcium fluxes at the junctional space. Image from [48]

4.1.3 Calcium and alternans

A cardiac alternans is a disturbance in the normal rhythm of the heart characterized by beat-to-beat alternations in the duration of the excited phase of the transmembrane potential, that is, in the action potential duration (APD) and in the concentration of cytosolic calcium because it initiates the contraction. [48] Several studies have been done on the relation between calcium and the presence of alternans, for example, Alvarez-Lacalle *et al* showed that depending on the kinetics of the RyR2, alternans may appear due to either SR load alternations, to a slow recovery of RyR2 from inactivation, or to a combination of both [49].

These results show that RyR2 refractoriness is a key to the presence of cardiac alternans. The goal of this chapter is to study a model that has been developed by [48] and that is able to reproduce cardiac alternans with just the essential elements, so we get a qualitative understanding on the dependence of the onset of alternans with parameters involved in RyR2 kinetics and SR release.

4.2 Model

In most whole cell models, because of the differences of concentration of calcium in the SR and the cytosol, the cell is splitted into different compartments. In our case, we will consider four compartments: cytosol, sarcoplasmic reticulum, subsarcolemma close to the cell membrane, and the junctional area close to the region of the membrane with L-type calcium channels (LCCs). The calcium concentration in each compartment will be c_i,c_{SR}, c_S and c_j respectively. We are going to reduce the dynamics of calcium to a minimal model that is able to reproduce calcium alternans and yet let us test its universal features due to RyR2 refractoriness in whole-cell calcium models. We need to follow several steps [48]:

- **Decoupling of the dynamics of calcium at the junctional space from that of calclium at the other compartments.** The behaviour of calcium at the junctional space follows the diagram of fluxes in Figure 43. We can describe how the concentration of calcium at the junctional area changes as

$$\frac{dc_j}{dt} = I_{CaL} + I_{SR} - I_{diff} \tag{4.2.1}$$

The SR release current is given by

$$I_{SR} = g_{rel} P_O (c_{SR} - c_j)$$

where g_{rel} is the conductance of the RyR2 channels and P_O the fraction of RyR2 channels that are in the open state.

The diffusive current

$$I_{diff} = (c_j - c_i)/\tau_{diff}$$

is proportional to the calcium concentration difference between two compartments.

Finally, I_{CaL}, the L-type calcium current, is an inward current that depends on the transmembrane voltage and calcium concentration.

To decouple the calcium dynamics at the junctional space from the other compartments we fix the concentrations of calcium at SR (c_{SR}), and at the cytosol ($c_i = c_0$). Thus, we exclude the possibility of alternans due to SR calcium alternations.

- **Simplification of the LCC type current**. We will consider the L-type calcium current as an external stimulus that introduces a fixed amount of calcium during a given time.

$$I_{CaL} = \begin{cases} I_{CaL}^{max}, & \text{if } \mathrm{mod}(t, T_{period}) \leq \Delta T = 10ms \\ 0, & \text{if } \mathrm{mod}(t, T_{period}) > \Delta T = 10ms \end{cases} \tag{4.2.2}$$

The L-type current described this way corresponds to the current through a LCC channel next to a cluster of RyR2 receptors, that matches what happens at the local level of the Calcium Release Unit where a cluster of RyR2 controls the release of calcium.

With this, we can revisit equation (4.2.1) and apply the changes, to get

$$\frac{dc_j}{dt} = I_{CaL}(t) + g_{rel} P_O (C_{SR} - c_j) - \frac{(c_j - c_0)}{\tau_{diff}} \tag{4.2.3}$$

where the dynamics of junctional calcium is only coupled to the dynamics of the RyR2 through the fraction of open RyR2 channels P_O.

- **Simplification of the dynamics of the RyR2**. The RyR2 channels consider transitions among four states: one open (O), one closed (C) and two inactivated (I_1, $_2$). The dynamics of this gating are represented in Figure **??**, and are given by the probability rate equations

$$\frac{dP_C}{dt} = k_{im} P_{I_1} - k_i c_j P_C - k_a c_j^2 P_C + k_{om} P_O \tag{4.2.4}$$

$$\frac{dP_O}{dt} = k_a c_j^2 P_C - k_{om} P_O - k_i c_j P_O + k_{im} P_{I_2} \tag{4.2.5}$$

$$\frac{dP_{I_1}}{dt} = k_{om} P_{I_2} - k_a c_j^2 P_{I_1} - k_{im} P_{I_1} + k_i c_j P_C \tag{4.2.6}$$

$$\frac{dP_{I_2}}{dt} = k_i c_j P_O - k_{im} P_{I_2} - k_{om} P_{I_2} + k_a c_j^2 P_{I_1} \tag{4.2.7}$$

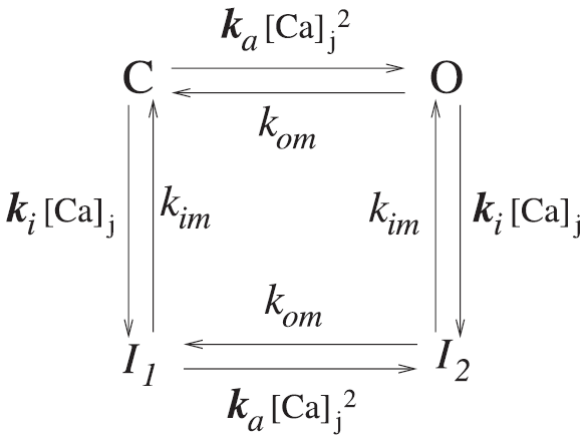

Figure 44: Representation of *RyR*2 gating dynamics. The four markovian states of the *RyR*2 are O (open), I_1 and I_2 (inactivated), and C (close). The respective rates for transitions between states are represented. The recovery time is defined as $\tau = \frac{1}{k_{im}}$. Image from [48]

This group of four equations can be simplified using the fact that it possesses two invariant manifolds [48] that allow us to work with a two dimensional system for p and q defined through

$$P_C = pq$$

$$P_O = q(1-p)$$

$$P_{I_1} = p(1-q)$$

$$P_{I_2} = (1-q)(1-p)$$

Thus, equations (4.2.4) - (4.2.7) become

$$\frac{dp}{dt} = k_{om}(1-p) - k_a c_j^2 p \tag{4.2.8}$$

$$\frac{dq}{dt} = k_{im}(1-q) - k_i c_j q \tag{4.2.9}$$

Equation (4.2.8) introduces the nature of calcium-induced calcium-released of calcium transient, while equation (4.2.9) dictates the possibility of inactivation of the RyR2.

An alternative way to express q is

$$q = P_C + P_O$$

where q is the fraction of RyR2 that are in the close or open state, that is, that have recovered from inactivation.

We have three equations, (4.2.3), (4.2.8) and (4.2.9) that define a three dimensional nonautonomous dynamical system for the junctional calcium concentration and the state of the RyR2. We can reduce it even more by considering that the opening of the RyR2 occurs almost instantaneously at the time scales of recovery. Thus, we consider that $dp/dt \simeq 0$ is in a quasisteady state, and

$$p \simeq \frac{k_{om}}{k_{om} + k_a c_j^2} \tag{4.2.10}$$

and therefore

$$P_O = q(1-p) \simeq q\frac{k_a c_j^2}{k_{om} + k_a c_j^2} \tag{4.2.11}$$

We can now get a two dimensional system by combining (4.2.3), (4.2.9) and (4.2.11) that is

$$\frac{dc_j}{dt} = I_{CaL}(t) + g_{rel} q \frac{k_a c_j^2}{k_{om} + k_a c_j^2}(c_{SR} - c_j) - \frac{c_j - c_0}{\tau_{diff}} \tag{4.2.12}$$

$$\frac{dq}{dt} = k_{im}(1-q) - k_i c_j q \tag{4.2.13}$$

These two equations represent a basic model that includes all relevant physiological information needed to test and study the appearance of calcium alternans disconnected from SR alternation and homeostatic effects [48].

Table 1 has the usual values for the parameters in these equations, though there is controversy about the order of magnitude of g_{rel} and k_i. To avoid dealing with problematical values, we will eliminate some parameters by normalizing the junctional calcium concentration c_j by $\sqrt{k_{om}/k_a}$ and time by $\tau = 1/k_{im}$.

Parameter	Dimensional	Non dimensional
RyR2 inactivation	$k_i = 0.5 mM^{-1}\ ms^{-1}$	$\gamma = {k_i}/{k_{im}\sqrt{k_{om}/k_a}} = 25$
RyR2 recovery from inactivation	$k_{im} = 0.002 ms^{-1}$	
RyR2 activation	$k_a = 12 mM^{-2}\ ms^{-1}$	
RyR2 closing	$k_{om} = 0.12 ms^{-1}$	
SR calcium concentration	$c_{SR} = 500 \mu M$	${c_{SR}}/{\sqrt{k_{om}/k_a}} = 5$
Cytosolic calcium concentration	$c_0 = 0.1 \mu M$	${c_0}/{\sqrt{k_{om}/k_a}} = 0.001$
Maximal L-type calcium current conductance	$I_{CaL_{max}} = 50 \mu M\ ms^{-1}$	$I_{CaL_{max}}\sqrt{k_a/k_{om}}/k_{im} = 25$
RyR2 channel conductance	$g_{rel} = 0.556 ms^{-1}$	$\alpha = {g_{rel}}/{k_{im}} = 278$
Diffusive time between dyadic and cytosolic spaces	$\tau_{diff} = 2ms$	$\beta = {1}/{k_{im}\tau_{diff}} = 250$

Table 1: Standard values of the parameters in Eqs. 4.2.12 and 4.2.13, taken from Ref. [48]

Thus, the model we will study is

$$\frac{dc_j}{dt} = I_{CaL}(t) + \alpha q\left(\frac{c_j^2}{1+c_j^2}\right)(c_{SR} - c_j) - \beta(c_j - c_0) \tag{4.2.14}$$

$$\frac{dq}{dt} = 1 - q - \gamma c_j q \tag{4.2.15}$$

with adimensional parameters α, β and γ.

4.3 Analysis of the model

We will work with the nonautonomous system:

$$\frac{dc_j}{dt} = I_{CaL}(t) + \alpha q\left(\frac{c_j^2}{1+c_j^2}\right)(c_{SR} - c_j) - \beta(c_j - c_0) \tag{4.3.1}$$

$$\frac{dq}{dt} = 1 - q - \gamma c_j q \tag{4.3.2}$$

where the parameters have been adimensionalized and we have that they are related to different features of the dynamics:

- α is related to the release strength of the RyR2
- β is related to diffusion
- γ is related to the relevance of the inactivation (or termination process) of the receptor.

Our goal is to leave all parameters fixed but I_{CaL}, and then study the equilibria, the stability of that equilibria, the periodic solutions and the bifurcation that happens at certain values. To do so, we will use the bifurcation diagram and will use Poincaré Maps to get a better understanding of what happens at certain values of the T : *period*. Most of the work will be done numerically using MatLab, but if analytic study is possible, it will be performed. We will specify the details of the numerical methods that MatLab uses to solve systems of ODEs and all codes used will be on Appendix A. To write the codes [50] has been used.

4.3.1 Nullclines and fixed points

We start by finding the nullclines analytically and their corresponding trajectories in the phase space. The nullclines correspond to

$$\frac{dc_j}{dt} = f(q, c_j, I_{CaL}) = 0 \qquad \frac{dq}{dt} = g(q, c_j) = 0 \tag{4.3.3}$$

and give the following curves

$$q_1 = \frac{\beta(c_j - c_0) - I_{CaL}}{\alpha(c_{SR} - c_j)}\left(\frac{1 + c_j^2}{c_j^2}\right)$$

$$q_2 = \frac{1}{1 + \gamma c_j}$$

The curve q_1 sets the excitability threshold and q_2 the termination of release. We know that the equilibria will be those points where nullclines cross. We can find a polinomyal for c_j which will have as roots the fixed points of the system when we choose the parameters. The polynomial is:

$$p(c_j) = \beta\gamma c_j^4 + (\beta - \beta\gamma c_0 + \gamma I_{CaL} + \alpha)c_j^3 + (\beta\gamma - \beta c_0 + I_{CaL} - \alpha c_{SR})c_j^2 + (\beta - \beta\gamma c_0 + \gamma I_{CaL})c_j - \beta c_0 + I_{CaL}$$

It is not a practical expression to work with, but it is easy to use in MatLab to check whether the fixed points are correct or not.
Once we have found the fixed points, we will want to find their stability. As we have seen on chapter 1, we do that by checking the sign of the real part of the eigenvalue of the Jacobian of the system evaluated at said point. The Jacobian can be found analytically, though in the codes has been calculated by MatLab, and is:

$$Df(c_j, q) = \begin{pmatrix} \frac{\partial f_1}{\partial c_j} & \frac{\partial f_1}{\partial q} \\ \frac{\partial f_2}{\partial c_j} & \frac{\partial f_2}{\partial q} \end{pmatrix} = \begin{pmatrix} \frac{\alpha q c_j}{(1+c_j^2)^2}(2c_{SR} - 3c_j - c_j^3) - \beta & \frac{c_j^2\alpha}{1+c_j^2}(c_{SR} - c_j) \\ -\gamma q & -1 - \gamma c_j \end{pmatrix}$$

We will get the eigenvalues with the code that is available at the Appendix A.
We consider the discretized model, where we fix I_{CaL} to a constant value in order to study the behaviour of the system when it is zero and when $I_{CaL} = 25$. If we plot the nullclines for both values of I_{CaL} in phase space, we get Figure 45 and Figure 46.

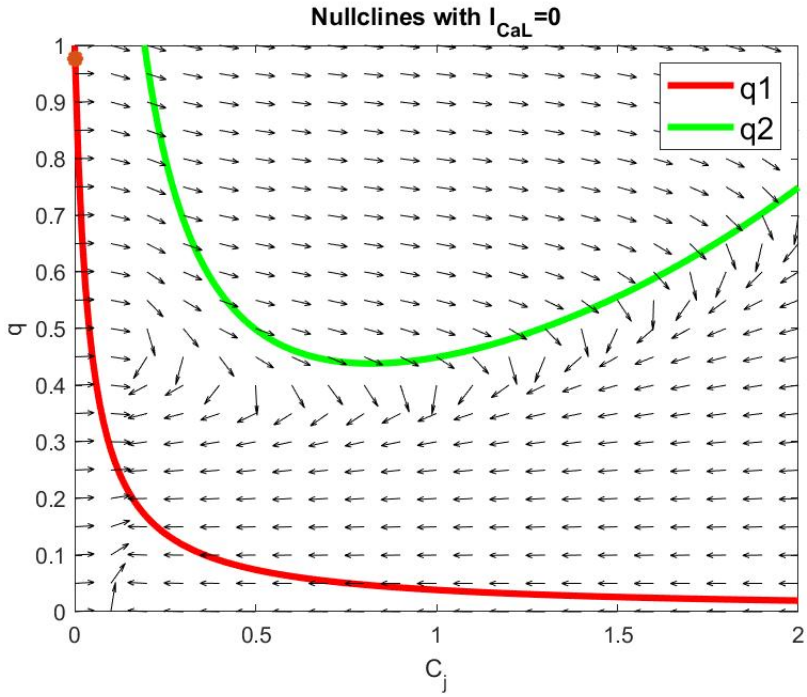

Figure 45: Nullclines with $I_{CaL} = 0$

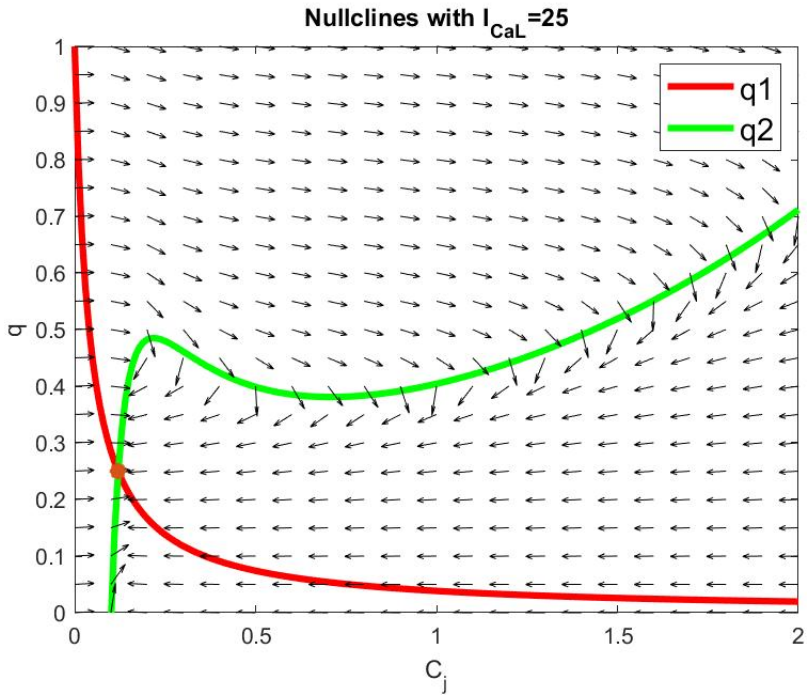

Figure 46: Nullclines with $I_{CaL} = 25$

For $I_{CaL} = 25$ the curves intersect at

$$p_{25} = [0.120, \quad 0.249]$$

It's clear in the phase diagram that the point is stable, but if we check the eigenvalues of the Jacobian of the system at this point, we get

$$(\lambda_1, \lambda_2) = (-4.731, \quad -171.128)$$

Both eigenvalues are real and strictly negative, so we check that the fixed point for $I_{CaL} = 25$, p_{25}, is an stable equilibrium.
For $I_{CaL} = 0$ the curves intersect at

$$p_0 = [0.001, \quad 0.975]$$

The point is an attractor as can be seen in the phase diagram, but again, we can check the eigenvalues of the Jacobian of the system at this point and get

$$(\lambda_1, \lambda_2) = (-1.025, \quad -247.273)$$

Since, as with the previous case, both eigenvalues are real and strictly negative, we confirm that the point is an stable equilibrium.
When we "turn-off" the LCC and do not give the system a peak of calcium, that is, we set $I_{CaL} = 0$, the fixed point is located at low values of c_j. However, when we turn it back on, the fixed point changes position and moves to lower values of q and larger values of c_j. Moreover, the flow on the phase space also changes.
To further analyze the behaviour of solutions, it is helpfull to plot the phase portrait (Figure 47 and Figure48). We have used two models in the MatLab codes, one discretized and one with I_{CaL} as a forced periodic function. To be able to understand how the phase portrait changes with and without the presence of active LCC, we will plot the phase diagram as we have done for the nullclines, with the discretized model for $I_{Cal} = 0$ and $I_{CaL} = 25$.
Now we can see the behaviour of the solutions and how it changes when we turn on the LCC. First, during a brief period of time, the nullclines with $I_{CaL} = 25$ determine the flow. The final point when I_{CaL} closes can end up at the right or at the left of the nullcline q_1. If to the right, then the solution goes away before returning to the fixed point (a calcium transient). On the other hand, if the final point is on the left of the nullcline there is a short return to the stable fixed point.
Suppose that the system starts at the position of the fixed point when $I_{CaL} = 0$. When the LCC is turned on, the system will move from this point and assuming that the inactivation is slow compared with the time scale in which I_{CaL} is acting, we can consider q constant during this first stage. Then, if we integrate the equation (4.3.1) is possible to compute an estimation of the threshold value of q_{thr} above which the trajectory crosses the nullcline q_1 [48]

$$q_{thr} = \frac{\beta^2}{4 I_{CaL} \alpha c_{SR}} \left[1 + \left(\frac{2\pi}{4 + \frac{\beta \Delta t}{\tau}} \right)^2 \right] \tag{4.3.4}$$

The existence of this limiting value makes the dependence of the trajectory with q very nonlinear. During alternans, one has to expect that the crossing of the nullcline happens only at non-consecutive beats. In one beat the number of recovered RyR2s is at a high value of q, a value large enough so the trajectory starting at that point crosses the excitability threshold. If the period is not large enough, however, by the time the next stimulation arrives, the number of recovered RyR2s q is at a much lower value than before.

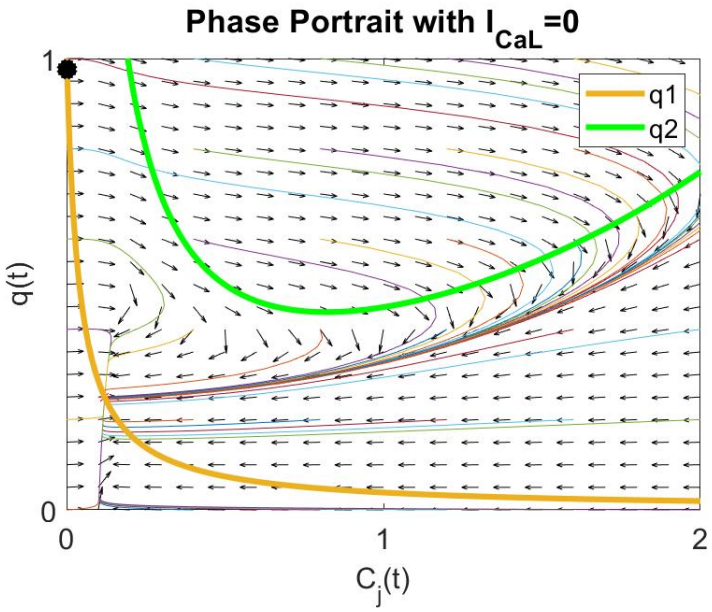

Figure 47: Phase portrait when $I_{CaL} = 0$

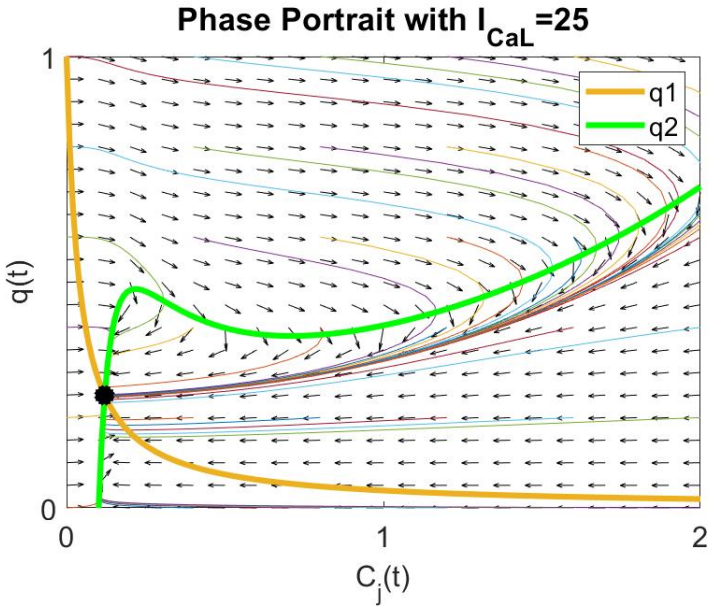

Figure 48: Phase portrait when $I_{CaL} = 25$

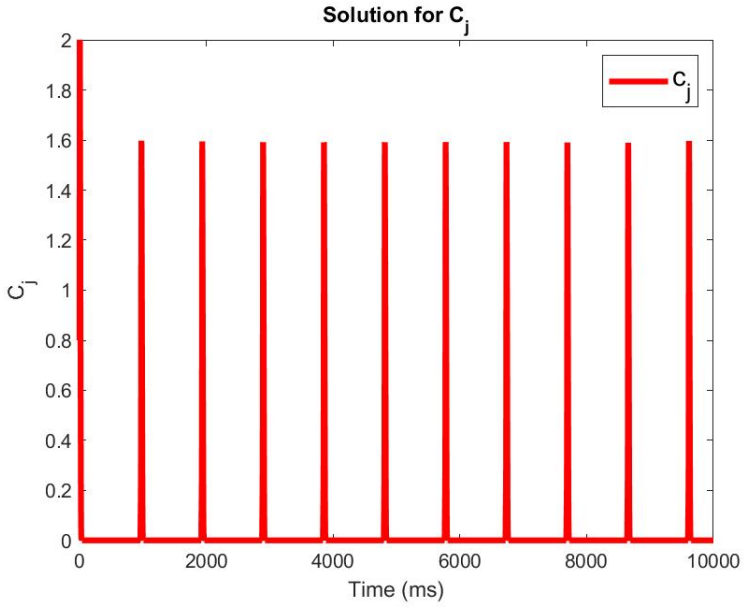

Figure 49: Phase diagram for c_j when I_{CaL} has a $T_{period} = 1.92$

Then, in this case, the nullcline q_1 is further to the right in phase space and the time is too short to increase the calcium level beyond the nullcline. The system, consequently, returns to the fixed point, resulting in a short transient. At the next beat, however, the value of q has recovered enough so as to cross the threshold generating 2:1 alternans.

4.3.2 Phase diagrams

Let's try to understand more the behaviour of calcium transients and alternans. We can solve the nonautonomous model and see the solutions for c_j, q and how they look like. We have considered the periodic I_{CaL} with a period $T_{period} = 1.92$ which gives a standard calcium transient.
As we can see in Figure 49 and Figure 50, both solutions are clearly periodical, and if we plot one on top of the other (Figure 51), we see that the periodicities match. LCC triggers the calcium-induced calcium-release opening of the RyR2 that results in a sharp increase in the level of junctional calcium. Upon the closing of the LCC, the release of calcium finishes due to the inactivation of the RyR2 opening. The variable q drops, closing the release and calcium is then diffused away, getting back to the basal level fixed in the model at c_0.
If we now focus on the trajectories (Figure 52), we see that they complete the whole calcium transient, as we expected.
If we change the T_{period} to $T_{period} = 1.01$ we find a 2:1 period doubling bifurcation with alternation of the strength in the calcium transient from one beat to the next, as we can see in Figure 53 and Figure 54
Now we see how the waves have the double amount of waves in the same time, because we have a period doubling bifurcation due to the appearance of cardiac alternans. If we plot the trajectories (Figure 55), we clearly see that now we have two different trajectories, a big one and at the next beat, a smaller one.
If, at a given beat, the number of recovered RyR2, q, is large, then, given the nonlinear relation between the calcium release strength and the number of recovered RyR2, release is also very large. However, this drives the inactivation of the receptors in the cluster, i.e., q drops dramatically for this release. Provided

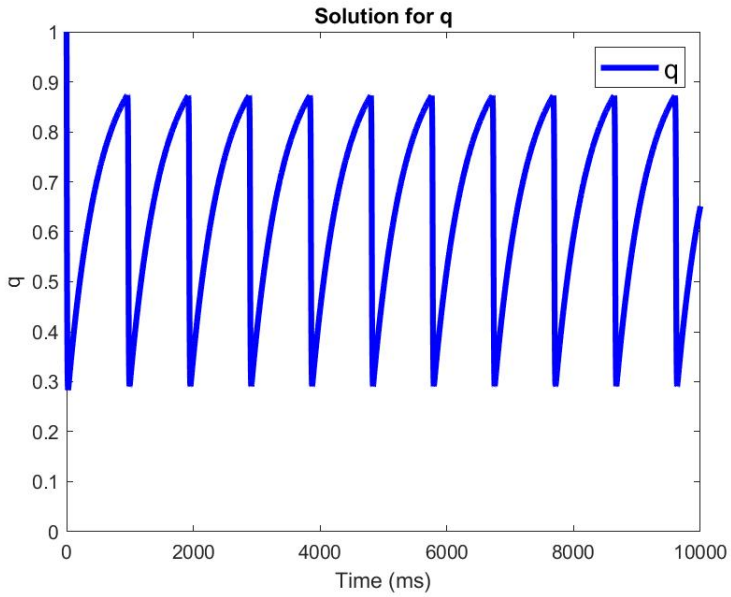

Figure 50: Phase diagram for q when I_{CaL} has a $T_{period} = 1.92$

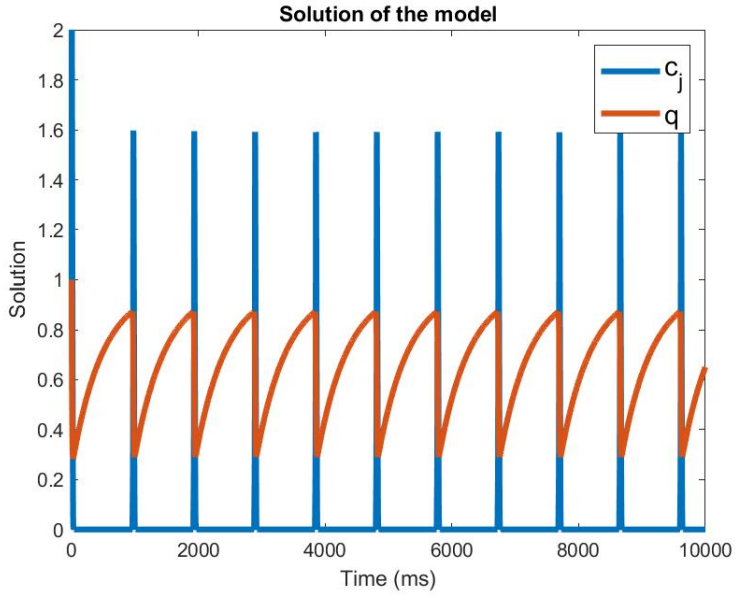

Figure 51: Evolution as of a function of time of normalized junctional calcium and RyR2 recovey variable for a pacing of the LCC at $T_{period} = 1.92$

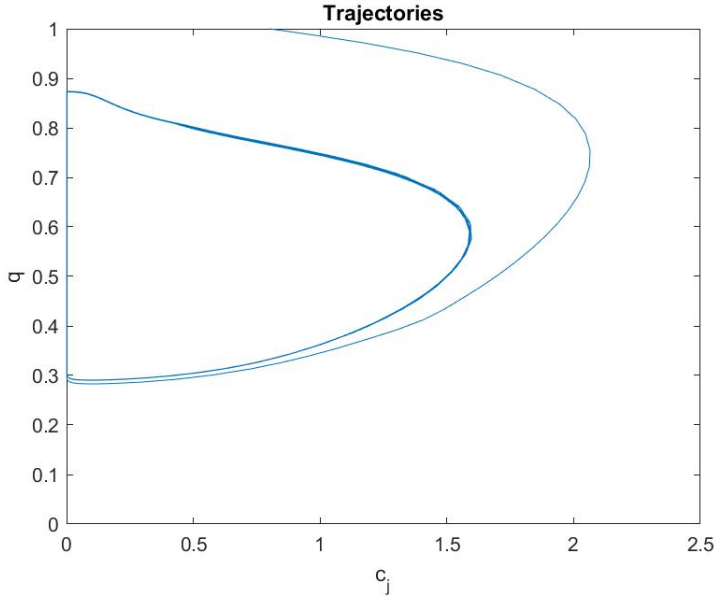

Figure 52: Trajectories that complete calcium transients

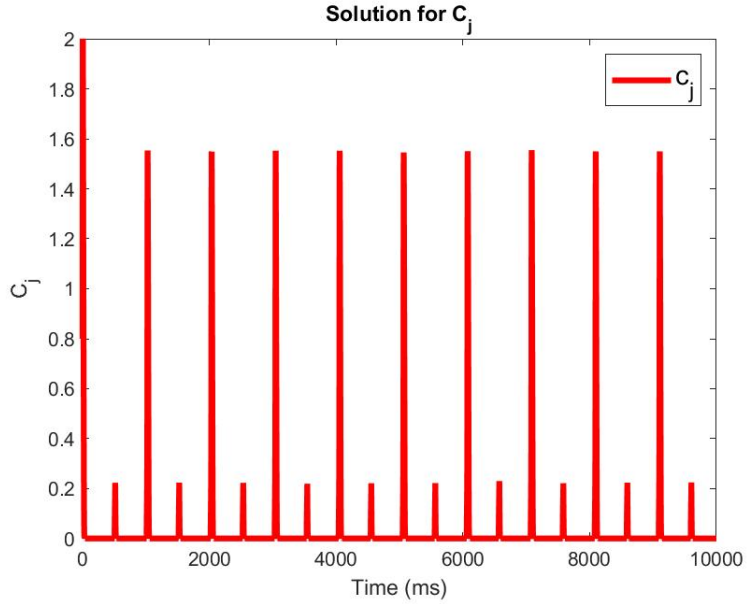

Figure 53: Phase diagram for c_j when I_{CaL} has a $T_{period} = 1.01$

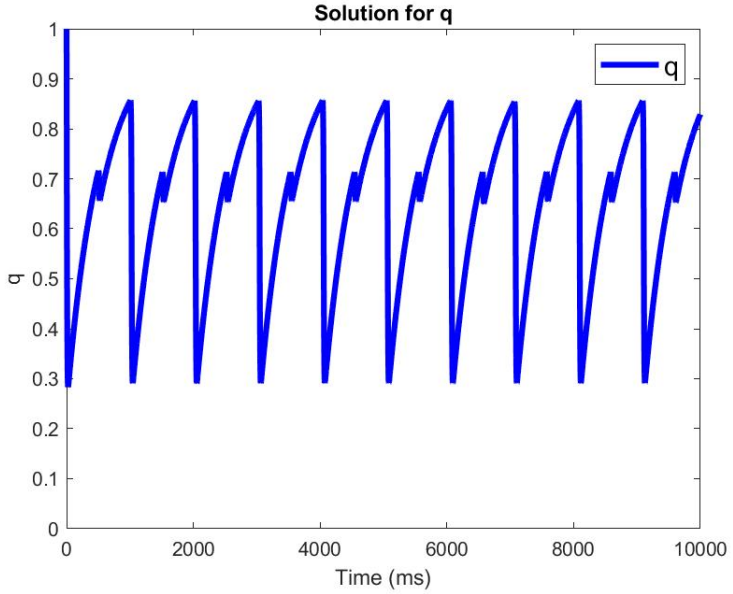

Figure 54: Phase diagram for q when I_{CaL} has a $T_{period} = 1.01$

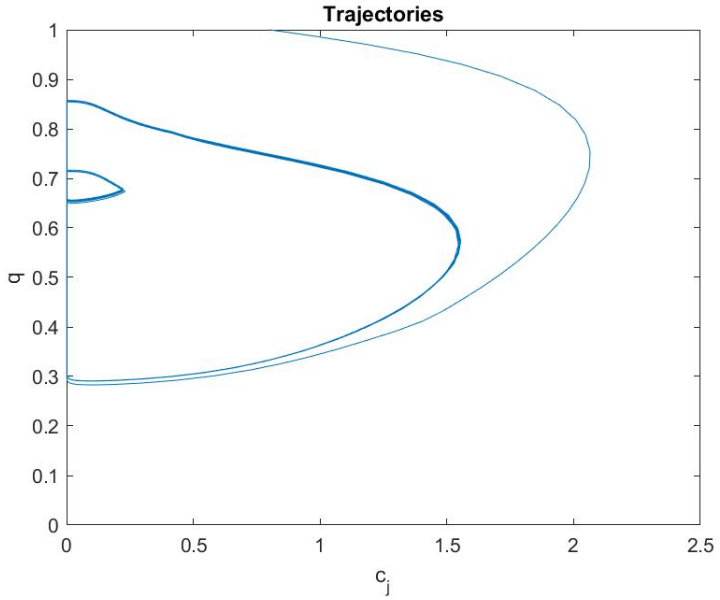

Figure 55: Trajectories with cardiac alternans

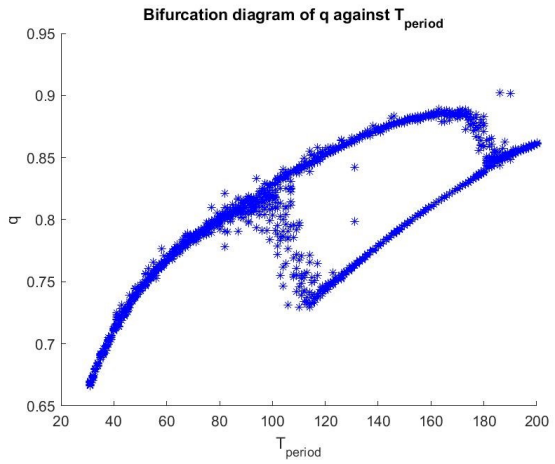

Figure 56: Bifurcation diagram when $\gamma = 50$

that the recovery from inactivation is slow enough, at the next beat the number of recovered receptors is low. This produces a small release and also small inactivation with q not dropping as much as in the previous beat. At the next beat the receptors are then fully recovered, starting the same process all over again. The release depends linearly on q and it is only through the nonlinearity of the calcium-induced calcium-release process that a nonlinear interaction is generated [48].

4.3.3 Bifurcation diagram and Poincaré Map

Now we get back to [48]. We see that they found that for $\gamma = 50$ a clear period doubling bifurcation appears in the model. We are going to plot the bifurcation diagram for q, because it will be easier to understand at sight, and study the bifurcation with the help of Poincaré maps. If we check Figure 56 we can see that around $T_{period} = 180$ a branch bifurcates. We could plot a closer bifurcation diagram to get a better view and we see how a solution splits in two. To check that it is actually a period doubling bifurcation, we sould have to plot a Poincaré section for a value of T_{period} higher than the bifurcation value along with the solution q, and repeat the plotting for a value lower than the bifurcation value.
The study of the bifurcation when γ is 50 is well detailed in [48]. In order to gain a better understanding of the bifurcations in the model and how Poincaré maps are useful to understand them, we are going to set $\gamma = 25$ again, and by repeating the simple analysis should be performed, we will try to understand the dynamics of q. Again, we plot a bifurcation diagram of q as a function of the T_{period} to see how the period orbits behave. The result is in Figure 57. Now we do not see the bifurcations,
we can clearly see two branches, but they never collide. This is probably because we are dealing with a subcritical period doubling, where $T_{period} \in (0.85, 1.40)$ approximately. There is an interval of T_{period} where we have 3 branches, around $T_{period} \in (0.60, 0.80)$ and for lower values of T_{period} we see two branches and a cloud of points, which indicates that we will probably find quasiperiodic behaviour.
First, we are going to plot the bifurcation diagram again, but focusing on the bifurcating points. We will start with the interval where the period doubling occurs, that is, $T_{period} \in (1.20, 1.50)$
We can see at Figure 58 that the bifurcation point is around $T_{period} = 1.37$. We can plot Poincaré maps for values of T_{period} higher, where we expect to see a single point because is a periodic orbit, for lower values, where we expect to see two points because the orbit has bifurcated in two, and at the bifurcation value we expect to see quasiperiodic behaviour. Also, we will plot the solution of q to be able to see how it behaves against time (Figure 60).

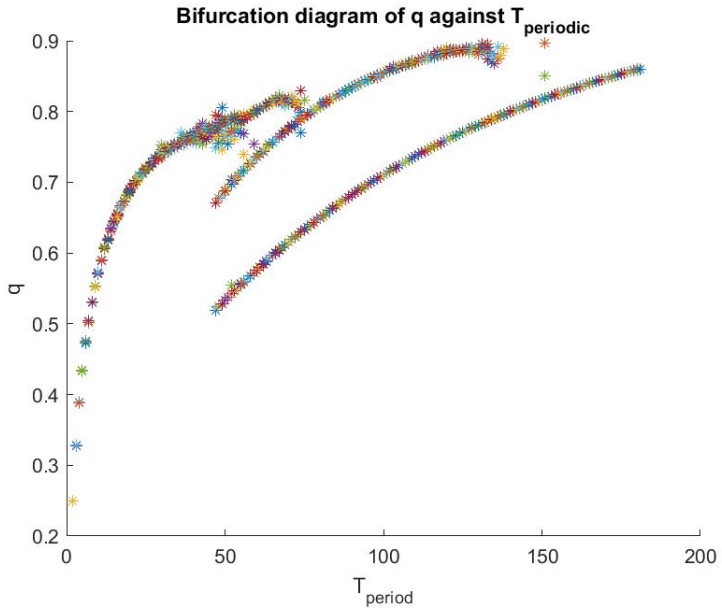

Figure 57: Bifurcation diagram when $\gamma = 25$

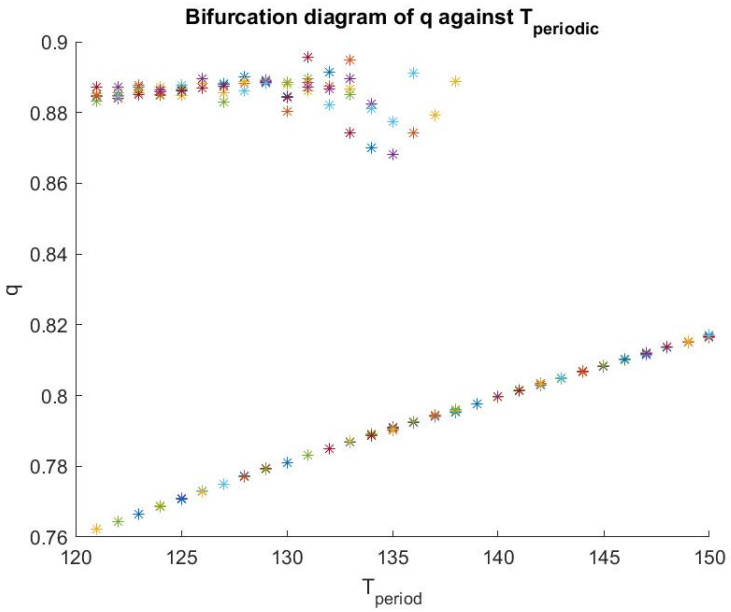

Figure 58: Bifurcation diagram

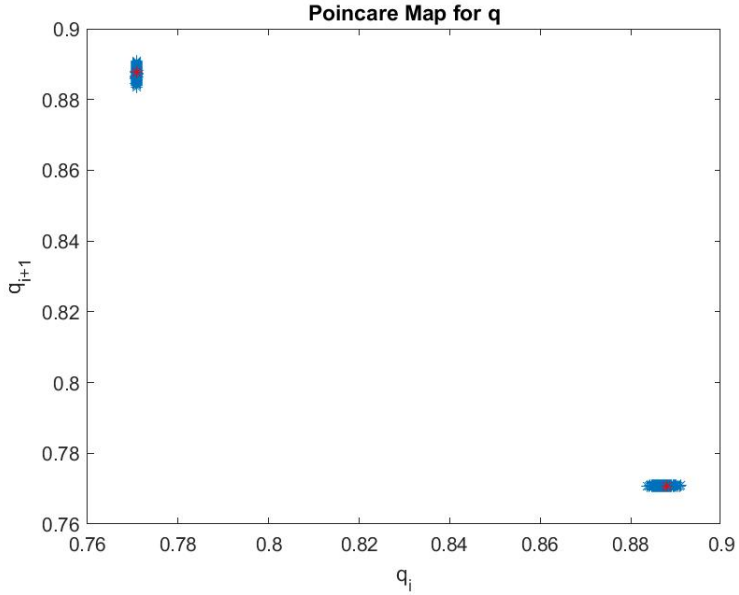

Figure 59: Poincaré map for $T_{period} = 1.25$

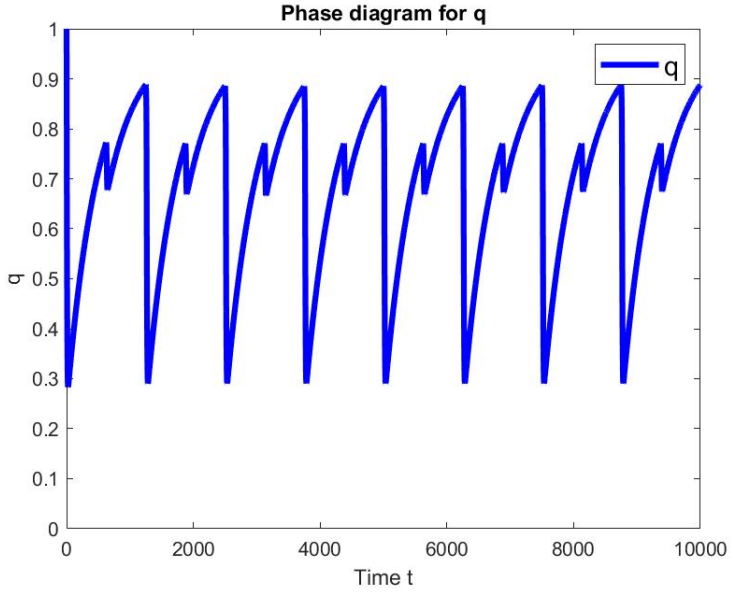

Figure 60: Solution of q when $T_{period} = 1.25$

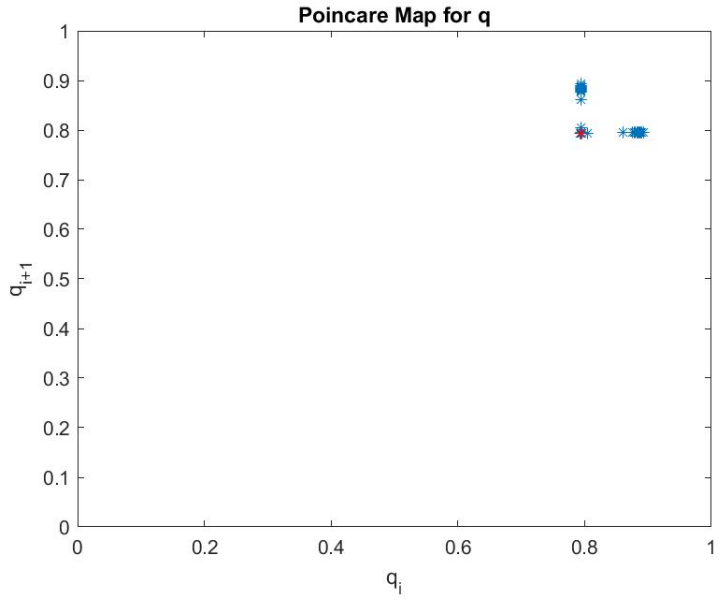

Figure 61: Poincaré map for $T_{period} = 1.37$

As expected, for values of T_{period} lower than the bifurcation value, we see two points in the Poincaré map (Figure 59) because we have a doubled period orbit when we plot the solution of q.
At the bifurcation value, we see how the Poincaré map (Figure 61) does not show one or two points, but a form of points. That is quasiperiodic behaviour, as can be seen in the plot of q (Figure 62).
Finally, the Poincaré map for $T_{period} = 1.50$ represents a point (Figure 63), which fits the simple periodic solution of q (Figure 64).

We can now repeat this study, now for the interval of T_{period} where a third branch appears. We will take $T_{period} \in (0.65, 0.80)$ and study the Poincaré maps and behaviour of solutions at the low and high part of the interval, and at an approximate value of the bifurcation value. To be able to be more specific with the values of T_{period}, we repeat the bifurcation diagram for this section.
Now we can see how, what resembles a branch, merges to one of the branches we already had in Figure 65. We can say that the bifurcation value is approximately $T_{period} = 0.74$, so we are going to plot Poincaré maps and the solution of q for higher, lower and that exact value to see the behaviour.
As we have three branches in the bifurcation diagram, we see that the wave of q is triple periodic (Figure 67), and we can see that on the Poincaré map because we have 3 points (Figure 66).
For the bifurcation value we have quasiperiodic behaviour again as can be seen in both the Poincaré map and the plot of q (Figure 68 and Figure 69).
For a higher value than the bifurcation value, we had two branches on the bifurcation diagram, and that is exactly what represents the Poincaré map with the two points (Figure 70), and can also be seen on the double waves of the phase diagram of q (Figure 71).

Finally, we can check the lowest values of T_{period} at the bifurcation diagram, $T_{period} \in (0.15, 0.60)$. At a certain value, almost simultaneously, two branches disappear, while a cloud of points remains.
We can choose, $T_{period} = 60$ because all branches are still alive, and see that there is still a triple wave for q (Figure 73. As T_{period} decreases, the behaviour looses its periodicity and becomes quasiperiodic because

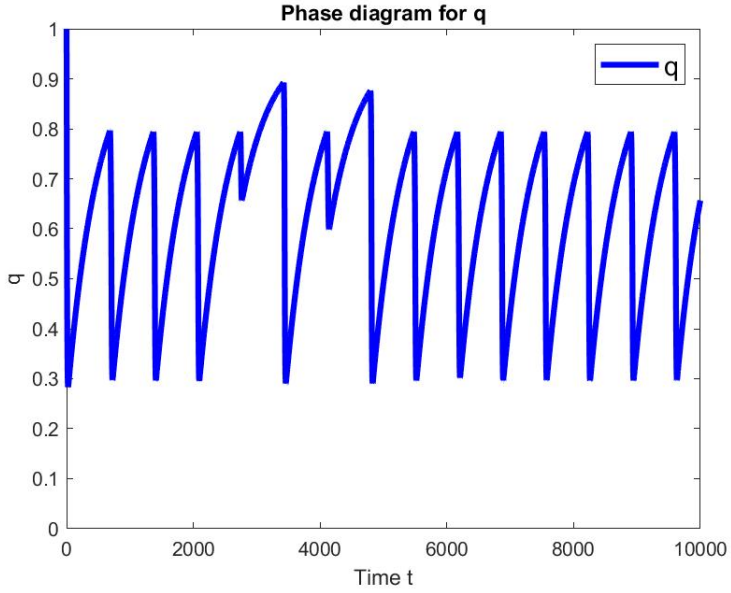

Figure 62: Solution of q when $T_{period} = 1.37$

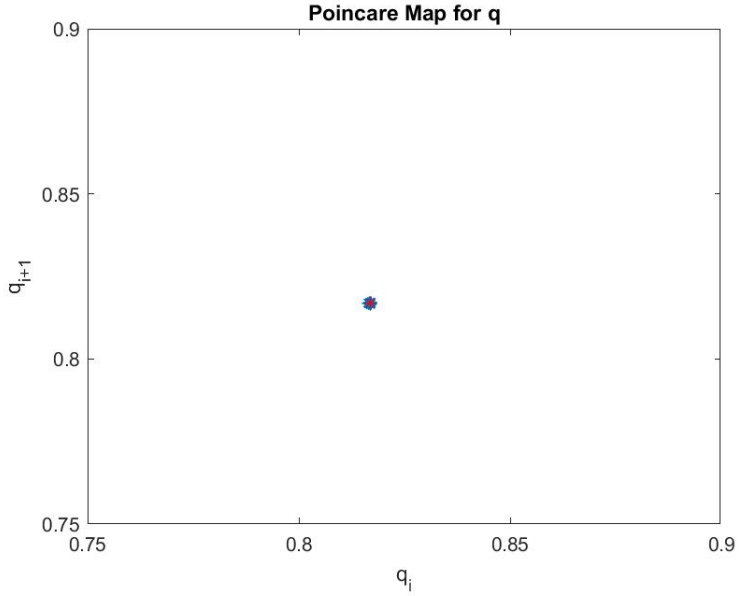

Figure 63: Poincaré map for $T_{period} = 1.50$

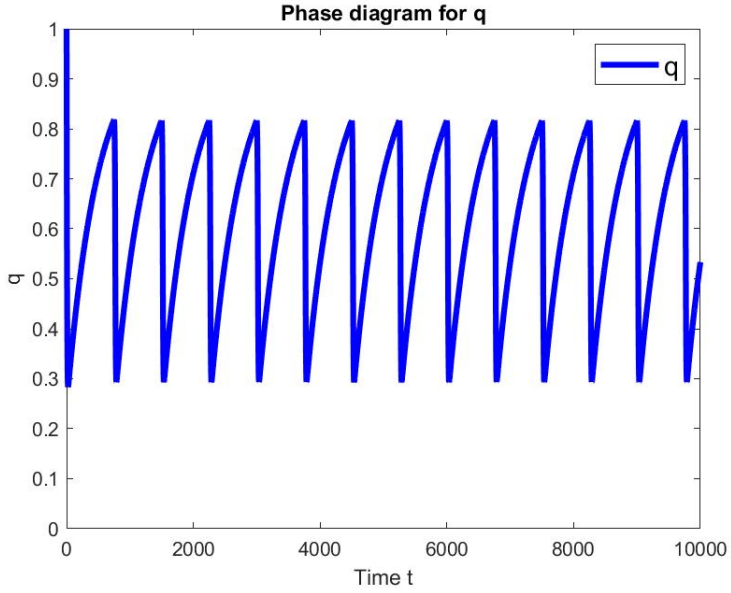

Figure 64: Solution of q when $T_{period} = 1.50$

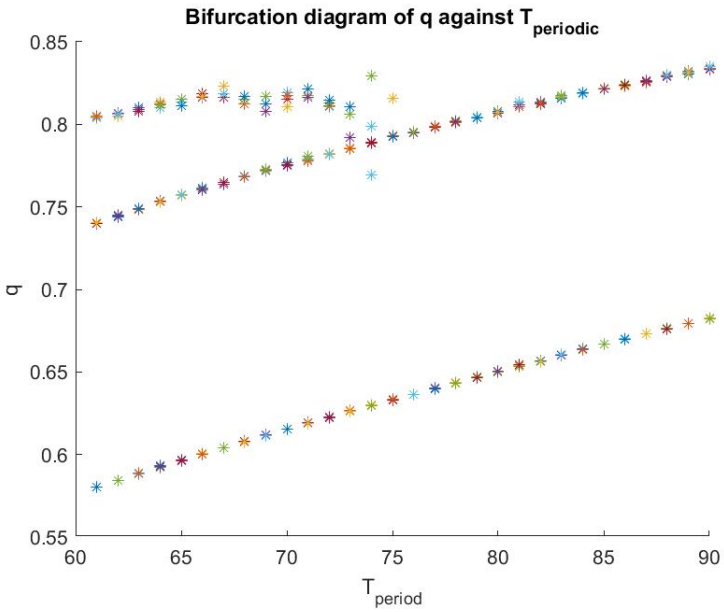

Figure 65: Bifurcation diagram

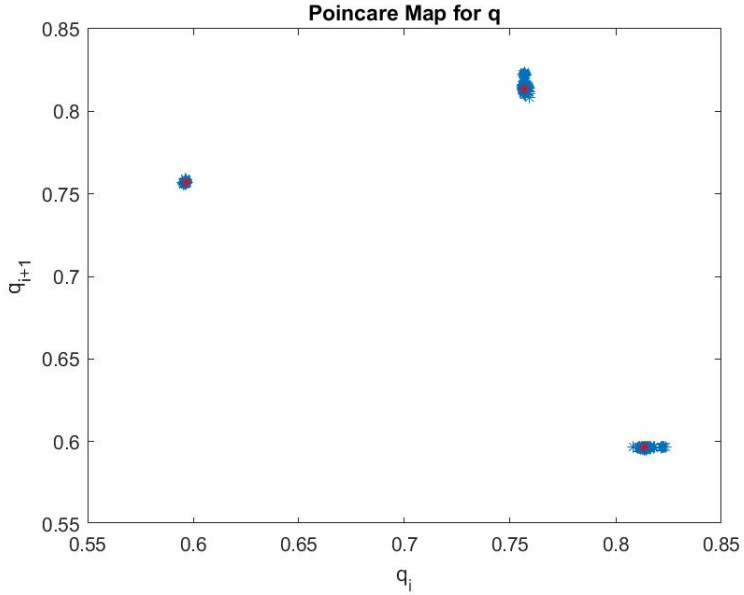

Figure 66: Poincaré map for $T_{period} = 0.65$

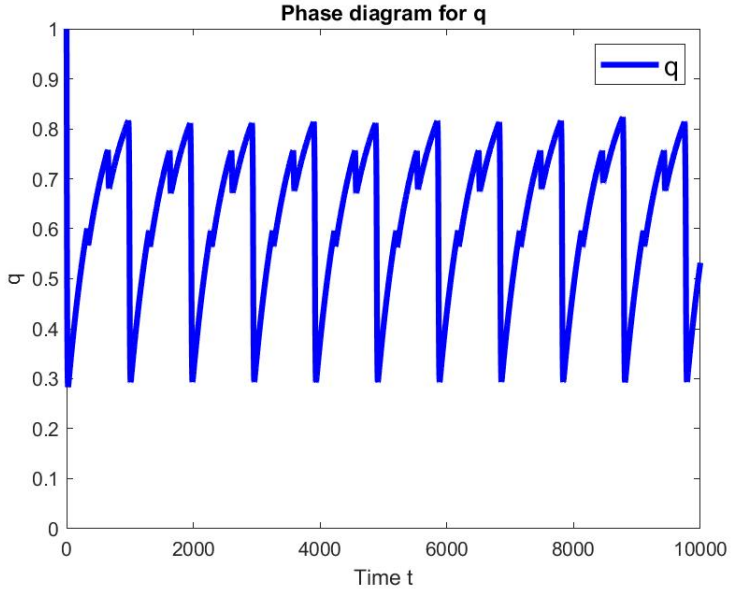

Figure 67: Solution of q when $T_{period} = 0.65$

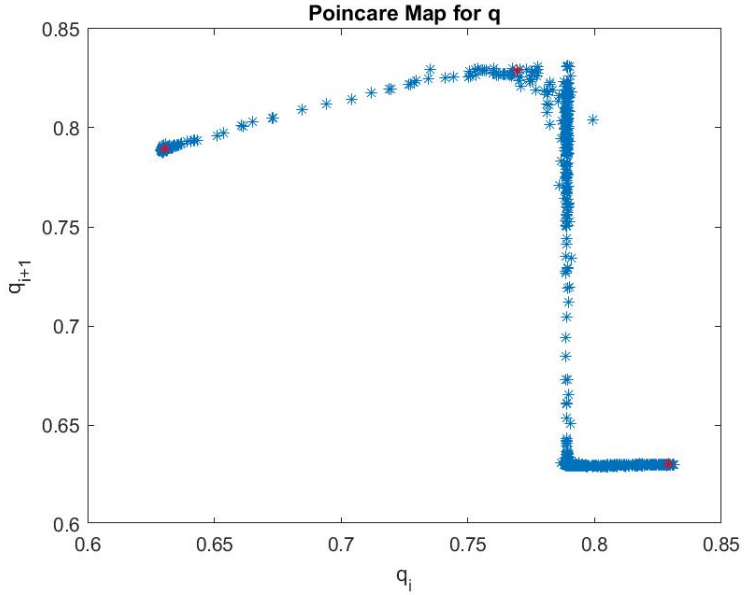

Figure 68: Poincaré map for $T_{period} = 0.74$

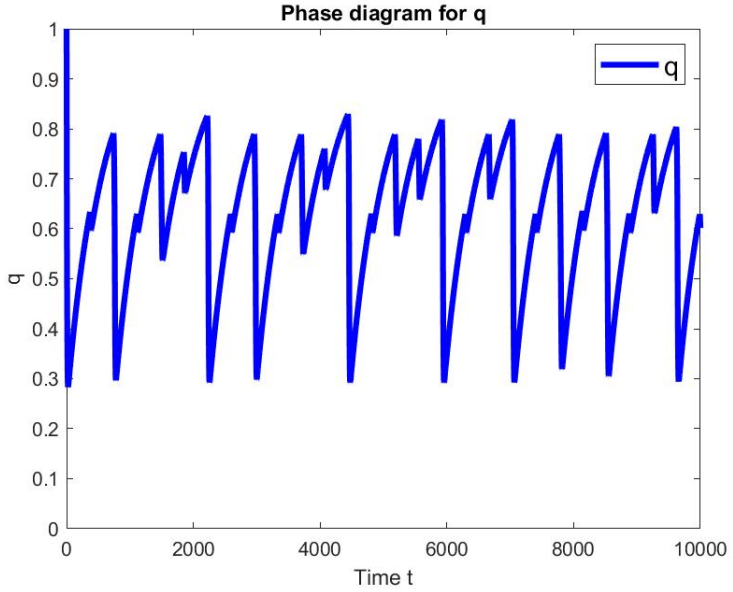

Figure 69: Solution of q when $T_{period} = 0.74$

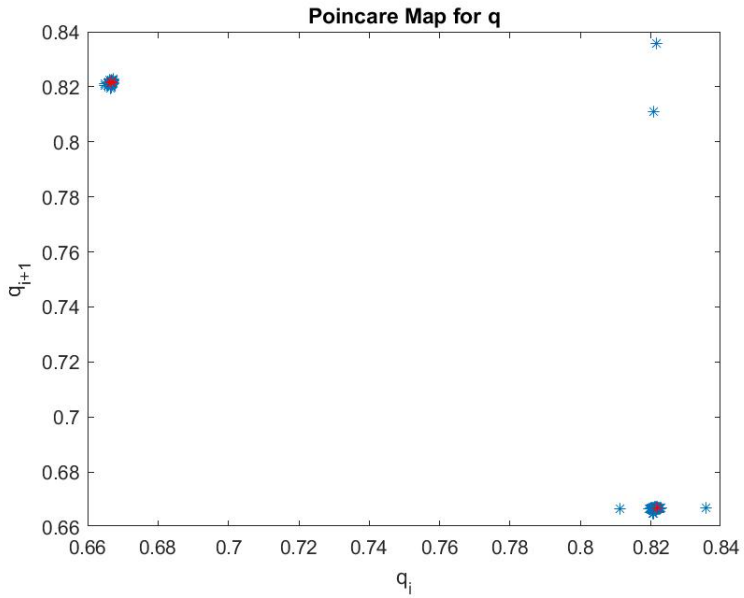

Figure 70: Poincaré map for $T_{period} = 0.85$

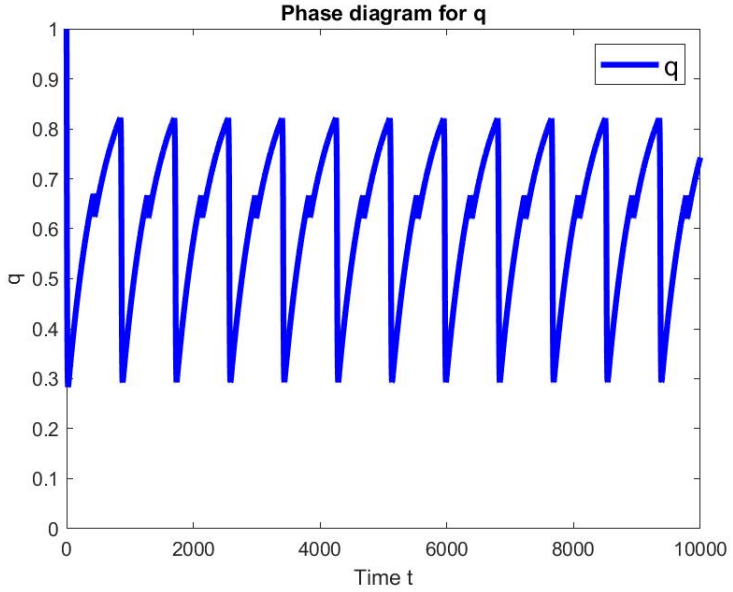

Figure 71: Solution of q when $T_{period} = 0.85$

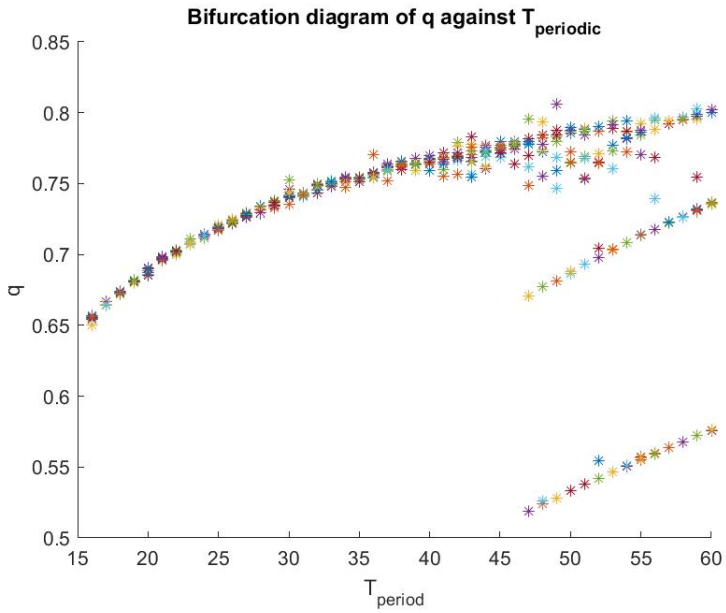

Figure 72: Bifurcation diagram

we have a cloud of points. Eventually, for $T_{period} = 20$ there is no quasiperiodic behaviour but just a pulse that fades because the spike of I_{CaL} is not enough to start the periodic behaviour of q. It's important to remark that when the two branches dissapear, the behaviour declines to a stationary state quickly. We plot the solution q for some values of T_{period} as a prove of this reasoning in Figure 74 to Figure 77.

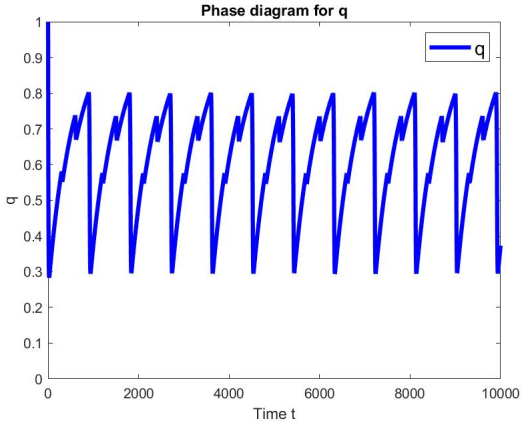

Figure 73: Solution of q when $T_{period} = 0.60$

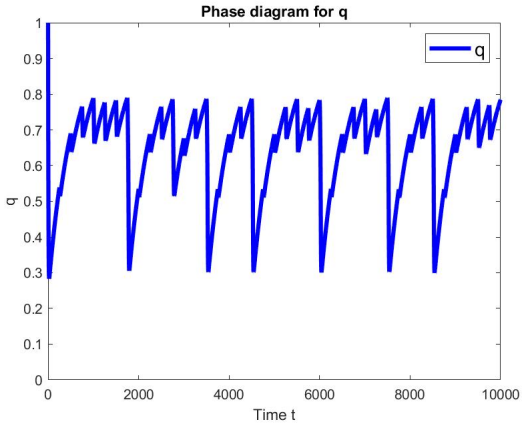

Figure 74: Solution of q when $T_{period} = 0.50$

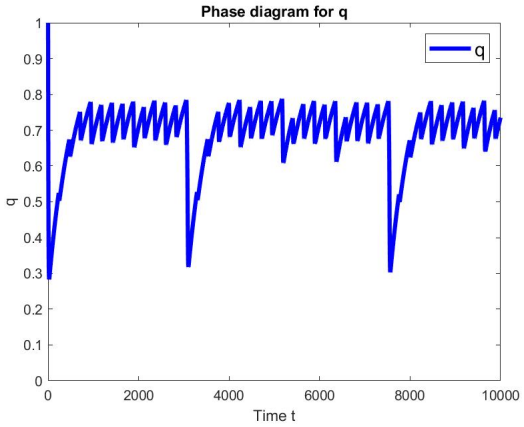

Figure 75: Solution of q when $T_{period} = 0.47$

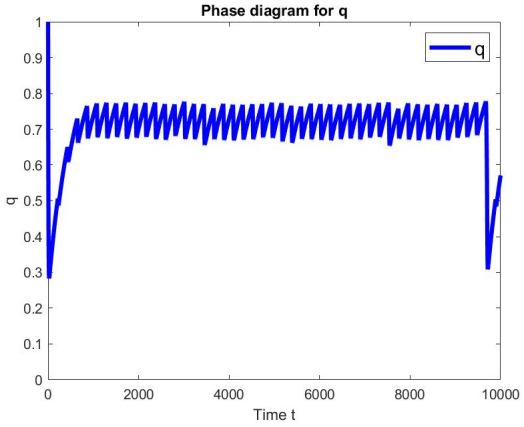

Figure 76: Solution of q when $T_{period} = 0.43$

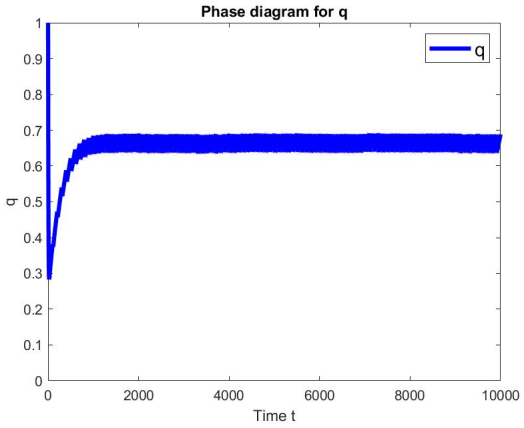

Figure 77: Solution of q when $T_{period} = 0.20$

4.4 Conclusions

We have worked with a simplified model of calcium release that reproduces calcium alternans due to refractoriness because of inactivated states of the RyR2. The model can be considered as a reduction of a whole cell-model where the calcium concentration in each compartment corresponds to average values on the cell and where alternation appears. Mathematically, alternans are period doubling bifurcations of the calcium transient, and along them, different transitions to higher order periodicities appear as the value T_{period} decreases.

We have studied the behaviour of q and seen that there is a strong nonlinear dependence of calcium release with the level of recovered receptors, which is linked to the excitable gap defined by the nullclines of the model. There is a critical value of the number of recovered receptors that leads to a large calcium release, which gives rise to an on/off process. Close to this critical value, the system easily transits from release to non-release events, leading to high order periodicity.

It has been impossible to determine properly and without a doubt the type of bifurcations for the model when $\gamma = 25$. That is because the transitions are to difficult to understand just with a MatLab solver, and probably continuation methods and specific software is necessary to make a more relevant study.

5. Conclusions

The model analyzed in the third chapter has very interesting transitions when it bifurcates. It is out of scope to further analyze those transitions, but it's important to remark that just with MatLab software is not possible to get good results. While the two first chapters, and the ODE course of the degree, have given a great background to study the model, more analytical knowledge is required to get a better understanding of how periodic solutions of the model behave, and why and how they change period. It is probably because chaos is involved at some level, so further analysis should be done.

References

[1] John Guckenheimer and Philip Holmes. *Nonlinear Oscillations, Dynamical Systems, and Bifurcations of Vector Fields*, pages 1–8. Springer, 1983.

[2] Jordi Villanueva. Equacions diferencials ordinaries. https://mat-web.upc.edu/people/rafael.ramirez/edos/apunts_edos1.pdf, 2009.

[3] Steven H. Strogatz. *Nonlinear Dynamics and Chaos*, pages 18–21. Addison-Wesley Publishing Company, 1994.

[4] Hassan K. Khalil. *Nonlinear Systems (3rd Edition)*, chapter 4. Lyapunov Stability. Prentice-Hall, 2002.

[5] D. R. J. Chillingworth. *Differential Topology with a view to applications*, pages 188–187. Pitman, 1976.

[6] Earl A. Coddington & Norman Levinson. *Theory of ordinary differential equations*. McGraw-Hill, 1955.

[7] John Guckenheimer and Philip Holmes. *Nonlinear Oscillations, Dynamical Systems, and Bifurcations of Vector Fields*, pages 10–12. Springer, 1983.

[8] Rafael Ramirez. Sistemas de edos lineales. https://mat-web.upc.edu/people/rafael.ramirez/edos/sl.pdf, 2013.

[9] Axelle Amon. *Nonlinear dynamics*, pages 26–38. Hal Archives Ouvertes, 2007.

[10] Scott Zimmerman. An undergraduates guide to the hartman-grobman and poincare-bendixon theorems. https://www.math.hmc.edu/ levy/181_web/Zimmerman_web.pdf, 2008.

[11] Phillip Hartman. *Ordinary Differential Equations, 2nd Edition*, pages 228–272. Siam, 2002.

[12] John Guckenheimer and Philip Holmes. *Nonlinear Oscillations, Dynamical Systems, and Bifurcations of Vector Fields*, pages 16–22. Springer, 1983.

[13] John Guckenheimer and Philip Holmes. *Nonlinear Oscillations, Dynamical Systems, and Bifurcations of Vector Fields*, pages 33–38. Springer, 1983.

[14] John Guckenheimer and Philip Holmes. *Nonlinear Oscillations, Dynamical Systems, and Bifurcations of Vector Fields*, pages 38–42. Springer, 1983.

[15] C. Pugh and M. Matos Peixoto. Structural stability. *Scholarpedia*, 3(9):4008, 2008. revision #137910.

[16] Joris Vankerschaver. Lectures on periodic orbits. http://www.cds.caltech.edu/archive/help/uploads/wiki/files/224/perorb.pdf.

[17] J. Moehlis, K. Josic, and E. T. Shea-Brown. Periodic orbit. *Scholarpedia*, 1(7):1358, 2006. revision #153208.

[18] John Guckenheimer and Philip Holmes. *Nonlinear Oscillations, Dynamical Systems, and Bifurcations of Vector Fields*, pages 42–60. Springer, 1983.

[19] Norman R. Lebovitz. Stability ii: Maps and periodic orbits. http://people.cs.uchicago.edu/ lebovitz/Eodesbook/stabper.pdf.

[20] W.S Koon. Poincaré map, floquet theory, and stability of periodic orbits. http://www.cds.caltech.edu/archive/help/uploads/wiki/files/190/Lecture6$_0$6.*pdf* .

[21] John Guckenheimer and Philip Holmes. *Nonlinear Oscillations, Dynamical Systems, and Bifurcations of Vector Fields*, pages 22–32. Springer, 1983.

[22] Joseph Romeo William Michael Picard. Impredicativity and turn of the century foundations of mathematics : presupposition in poincare and russell. https://dspace.mit.edu/bitstream/handle/1721.1/84612/12-006j-fall-2006/contents/lecture-notes/lecnotes8.pdf.

[23] David Jerison Jennifer French Jeremy Orloff Arthur Mattuck, Haynes Miller. Limit cycles. https://math.mit.edu/ jorloff/suppnotes/suppnotes03/lc.pdf.

[24] Ferdinand Verhulst. *Nonlinear Differential Equations and Dynamical Systems*. Springer-Verlag Berlin Heidelberg, 1996.

[25] Axelle Amon. *Nonlinear dynamics*, pages 39–45. Hal Archives Ouvertes, 2007.

[26] John Guckenheimer and Philip Holmes. *Nonlinear Oscillations, Dynamical Systems, and Bifurcations of Vector Fields*, pages 118–123. Springer, 1983.

[27] John Guckenheimer and Philip Holmes. *Nonlinear Oscillations, Dynamical Systems, and Bifurcations of Vector Fields*, pages 123–138. Springer, 1983.

[28] Dr. Yanghong Huang. *Applied Dynamical Systems*, pages 63–65. School of Mathematics, University of Manchester.

[29] Dr. Yanghong Huang. *Applied Dynamical Systems*, pages 69–72. School of Mathematics, University of Manchester.

[30] John Guckenheimer and Philip Holmes. *Nonlinear Oscillations, Dynamical Systems, and Bifurcations of Vector Fields*, pages 138–145. Springer, 1983.

[31] Steven H. Strogatz. *Nonlinear Dynamics and Chaos*, pages 45–50. Addison-Wesley Publishing Company, 1994.

[32] Jean-Michel Grandmont. *Nonlinear difference equations, bifurcations and chaos:An introduction*, pages 136–142. Elsevier Ltd., 2008.

[33] Moo. Transcritical bifurcation phase portraits. https://mathematica.stackexchange.com/questions/115653/transcritical-bifurcation-phase-portraits.

[34] Nasser M. Abbasi. My math 703, methods of applied mathematics i, 3.6 hw 6, due dec 10, 2014. https://www.12000.org/my_courses/univ_wisconsin_madison/fall_2014/math_703_applied_math/inse7.htm.

[35] Canan elik Karaaslanl. *Numerical Simulation - From Theory to Industry*, pages 10–15. Edited by Mykhaylo Andriychuk, 2012.

[36] John Guckenheimer and Philip Holmes. *Nonlinear Oscillations, Dynamical Systems, and Bifurcations of Vector Fields*, pages 145–156. Springer, 1983.

[37] Y. A. Kuznetsov. Andronov-Hopf bifurcation. *Scholarpedia*, 1(10):1858, 2006. revision #90964.

[38] Dr. Yanghong Huang. *Applied Dynamical Systems*, pages 74–78. School of Mathematics, University of Manchester.

[39] Canan elik Karaaslanl. *Numerical Simulation - From Theory to Industry*, pages 15–19. Edited by Mykhaylo Andriychuk, 2012.

[40] Dr. Yanghong Huang. *Applied Dynamical Systems*, pages 80–82. School of Mathematics, University of Manchester.

[41] John Guckenheimer and Philip Holmes. *Nonlinear Oscillations, Dynamical Systems, and Bifurcations of Vector Fields*, pages 155–165. Springer, 1983.

[42] C. Tresser, P. Coullet, and E. de Faria. Period doubling. *Scholarpedia*, 9(6):3958, 2014. revision #142883.

[43] De Los Nietos Miguel C. Nociones basicas de anatomia, fisiologia y patologia cardiaca: bradiarritmias y taquiarritmias. *Enfermeria en Cardiologia N 40*, pages 7–20, 1er cuatrimestre 2007.

[44] Eric Pierce. File:heart labelled large.png. https://en.wikipedia.org/wiki/Heart.

[45] Martin L. Buist Andrew J. Pullan, Leo K. Cheng. *Mathematical modelling the electrical activity of the heart: from cell to body surface and back again*, pages 1–147. World Scientific Publishing, 2005.

[46] Richard E. Klabunde. *Cardiovascular Physiology Concepts, Second Edition*. Lippincott Williams & Wilkins, 2011.

[47] Donald M. Bers. Cardiac exciaion-contraction coupling. *Macmillan Magazines Ltd*, 415:198–202, 2002.

[48] Angelina Pearanda Inma R. Cantalapiedra, Enrique Alvare-Lacale and Blas Echebarria. Minimal model for calcium alternans due to sr release refractoriness. *Chaos*, 27(093928), 2017.

[49] A. Pearanda J. Cinca L. Hove-Madsen E. Alvarez-Lacalle, I. R. Cantalapiedra and B. Echebarria. Dependency of calcium alternans on ryanodine receptor refractoriness. *PLoS One*, 8:e55042, 2013.

[50] Stephen Lynch. *Dynamical Systems with Applications using MATLAB*. Birkhauser, Manchester, United Kindom, 2004.

A. MATLAB Codes

A.1 Model

```
%MODEL
function system = model(t, y)
T=1.44; %Period
I=0; %L-type calcium current conductance
if(mod(t,T)<0.02)
I = 25.; %maximal L-type calcium current conductance
end
a = 278; %strenght release of the RyR2 (adimensional)
b = 250; %difussion (adimensional)
g = 25; %relevance of the inactivation of the receptor (adimensional)
csr = 5; %SR calcium concentration
c0 = 0.001;%cytosolic calcium concentration
system = [I + a*y(2)*y(1)^(2)/(1+y(1)^(2))*(csr - y(1)) - b*(y(1) - c0); 1 - y(2) ...
    - g*y(1)*y(2)];

%y(1) = cj (calcium concentration at the junctional space
%y(2) = q (fraction of RyR2 that have recovered from inactivation)
```

A.2 Discretized Model

```
%MODEL DISCRETIZED
function system = modeldis(t, y)
I = 25; %L-type calcium current conductance
a = 278; %strenght release of the RyR2 (adimensional)
b = 250; %difussion (adimensional)
g = 25; %relevance of the inactivation of the receptor (adimensional)
csr = 5; %SR calcium concentration
c0 = 0.001;%cytosolic calcium concentration
system = [I + a*y(2)*y(1)^(2)/(1+y(1)^(2))*(csr - y(1)) - b*(y(1) - c0); 1 - y(2) ...
    - g*y(1)*y(2)];

%y(1) = cj (calcium concentration at the junctional space
%y(2) = q (fraction of RyR2 that have recovered from inactivation)
```

A.3 ModelT

```
function system = modelT(t,y)
global T;
I=0; %L-type calcium current conductance
if(mod(t,T)<0.02)
I = 25.; %maximal L-type calcium current conductance
end
a = 278; %strenght release of the RyR2 (adimensional)
```

```
b = 250; %difussion (adimensional)
g = 25; %relevance of the inactivation of the receptor (adimensional)
csr = 5; %SR calcium concentration
c0 = 0.001;%cytosolic calcium concentration
system = [I + a*y(2)*y(1)^(2)/(1+y(1)^(2))*(csr - y(1)) - b*(y(1) - c0); 1 - y(2) ...
    - g*y(1)*y(2)];
end
```

A.4 Fixed Points

```
function [fp] = FixedPoints(I, g)
syms cj q;
a = 278;
b = 250;
csr = 5;
c0 = 0.001;

eq1 = I + a.*q.*cj^(2)/(1+cj^(2)).*(csr - cj) - b.*(cj - c0)==0;
eq2 =1 - q - g.*cj.*q==0;

eqns = [eq1,eq2];
vars = [cj q];
[solcj, solq]=solve(eqns, vars);
scj = vpa(solcj);
sq = vpa(solq);
n = size(solcj);
FP = [];
for i=1:n
    if abs(imag(scj(i)))<0.00001 && abs(imag(sq(i)))<0.00001
        if real(scj(i))>0 && real(sq(i))>0
            FP = vertcat(FP,[real(scj(i)) real(sq(i))]);
        end
    end
end
fp = FP;
end
```

A.5 Vector Field

```

%vector field

function vectorfield(deqns, xval, yval, t)
if nargin == 3;
    t=0;
end

m = length(xval);
n = length(yval);
x1 = zeros(n, m);
```

```
y1 = zeros(n, m);
for a=1:m
    for b=1:n
        pts = feval(deqns, t, [xval(a);yval(b)]);
        x1(b, a) = pts(1);
        y1(b, a) = pts(2);
    end
end
arrow = sqrt(x1.^2+y1.^2);
quiver(xval, yval, x1./arrow,y1./arrow,.5,'black');
axis tight;
```

A.6 Nullclines

```
%Plot nullclines and fixed points
clear all;

dlgtitle = 'Input';
prompt = {'Enter I:'};
dims = [1 35];
definput = {''};
userInput = inputdlg(prompt,dlgtitle,dims,definput);

I = str2double(userInput(1));
g = 25;
a = 278;
b = 250;
csr = 5;
c0 = 0.001;



A = Fixedpoints(I,g)
[m, n] = size(A); %m es num de fixed points

cj=[0:0.01:2];

q1=1./(1+g.*cj);
q2=(b*(cj-c0)-I).*(1+cj.^2)./(a*cj.^2.*(csr-cj));

fig=figure(1);
p1=plot(cj,q1,'r','LineWidth',3);
hold on;
p2=plot(cj, q2,'g','LineWidth',3);
vectorfield(@modeldis, 0:.1:2.5, 0:.05:1);
hold on;
for i=1:m
    p3=plot(A(i,1),A(i,2),'*','LineWidth',5);
end
axis([0 2 0 1]);
hold off;
lgd=legend([p1 p2],'q1','q2');
lgd.FontSize = 14;
xlabel('C_j')
```

```
ylabel('q')
title(sprintf('Nullclines with I_{CaL}=%d',I));

savePath=sprintf('/figures/nullclines_%d.jpg',I);
saveas(fig,[pwd savePath],'jpeg');
```

A.7 Stability Fixed Points

```
%Stability Fixed Points
clear all;

dlgtitle = 'Input';
prompt = {'Enter I:'};
dims = [1 35];
definput = {''};
userInput = inputdlg(prompt,dlgtitle,dims,definput);

I = str2double(userInput(1));
g = 25;
a = 278;
b = 250;
csr = 5;
c0 = 0.001;
FP = Fixedpoints(I,g);
syms cj q;
DF = jacobian([I + a*q*cj^(2)/(1+cj^(2))*(csr - cj) - b*(cj - c0), 1 - q - ...
    g*cj*q], [cj;q]);
[n, m] = size(FP);
for i=1:n
    disp('eigenvalues for fixed point ')
    fp = [FP(i, 1) FP(i, 2)]
    B = subs(DF, [cj q], fp);
    disp('are ')
    eigen = eig(B)
end
```

A.8 Phase Portrait

```
clear all;
%Phase portrait

dlgtitle = 'Input';
prompt = {'Enter I:'};
dims = [1 35];
definput = {''};
userInput = inputdlg(prompt,dlgtitle,dims,definput);

I = str2double(userInput(1));
g = 25;
a = 278;
```

```
b = 250;
csr = 5;
c0 = 0.001;
warning off MATLAB:divideByZero
vectorfield(@model, 0:.1:2.5, 0:.05:1);
    hold on
    for y1=0:0.4:2
        for y2=0:0.2:1
            [ts, ys]= ode45(@model, [0 10], [y1 y2]);
            plot (ys(:,1), ys(:,2))
            plot (ys(end,1), ys(end,2),'*')

        end
    end
axis([0 2 0 1])
fsize = 15;
set(gca, 'xtick', [-1:1:5], 'FontSize', fsize)
set(gca, 'ytick', [-1:1:5], 'FontSize', fsize)
xlabel('C_j(t)', 'FontSize', fsize)
ylabel('q(t)', 'FontSize', fsize)



cj=[0:0.01:2];
q1=1./(1+g.*cj);
q2=(b*(cj-c0)-I).*(1+cj.^2)./(a*cj.^2.*(csr-cj));
figure(1)
plot(cj,q1,'LineWidth',3);
hold on;
plot(cj,q2,'g','LineWidth',3);
axis([0 2 0 1]);
hold off;

title(sprintf('Phase Portrait with I_{CaL}=%d',I));

savePath=sprintf('/figures/phasePortrait_%d.jpg',I);
saveas(figure(1),[pwd savePath],'jpeg');
```

A.9 Phase Diagrams

```
clear;
[t,y] = ode45(@model,[0 20],[0.8; 1]);


%Phase diagram for cj
fig1 = figure(1);
plot(t*500,y(:,1),'r','LineWidth',3);
title('Phase diagram for C_j');
xlabel('Time t');
ylabel('C_j');
lgd=legend('c_j');
lgd.FontSize = 14;
axis([0 10000 0 3]);

```

```
%Phase diagram for q
fig2 = figure(2);
plot(t*500,y(:,2),'b','LineWidth',3);
title('Phase diagram for q');
xlabel('Time t');
ylabel('q');
lgd=legend('q');
lgd.FontSize = 14;
axis([0 10000 0 3]);


%Solution Curves
fig3 = figure(3);
plot(t*500,y(:,1),'-o',t*500,y(:,2),'-o')
title('Solution of the model with ODE45');
xlabel('Time t');
ylabel('Solution');
lgd=legend('c_j','q');
lgd.FontSize = 14;


saveas(figure(1),[pwd '/figures/phaseDiagramsCj.jpg'],'jpeg');
saveas(figure(2),[pwd '/figures/phaseDiagramsQ.jpg'],'jpeg');
saveas(figure(3),[pwd '/figures/phaseDiagramsSol.jpg'],'jpeg');
```

A.10 Bifurcation Diagram

```


%para diferentes valores de T, me guardo los ultimos 10 valores de qi(end) y entonces
%dibujo contra T
%Bifurcation diagram
clear all;
global T;
A = [];
for i=1:180
    iT=i+30;
    T = iT/100;
    [ts, ys] = ode45(@modelT,[0:0.01:1000],[0.8; 1]);
    q = ys(:, 2);
    n=size(q);
    qi=1+iT*10:iT:n-iT;
    A(i, 1)= iT;
    A(i, 2)=q(qi(end));
    for j=1:10
       A(i, 1+j) = q(qi(end - j));
    end
end
[f, h] = size(A);
fig = figure(1);
hold on;
for s=1:f
        plot(A(s, 1), A(s, 2:h), '*');
end
```

```
hold off;
%saveas(fig, 'bifurcationdiagram.jpg')
```

A.11 Poincaré Section

```
clear all;
global T; %value between 0 and 2

dlgtitle = 'Input';
prompt = {'Enter T:'};
dims = [1 35];
definput = {''};
userInput = inputdlg(prompt,dlgtitle,dims,definput);

T = str2double(userInput(1));

[t, y] = ode45(@modelT,[0:0.01:1000],[0.8; 1]);
iT= T*100; %period value between 62 and 200

% cj = y(:,1);

% Poincar  Map for q
fig=figure(2);
q = y(:,2);
n=size(q);
qi=1+iT*10:iT:n-iT;
qj=1+iT*11:iT:n;
plot(q(qi), q(qj),'*');hold on
plot(q(qi(end)), q(qj(end)),'r*')
plot(q(qi(end-1)), q(qj(end-1)),'r*')
plot(q(qi(end-2)), q(qj(end-2)),'r*')
title('Poincare Map for q');
xlabel('q_i')
ylabel('q_{i+1}')

savePath=sprintf('/figures/poincareSection_%.1f.jpg',T);
saveas(fig,[pwd savePath],'jpeg');
```